Boston University

OpenBU **http://open.bu.edu**

Boston University Theses & Dissertations Boston University Theses & Dissertations

2012

The effects of shockwaves on cultured mammalian neurons and their implications for mild traumatic brain injury

https://hdl.handle.net/2144/31551

Downloaded from DSpace Repository, DSpace Institution's institutional repository

BOSTON UNIVERSITY

GRADUATE SCHOOL OF ARTS AND SCIENCES

Dissertation

THE EFFECTS OF SHOCKWAVES ON CULTURED MAMMALIAN NEURONS AND THEIR IMPLICATIONS FOR MILD TRAUMATIC BRAIN INJURY

by

MATTHEW TEAGUE FERENC

B.S., Bucknell University, 2002
M.S., Bucknell University, 2004

Submitted in partial fulfillment of the

requirements for the degree of

Doctor of Philosophy

2012

Ph2
2012
Fer
cop.1

Approved by

First Reader [redacted]

James O. Deshler, Ph.D.
Assistant Professor of Biology

Second Reader [redacted]

Hengye Man, Ph.D.
Assistant Professor of Biology

ACKNOWLEDGMENTS

I would first like to thank my advisor, Dr. James Deshler, for the amazing research opportunity he provided me with and for all his help in analyzing data, trouble-shooting experiments, preparing seminar talks and, of course, my thesis. I have grown both as a person and a scientist under his guidance.

I also want to thank all the students in the Deshler lab that I've had the good fortune to work with over the years, Dr. Bianca Heinrich, Dr. Zhao Chen and Vanessa Obourn. Without your help and support I would not have reached this milestone.

I would also like to thank my committee—Dr. William Eldred, Dr. Angela Ho, Dr. Ulla Hansen, Dr. Hengye Man and Dr. Robert Hausman for sharing their time and expertise as well as their support.

I would also like to thank Dr. Man and the members of his lab for the neuronal cultures they unfailingly made for me every week, without which my work would not have been possible. In particular I would like to thank Larissa Jarzylo and Steve Amato for their instruction on the use of their microscope as well as their patience for my endless questions.

I need to thank my classmates for their camaraderie and support during long hours studying, desperate searching for reagents, struggling data analysis

and general commiserating over data- good, bad and ugly. I especially need to thank Jack Stopa and Jan Blom for always being there whenever, for whatever.

Thank you to my parents, Thomas and Christie Ferenc who taught me to work hard and persevere. Their love and support over the years has kept me going and I don't think I can ever fully thank them for everything they've done for me. I love you both.

Most importantly I would like to thank my amazing wife Natalie for the continued support that she has provided throughout my graduate school experience. She is the most amazing person I know and without her I would be lost. You carry my heart.

THE EFFECTS OF SHOCKWAVES ON CULTURED MAMMALIAN NEURONS AND THEIR IMPLICATIONS FOR MILD TRAUMATIC BRAIN INJURY

(Order No. 3500887)

MATTHEW TEAGUE FERENC

Boston University Graduate School of Arts and Sciences, 2012

Major Professor: James O. Deshler, Professor of Biology

ABSTRACT

The widespread use of Improvised Explosive Devices (IEDs) in the Wars in Iraq and Afghanistan has caused a dramatic increase in shockwave-induced mild Traumatic Brain Injury (mTBI), leading mTBI to be dubbed the 'signature injury' of modern warfare. Currently, the pathology of shockwave-induced mTBI is unknown, and its diagnosis is based on self-reported symptoms and combat history. While the etiological mechanism has not yet been determined, it is becoming increasingly accepted that shockwaves themselves are the brain-damaging agent that emanate from IEDs. To assess how mild, sub-lethal shockwaves might damage brain tissue, we developed an *in vitro* assay to deliver shockwaves to neuronal cells in culture, and then assayed several properties of these cells that affect their function. This assay involved exposing rat cortical and hippocampal primary neuronal cultures to shockwaves of increasing magnitude generated with a biolistic Gene Gun. The Gene Gun produces shockwaves of sufficient overpressure to cause cognitive impairment in

animal models of shockwave-induced mTBI. Our results show that overpressures of ~1.0 pound per square inch (psi) caused transient membrane permeability for molecules up to ~12 nanometers in diameter. This change in membrane permeability was accompanied by a transient decrease in cellular ATP levels and synaptic densities. This synaptic degeneration correlated with changes in the level and phosphorylation state of several synaptic proteins examined. Similar results were observed in dissected rat retinas suggesting that these shockwave-induced effects can occur in complex tissues, such as the brain. Based on these findings we propose that shockwaves damage cellular membranes, leading to a decrease in intracellular ATP, and ultimately to a reduced numbers of synapses, the part of neurons most important for learning, memory and behavior. Additional experiments in whole animals will be required to ascertain whether shockwave-induced cellular damage and synaptic degeneration plays an etiological role in shockwave-induced mTBI.

TABLE OF CONTENTS

LIST OF TABLES

LIST OF FIGURES

LIST OF ABBREVIATIONS

ACRAM	American College of Rehabilitation Medicine
ACSF	Artificial Cerebral Spinal Fluid
AD	Alzheimer's disease
AMPA	α-amino-3-hydroxy-5-methyl-4-isoxazolepropionic acid
ATP	Adenosine Triphosphate
BCA	Bicinchoninic Acid
BOLD	Blood Oxygen Level-Dependent
BSA	Bovine Serum Albumin
C	Celsius
$CaCl_2$	Calcium Chloride
CAMII	Ca^{2+}/Calmodulin-dependent Kinase II
CAPS	Clinician-Administered PTSD Scale
CASK	Ca^{2+}/Calmodulin-dependent Serine Protein Kinase
CAT/CT	Computer Aided Tomography
CDC	Centers for Disease Control and Prevention
CO_2	Carbon Dioxide
CPG	Clinical Practice Guideline
DAB	Diaminobenzidine
DAI	Diffuse Axonal Injury

DAPI	4',6-diamidino-2-phenylindole
df	Degrees of Freedom
DIC	Differential Interference Contrast
DIV	Days *in vitro*
DNA	Deoxyribonucleic acid
DoD	Department of Defense
DSM-III	Diagnostic and Statistical Manual of Mental Disorders 3rd edition
DSM-IV-TR	Diagnostic and Statistical Manual of Mental Disorders 4th Edition Text Revisions
DTI	Diffusion Tensor Imaging
eEFA1a	Eukaryotic Translation Elongation Factor 1α1
ESW	Extracorporeal Shockwave
FdU	Fluorodeoxyuridine
fMRI	Functional Magnetic Resonance Imaging
GAP43	Growth Associated Protein 43
GK	Guanylate Kinase-like Domain
GluR1	Glutamate Receptor Subunit 1
GluR2	Glutamate Receptor Subunit 2
Grip1	Glucocorticoid Receptor Interacting Protein 1
HD	Huntington's disease

HEPES	4-(2-hydroxyethyl)-1-piperazineethanesulfonic acid
HRP	Horseradish Peroxidase
IACUC	Institutional Animal Care and Use Committee
IED	Improvised Explosive Device
ImPACT	Immediate Post-Concussion Assessment and Cognitive Testing
iNOS	Inducible Nitric Oxide Synthase
KCl	Potassium Chloride
kDa	Kilodalton
kHz	Kilohertz
kpa	Kilopascal
lbs	pounds
MACE	Military Acute Concussion Evaluation
MAGUK	Membrane Associated Guanylate Kinase
$MgSO_4$	Magnesium Sulfate
MGV	Mean Grey Value
mM	Millimolar
MRI	Magnetic Resonance Imaging
mTBI	Mild Traumatic Brain Injury
Na_2HPO_4	Disodium Hydrogen Phosphate
NaCl	Sodium Chloride
NCBI	National Center for Biotechnology Information

NFL	National Football League
NIH	National Institute of Health
NMDA	N-methyl-D-aspartic acid
NSE	Neuronal Specific Enolase
OEF	Operation Enduring Freedom
OIF	Operation Iraqi Freedom
PAGE	Polyacrylamide Gel Electrophoresis
PBS	Phosphate Buffered Saline
PCL	PTSD Checklist
PDZ	*P*ost Synaptic Density Protein (PSD95), Drosophila *D*isc Large Tumor Suppressor (Dlg1), *Z*onula Occludens-1 Protein (zo-1)
PFA	Paraformaldehyde
PSD93	Post Synaptic Density protein 93
PSD95	Post Synaptic Density Protein 95
psi	Pound Per Square Inch
PTSD	Post Traumatic Stress Disorder
PVDF	Polyvinylidene Fluoride
RNA	Ribonucleic Acid
RNP	Ribonucleoprotein
ROI	Region of Interest
SAC	Standardized Assessment of Concussion
SAP97	Synapse Associated Protein 97

SDS	Sodium Dodecyl Sufate
SEM	Standard Error of the Mean
SH3	SRC Homology 3
siRNA	Short Interfering RNA
SR	Stokes Radius
SSC	Saline-Sodium Citrate
TBI	Traumatic Brain Injury
TBST	Tris-Buffered Saline and Tween 20
TUNEL	Terminal Deoxynucleotidyl Transferase dUTP Nick End Labeling
WHO	World Health Organization

CHAPTER 1

INTRODUCTION

1.1 Shockwave definition

The original goal of this work was to develop an experimental model to test the biological effects of shockwaves on neuronal cells. A shockwave is a moving disturbance resulting from rapid expansion of a substance and the subsequent compression of the surrounding medium. The rapid expansion of a substance associated with a shockwave is most often the result of an explosion, the near instantaneous conversion of a solid or liquid into a gaseous state. After the explosion the gas initially occupies the same volume as it did when a solid or liquid, but is now under extremely high pressure. As the gaseous matter expands, it pushes the medium around it, compressing the it and driving it outwards creating a wave of high pressure (overpressure) followed by a wave of low pressure (underpressure). The resulting shockwave (also known as a blastwave when the result of an explosion) travels outward in all directions from the center of the explosion. In ideal conditions, a shockwave (or blastwave) can be described as a Friedlander Wave Form, rapidly reaching a distinct maximum overpressure followed by a lesser magnitude underpressure with both ascension and decline occurring in smooth distinct phases (Figure 1.1).

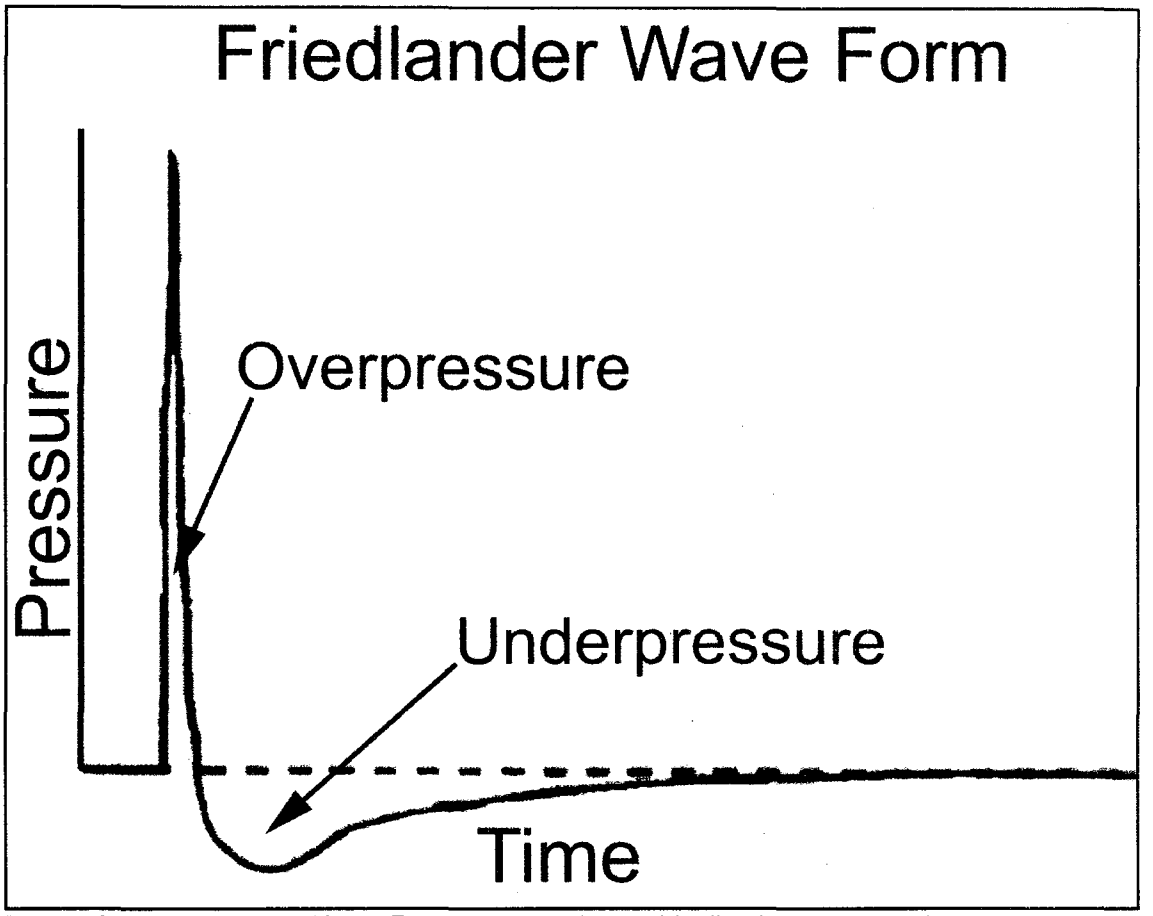

Figure 1.1: A Friedlander Wave Form, representing an idealized shockwave. Any pressure change which reaches its maximum overpressure in less than 0.3 msec is generally defined as a shockwave. The overpressure phase is followed by a smaller magnitude, longer lasting, negative pressure, the underpressure phase.

However, even under the most controlled laboratory conditions measurements of shockwaves rarely produce smooth, ascending and descending pressure profiles, but more often a large initial peak followed by a series of smaller peaks (Figure 1.2). The pressure vs time profile of an actual explosion may not seem to resemble the smooth ascension and decline of a Friedlander Wave Form, but the important and defining characteristic of a shockwave is the rapid initial rise to the peak overpressure, which should occur in less than 0.3 msec to be considered a true shockwave (de Candole, 1967).

The overpressures generated by shockwaves are often measured in kilopascals (metric, kpa) or pounds per square inch (English, psi).

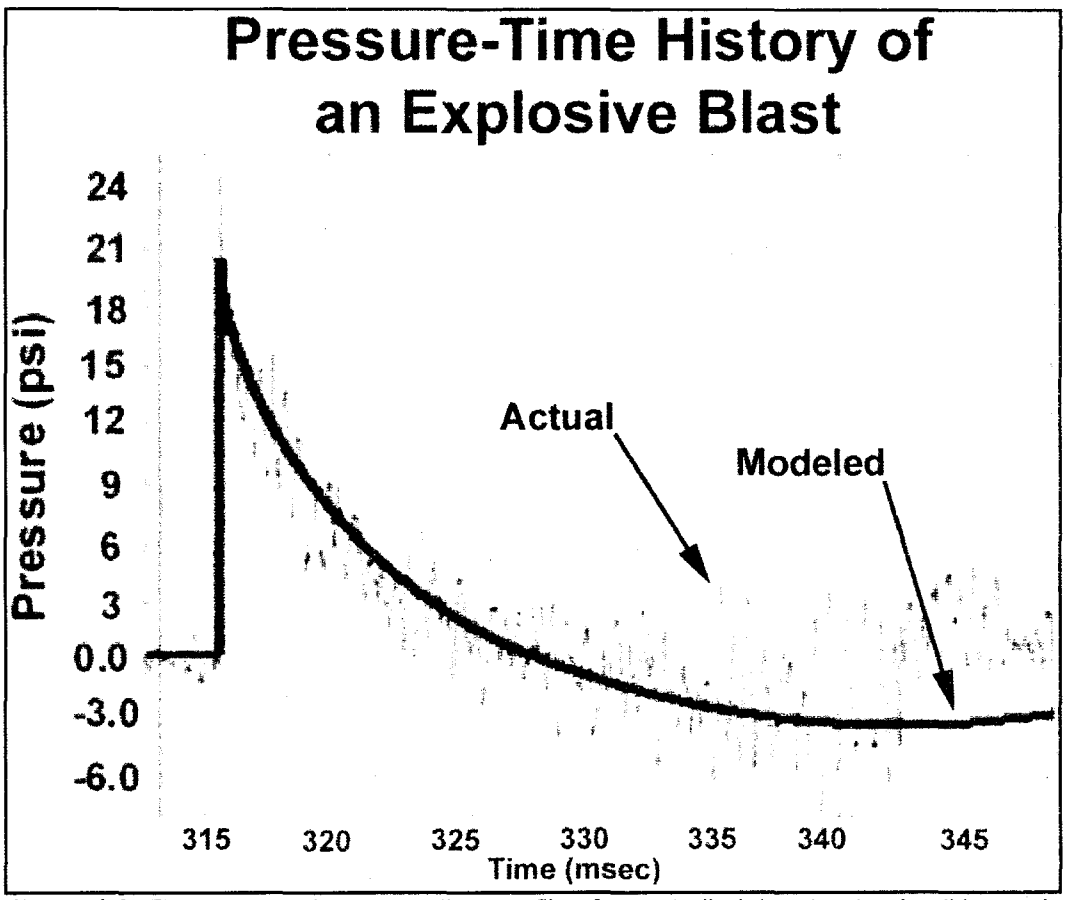

Figure 1.2: The measured pressure-time profile of a controlled, 'moderate-sized' improvised explosive device (IED) explosion in a laboratory setting with an overlaid modeled Friedlander Wave Form (solid line). These recordings were measured 15 feet from the source of detonation and are in pounds per square inch (psi). Note the almost instantaneous rise to peak overpressure marking this as a shockwave. The actual pressure-time profile shows many smaller peaks as the shockwave passes the sensor, common for complex explosive blasts. Bauman *et al* Journal of Neurotrauma 2009.

The modeling of shockwaves as they move through and interact with an environment is an extremely complicated endeavor. Similar to how dropping a stone into a calm, smooth pool causes ripples to expand outward, an explosion causes shockwaves to propagate out from the point of detonation. When the ripple in the pool meets an object of greater density than the water it is traveling

through, for instance the wall of the pool, the ripple bounces back and begins interacting with other ripples, sometimes creating bigger ripples (positive interference), sometimes smaller (negative interference). These types of positive and negative interactions are true of shockwaves as well (Elsayed, 1997, Wightman and Gladish, 2001). When a shockwave traveling through air meets an object that is not dense enough to bounce the wave, it travels through the object, imparting some of its energy to the object. Rarely are real life environments uniform in pressure before an explosion. To use the stone and pool analogy, instead of a calm smooth pool, a stone is dropped into a turbulent pool with some pre-existing waves, making the path of the ripples harder to predict and measure. Further complicating predictions are the multiple, non-uniform surfaces found in real life environments, which further disrupt the wave pattern. Predicting the pressure for any space at any given time during an explosion quickly becomes extremely difficult to reliably model computationally. The reflections and interactions of the traveling shockwave are responsible for the complex profiles recorded during actual explosions. The result of all of these factors is that two individuals standing side by side, equidistant from the epicenter of an explosion, can experience very different peak overpressures as a result of that explosion.

1.2 History of blast injury

Explosions, and by association shockwaves, have been utilized by humans for their destructive power for hundreds of years. The powerful effects of shockwaves on living tissue have been scientifically observed over the last several decades and have gained particular attention in the theater of war. Early accounts from World War I document the lethal damage shockwaves can cause to the human body both externally and internally. Today, the damage caused by an explosion is categorized into one of four distinct groups; quaternary or miscellaneous effects which are injuries due to burns, asphyxia, radiation or poison; tertiary effects which are injuries sustained as a result of the victim being propelled by the blast; secondary effects which are injuries due to shrapnel either from the explosive device itself or surrounding material subsequently accelerated due to the shockwave; and primary damage is any injury resulting from the shockwave itself (de Candole, 1967, Mayorga, 1997, Ritenour and Baskin, 2008). Research into the primary effects of blast damage has generally been limited to the hollow organs of the body. It is only in the last ten years that research has begun to focus on the subtle effects of primary blast damage on the brain. This is, in part, due to the triage treatment that secondary, tertiary and quaternary effects receive immediately after an explosion, since damage inflicted by them is physically apparent. In addition, advancements in body armor for soldiers and vehicles and greater access to advanced trauma centers close to the battlefield have resulted in increased survival rates for victims of primary blast exposure

that otherwise would have been fatal (Sayer et al., 2008). Taken together, these advancements in protection and treatment have decreased the lethal occurrences of secondary, tertiary and quaternary affects allowing symptoms of primary effects to come to light.

The other major factor leading to the increased interest in the primary effects of shockwaves is the increased use of Improvised Explosive Devices (IEDs) in the wars in Iraq and Afghanistan. Injuries from explosive devices account for the majority of injuries and fatalities in modern warfare. A study conducted between 2001 and 2004 found that 88% of soldiers treated at military hospitals in Iraq had been injured in some type of explosion from either IEDs or mines and 47% of those treated sustained a head injury (Murray et al., 2005). A similar study following one Marine unit in Iraq during 2002 found that 97% of the injuries sustained in combat were due to explosive devices and 53% of those involved a head injury (Gondusky and Reiter, 2005). In 2005, the U.S. military reported almost eleven thousand IED attacks, an average of thirty per day (Xydakis et al., 2007). A study conducted on all medical evacuations in Operation Enduring Freedom (OEF) and Operation Iraqi Freedom (OIF) in 2006 report that almost 2/3 of medical evacuations were due to injuries from explosions ((AMEDD), 2006). The increased use of explosives has created a situation where blast injury has become the 'signature injury' in modern warfare (Tanielian and Jaycox, 2008).

A shockwave is rated by lethality based on the damage it is capable of inflicting to the major organs in the body. The lethality of explosions first gained attention during the trench warfare of World War I when soldiers would be found dead with no apparent physical injury (Mott, 1917, Hooker, 1924). It was nearly thirty years before the mechanism of lethality for shockwaves was determined. The first attempts to categorize explosions and the damage they cause took place in the early 1960's, and were primarily focused on the shockwaves generated from nuclear explosions (White et al., 1961, White et al., 1965). First used in 1950, the term 'blast lung' was the result of the shockwave shearing the alveolar interface with the lung capillaries causing the victim to asphyxiate (Clemedson and Granstom, 1950). Lung damage remained the primary concern with blasts followed by bowel perforation, tympanic membrane rupture and ocular dislocation (White et al., 1961, White et al., 1965, Elsayed, 1997, Mayorga, 1997). The majority of these kinds of injuries involved gas filled organs containing air-tissue interfaces where the shockwave could impart a great deal of energy to the body due to the differential density at these sites. All of these injuries were associated with recognizable physical trauma internally and almost always externally as well.

In addition to physical damage, blast exposure often causes emotional damage as well. In World War I, when casualties due to explosions were on the rise, another seemingly blast-related injury was being observed and was termed 'shell shock'. Shell shock described a general set of emotional and psychological

maladies that could manifest after blast exposure, but without apparent physical injury. Victims of shell shock experienced ringing of the ears (tinnitus), hypersensitivity to noise, memory loss, headache, attention problems and tremors. Most importantly, shell shock victims were slow to recover, with many being discharged from service because of their condition. At this time shell shock was considered a physiological injury, though without clear pathology (Jones et al., 2007, Alexander, 2010).

By 1916 the British Armed Forces were stretched thin, and even with the employment of steel helmets, a significant number of troops were being disabled due to shell shock. By the end of 1917, it was reported that shell shock was responsible for one third of all British discharges if wounds were excluded, over 32,000 pensions for shell shock were awarded by the British government (Mitchell, 1931). The debate over diagnosis (physiological vs. psychological) and the resulting treatment regiment was never resolved and became so heated that by 1917 a British doctor was denied permission to publish a paper on shell shock in the British Medical Journal because of a media blackout on the subject issued by the government (Jones et al., 2007). A new definition for the symptoms was adopted to hasten the return of soldiers to the front lines. Instead of being classified as having received a battle related injury, and thus, become ineligible to return to combat, soldiers were diagnosed with a psychological disorder, such as 'nervous anxiety', which would allow them to return to active duty (Jones et al., 2007).

By World War II the British had officially banned the term shell shock in favor of a number of different diagnoses including 'post-trauma concussion state', 'posttraumatic psychoneurotic state' and the most ubiquitous, 'post concussion syndrome'. All these terms were used to describe any continuing symptoms involving disorder of consciousness without obvious physical trauma, with the most notable symptoms being tinnitus, headache, memory impairment, poor concentration and nervousness (Jones et al., 2007). Again, there was debate as to whether or not post concussion syndrome, and its ilk, were the result of a physiological or psychological trauma.

The issue of the nature and extent of injuries imparted by explosions is once again at the forefront of military, scientific and political thought. After almost a century of experience with the physiological and psychological effects of blasts, there has been surprisingly little progress made in discovering the mechanism by which shockwaves might damage the brain. It has become accepted that high magnitude blasts are capable of causing neurological impairment in the form of Traumatic Brain Injury (TBI) because damage in the form of intracranial contusions and hemorrhages can be seen with imaging technology (Taber et al., 2006, Warden, 2006). The debate currently centers on the minimum overpressure required for mild traumatic brain damage (mTBI), a current term defining a set of mental and emotional symptoms similar to shell shock. Both shell shock and mTBI are most often present without apparent physiological damage. The extremely high incidences of blast exposure and resulting brain

injury have led mTBI to be dubbed the 'invisible wound' of the Wars (Tanielian et al., 2008).

1.3 A perspective of damage

Medical treatments for damage from shockwaves have traditionally focused on the secondary blast effects, such as shrapnel penetration or the blunt trauma of tertiary effects as well as the range of quaternary effects (burns, radiation poisoning, etc). Primary effects of shockwaves, when considered, concentrated on the hollow organs, such as the lungs, the bowels and the ears. The hollow organs are particularly susceptible to damage due to the decreased density of air compared to biological tissue and cells. The effect of a shockwave leaving the tissue and moving into the air in the hollow organ is similar to a flag flapping in the wind; the distal edge from the pole always moves more vigorously than the edge anchored to the flag pole and well-worn flags show the most wear at the free-flapping edge. The damage a shockwave causes when it leaves the tissue and enters the cavity is called cavitation. Cavitation is a process which is similar to boiling, creating small bubbles at the interface of air and tissue which burst, and sends tissue fragments out into air filled cavities. The leading causes of death from primary blast effects are massive internal blood loss (hemorrhage) or embolism (de Candole, 1967, Elsayed, 1997, Mayorga, 1997, Wightman and Gladish, 2001, Ritenour and Baskin, 2008).

As mentioned earlier, blast lung is the most common primary effect fatality of explosions for initial survivors. Historical accounts suggest that it was first characterized in 1915 by Swiss researcher Franchino Rusca, who began experimenting with blast overpressure on rabbits after the examination of three soldiers, killed by a grenade, but had no apparent external injuries. His research with rabbits concluded that the force of the explosion had the capacity to kill without leaving any apparent external wounds (Jones et al., 2007). Extensive study of blast overpressures in the 1950s concluded that most fatalities lacking obvious external injuries were the result of blast lung (Clemedson and Granstom, 1950, White et al., 1961, White et al., 1965). An overpressure in the 40-75 psi can be lethal by causing blast lung in the victim (Mahoney PF, 2004).

Primary blast damage to the intestinal tract is uncommon with air based explosions, but often occurs in underwater explosions (Leibovici et al., 1996). The increased density of water compared to air leads to increased damage when it is compressed by the explosion and then expands (Mayorga, 1997). The damage inflicted to the intestinal tract often includes hemorrhaging and/or rupture of the bowel. Intestinal damage is rarely found in the absence of other primary blast damage particularly damage to the ear (Mayorga, 1997, Ritenour and Baskin, 2008) .

The ear is also extremely sensitive to changes in pressure. The ear senses and transfers pressure changes in the environment to the inner ear

where those pressure changes are converted to nerve impulses and sent to the brain for interpretation. It takes as little as 5 psi to rupture the tympanic membrane of the ear. Aural injury is often used as an indicator of other possible primary blast injuries, though the connection continues to be debated (Leibovici, 1991, Leibovici et al., 1996). Its link to blast lung is tenuous at best, with one study finding only 29% connection between tympanic membrane ruptures and blast lung (Leibovici, 1991, Mellor, 1992). Tympanic membrane rupture has, however, been linked with high significance to loss of consciousness from an explosion. A study conducted in 2005 by the US Military on blast victims in Iraq found that victims with tympanic membrane perforation were 2.76 times more likely to have also suffered a loss of consciousness with the injury, though they did not link loss of consciousness to any specific grade of TBI (Xydakis et al., 2007).

Lethal primary blast damage to the solid organs, including the brain, was thought to be minimal and generally not considered in the presence of more apparent damage to the lungs or ears (de Candole, 1967, Elsayed, 1997, Mayorga, 1997). Primary blast-induced brain injury (TBI) was often linked to skull fracture, severe cerebral hemorrhage and contusion to the brain with an extremely high mortality rate. One study conducted over 12 years on terrorist bombings found that head/skull trauma accounted for 6% of injuries and of those with head injuries, the overwhelming majority died within 24 hours (Bellamy et al., 1991).

As our ability to image the brain and subsequent damage increased, the threshold of detecting blast-induced brain trauma decreased and non-lethal blast-induced brain injury became more common (Murthy et al., 1979). The most common brain injury resulting from blast exposure is mTBI, sometimes referred to as concussion. It has been estimated that almost 400,000 US soldiers have suffered a mTBI between 2001 to 2007 (Tanielian et al., 2008). As currently defined by the US military, a mTBI is a physiological condition that is the result of either blast or blunt trauma to the brain resulting in an alteration in mental status with some or all of the following symptoms: headache, nausea, vomiting, dizziness/balance problems, fatigue, insomnia/sleep disturbances, drowsiness, sensitivity to light/noise, blurred vision, difficulty remembering or difficulty concentrating (Helmick, 2006). This definition is the result of combining a number of established definitions from various organizations, such as the American College of Rehabilitation Medicine (ACRAM), the National Athletic Trainers' Association, the Centers for Disease Control and Prevention (CDC) and the World Health Organization (WHO) (CDC, 2003, Guskiewicz et al., 2004, von Holst and Cassidy, 2004, Hart et al., 2006).

None of the definitions of mTBI from any of the above organizations include the presence of any abnormality by any type of medical imagining technique. In fact, many of the definitions specify the lack of diagnostic imaging as a characteristic of mTBI (Bruns and Jagoda, 2009). Currently all mTBI diagnostic techniques rely on patient relayed information and historical

information of the incident. The Military Acute Concussion Evaluation (MACE) is the currently employed field test for mTBI and concussion that is administered immediately following an event that could cause head injury. The MACE field manual lists a number of events after which the MACE should be administered, including being within 50 meters of an explosion. The MACE consists of a series of simple questions which can be answered within 5 minutes and is designed to test orientation, immediate memory, concentration and delayed recall. The speed with which an individual answers, as well as the accuracy of their answers, are taken into account for the diagnosis (DVBIC, 2006). The MACE is based on the Standardized Assessment of Concussion (SAC), the most widely employed diagnostic in athletics which has been shown to be accurate in detecting mTBI immediately after injury in 84-100% of cases (McCrea et al., 1998, Van Kampen et al., 2006). The effectiveness of the MACE decreases with time after the injury occurred, becoming much less effective if administered more than 12 hours post-injury (Coldren et al., 2010). However, there is evidence to suggest that patient-response driven diagnostic tests can be inaccurate leading to many attempts to incorporate a more rigorous methodology or brain imaging technique into the diagnosis of mTBI (Lovell, 2002).

The military recently developed a computer aided neuropsychological exam called the Immediate Post-Concussion Assessment and Cognitive Testing exam (ImPACT) which has demonstrated a significant sensitivity increase over the standard MACE protocol in diagnosing mTBI (Schatz et al., 2006, Van

Kampen et al., 2006). Computer aided exams such as ImPACT rely on a series of questions and simple memory tests to evaluate a subject's performance. One benefit of computer based exams is large test banks of sample questions which minimize "practice effects", from subjects memorizing test questions. In addition, the time to respond is calculated to the 1/100 second and does not vary between questions, as can happen with a human examiner. Finally, the most powerful benefit to computer based exams is the pre-deployment testing done to establish 'baseline' readings for each individual. The ImPACT protocol can be completed in less than 20 minutes, and the data is easily accessible (Schatz et al., 2006). While the use of computer-aided neurocognitive tests greatly increases our ability to diagnose mTBI, it does not increase our understanding of the pathology of the disease.

With increasingly sensitive imaging technology it has been conclusively shown in humans that high overpressure shockwaves damage the brain. This damage can be seen with Computer Aided Tomography (CAT, CT) scans as intracranial lesions or hemorrhages and is generally identified as moderate to severe TBI. Only a very small fraction (>15%) of patients suffering a mTBI have positive CT scans (Schwartz et al., 2008, Bruns and Jagoda, 2009). It has also been noted that initial CT scans may give negative results, but within 48 hours additional scans can show damage, suggesting blast-induced brain injury is not a discrete temporal event (Bochicchio et al., 2008).

Magnetic resonance imaging (MRI) is a more sensitive scanning technique than CT, but there is no currently published research on its effectiveness in detecting intracranial lesions in cases of blast-induced mTBI. Certain types of MRI have shown limited trial success in evaluating blast-induced mTBI. Functional MRI (fMRI) coupled with Blood Oxygen Level-Dependent (BOLD) computer analysis is capable of creating a macroscopic (in the order of millimeters) view of the activity of neurons in the brain (Kim et al., 2004). This analysis is based on the ratio of oxygenated to deoxygenated hemoglobin, which can be detected in a magnetic field. When cerebral blood volume, cerebral metabolic rate of oxygen and the cerebral blood flow are taken into account a local change in neuronal activity can be detected (Jantzen, 2010). Thus, more work is required to determine if MRI can be optimized to diagnose mTBI reliably.

Diffusion Tensor Imaging (DTI) is another new MRI technique which has shown some limited initial success diagnosing blast-induced mTBI (Huang et al., 2009). DTI utilizes the diffusion of water through the white mater of the brain to create extremely detailed three dimensional maps of bundles of axons (Levin et al., 2010). DTI can show subtle damage to the axons of neurons in the brain, called Diffuse Axonal Injury (DAI). The major downfall of the current imaging techniques is our lack of understanding of the mechanism of injury; we simply do not know what to look for.

There have also been recent discoveries of certain serum biomarkers in moderate and severe TBI. The glial cytoplasmic protein S100β and neuronal cytoplasmic protein Neuronal Specific Enolase (NSE) have been found to increase in the blood and spinal fluid after head trauma, though changes are only detectable within 6 hours post-injury (Bruns and Jagoda, 2009). Their use in diagnosing mild TBI has so far been unsuccessful.

The ability to conclusively diagnose a moderate to severe TBI based on diagnostic testing has greatly aided the treatment of the condition. Diagnosis of mild TBI, which accounts for half of all TBI reported from Iraq and Afghanistan, is improving though the etiology of mTBI remains unclear (Warden, 2006).

1.4 Differences between shockwave-induced TBI and non-shockwave induced TBI

The awareness of mild traumatic brain injury (concussion) by the public has risen dramatically due to increased attention from the media in the last 10 years. Thanks to a joint effort from the government and many different sporting leagues, notably the National Football League (NFL), to raise public awareness about the adverse effects of head trauma, there is a wide range of diagnostic information available on blunt force mTBI. The vast majority of information on mTBI comes from civilian traumas, with most injuries almost exclusively resulting from blunt trauma induced concussion (Bruns and Jagoda, 2009). In 2003 the CDC reported to Congress on the prevalence and dangers of civilian mTBI,

noting that there are over 1 million cases of civilian mTBI every year (CDC, 2003). All of the diagnostic techniques and treatment protocols employed by the military are adaptations of these civilian-developed protocols. The most significant change to the civilian protocols was the inclusion of 'blast' as a possible cause of mTBI (the MACE vs the SAC).

Many of the diagnostic imaging techniques (CT, MRI, fMRI, DTI) were first tested on civilian blunt trauma mTBI with success. One of the major drawbacks in their use for blast-induced mTBI is that the equipment necessary for the exam is not available in field hospitals. Most of the civilian cases were evaluated immediately following injury, a luxury not available to a soldier in the field.

There is great overlap between blunt force-induced mTBI and blast-induced mTBI, but due to the lack of information regarding the mechanism by which shockwaves injury the brain it has become recommended that these two injuries be treated as separate entities (Hoffer et al., 2009, Sponheim et al., 2011). Data on the recovery periods of blunt force induced mTBI and blast-induced mTBI seem to bear out the idea that different pathologies are at work. The majority (98%) of blunt force-induced mTBI symptoms are resolved within 1 year of the injury while up to 55% of blast-induced mTBI still have persistent symptoms 1 year after injury (Cernak et al., 1999, Cernak et al., 2001, Schretlen and Shapiro, 2003, Faux and Sheedy, 2008, Lew et al., 2009, Sponheim et al., 2011).

1.5 Post Traumatic Stress Disorder (PTSD) and the overlap with mTBI

Post Traumatic Stress Disorder (PTSD) was officially defined by the American Psychiatry Association in 1980 and included in the 3rd edition of Diagnostic and Statistical Manual of Mental Disorders (DSM-III) and listed with other Anxiety disorders. Its inclusion brought a fundamental change in thinking about the cause of an anxiety disorder, namely an external trauma rather than an internal weakness. A point of concern for the diagnosis of PTSD is the reliance on the recollection of the patient to provide the necessary criteria. In order to standardize the diagnostic process two established and reliable methods are currently used, the Clinician-Administered PTSD Scale (CAPS) and the self-reported PTSD Checklist (PCL). The CAPS has the advantage of a trained professional conducting the interview while the PCL can be broadly distributed to a large group of individuals. Both methods are based on the symptomology of PTSD in the DSM-IV-TR and rely on truthful answers from the patient.

The DSM-IV-TR (4th edition Text Revisions) was released in 2000, and contains the current definition and diagnostics of PTSD. There are three main categories of symptoms which must be present in order to be diagnosed with PTSD, in addition to other specific criteria. The first category is classified as re-experiencing: it includes recollections of the event that are both intrusive and reoccurring, reoccurring distressful dreams, any flashback, hallucination or illusion of the event, any exposure to any aspect of the event triggers intense

psychological distress and any physiological reaction to any aspect of the event. The second category is avoidance and numbing: it includes avoiding thoughts or feelings of the event including not speaking about it, avoiding persons/places/things involved with the event, failure to recall important facts concerning the event, marked disinterest in significant activities, feelings of detachment and alienation, changes in the range of affect and finally feelings of having no real future. The final category is increased arousal, and includes difficulty falling or staying asleep, irritability or outbursts of anger, problems concentrating, hyper-vigilance and finally an increased startle response. In order to be diagnosed with PTSD an individual must present with at least 1 symptom of re-experiencing, 3 symptoms of avoidance/numbing and 2 symptoms of increased arousal. Further, the trauma experienced must have been physical in nature, with either actual or threatened imminent violence to either the individual or others with the individual. The individual's response must have involved intense fear, helplessness or horror. The symptoms being experienced must persist beyond 30 days. Finally, the symptoms must significantly alter the functioning of the individual compared to pre-trauma. If all of the criteria are not met a diagnosis if PTSD cannot be made, instead a more general Acute Stress Disorder is often diagnosed (American Psychiatric Association., 2000). It should be noted, an individual can be diagnosed with PTSD without having suffered any physical injury, in contrast to a diagnosis of mTBI which requires a physical trauma.

A great deal of effort has been made to quantify the number of people with PTSD. A very comprehensive survey conducted in 2001-2002 called the National Comorbidity Survey-Replication interviewed ten thousand civilian volunteers. A standardized, fully structured diagnostic interview was conducted by trained lay-persons and all data was scored by computer. It was found that, among the general U.S. population, (over 18 years old) 6.8% of people have had PTSD in their lifetime (Kessler et al., 2005). It should not be surprising that the prevalence of PTSD among veterans and active duty soldiers is much higher given the increased threat of physical violence they face. Many studies have been conducted to quantitate the frequency of PTSD in soldiers and the general findings shows approximately 15% of current soldiers have had PTSD (Tanielian and Jaycox, 2008, Schnurr et al., 2010). There has been a dramatic increase in the number of PTSD diagnoses over the past 10 years. A study by Kang and Hyams (2005) quantitated the responses of almost fifty thousand active duty soldiers or recent veterans between 2003 to 2005 and found that PTSD diagnoses increased from 3% to 10% (Kang and Hyams, 2005). A similar study conducted between 2001 to 2008 used survey answers from almost three hundred thousand soldiers and found an increase in the diagnosis of PTSD from 0.2% to 21.8% (Seal et al., 2009).

There is a significant overlap in the diagnosis of PTSD with mTBI. A recently conducted survey of Veterans from OEF and OIF found that 81% Veterans diagnosed with PTSD also had suffered a mild TBI (Schneiderman et

al., 2008). A similar study found that 71.2% of soldiers diagnosed with PTSD had also suffered a mTBI (Hoge et al., 2008). As the diagnosis of PTSD has seen a dramatic increase so too has the diagnosis of mTBI. The diagnosis of mTBI has continually increased since 2002, but saw a nearly 200% jump when the Department of Defense (DOD) issued the Policy on Theater Screening and Management of Mild Traumatic Brain Injury (Concussion) Clinical Practice Guideline (CPG) in 2007 (Helmick, 2006). By 2009, almost 45% of all military injuries were classified as mTBI compared to less than 10% from 2002 to 2005 (Hettich et al., 2010). It became the goal of a great many researchers to clarify what, if any, boundaries exist between these two pathologies.

1.6 Summary of major questions in the field

Currently the question as to whether or not blunt force induced mTBI and blast-induced mTBI constitute similar pathologies and thus similar treatment courses is highly debated. There have been a number of different studies with opposite conclusions, but the majority of findings seem to point to a different pathology for blast-induced mTBI from blunt force induced mTBI (Lippa et al., 2010, Risling, 2010, Rosenfeld and Ford, 2010).

Another major need in the field of mTBI is a reliable diagnostic test both immediately in the field and later in a medical facility. There is evidence to suggest that the current field protocol used by the military, the MACE, is ineffective if administered more than 12 hours after blast exposure. The growing

use of computer aided neuropsychological tests (ImPACT) offers great sensitivity, but must rely on previously collected baseline readings for comparison. There is some promise with new, specific MRI techniques, but the resources required to equipment field hospitals with the technology are not available.

Differentiating between PTSD and mTBI for blast victims, if it is even possible, is another area of debate. Many different studies of soldiers suffering PTSD have found a high likelihood of mTBI as well. Animal models suggest the two conditions are linked and that PTSD exacerbates mTBI.

Finally, there is the question that was first asked by doctors during World War I, how do shockwaves specifically damage the brain? There has been a great deal of research with animal models attempting to mimic mTBI and the imaging of humans previously diagnosed with mTBI, but no clear pathology has yet been found.

A number of recent studies have attempted to discover the mechanism of shockwave damage to the brain through the use of animal models. Most of these studies use rats or mice and expose them to shockwaves generated from a shock-tube or a small explosion. Much like the early studies conducted in the 1960s to discern the lethality limits of primary blast effects these current studies must rely on body weight correlations in order to extrapolate their findings to humans (White et al., 1961). A major difference between the current studies and

the first attempts at quantitating primary blastwave effects is the nature of the damage being measured. Early studies focused on mortality and gross physical damage, things easily recognized and measured. By its very definition, mTBI is not detectable with any current scanning technology. Also complicating such studies is the complex nature of shockwaves and how they interact with the environment and one another. All this creates a scenario where the pathology being studied cannot be detected and the force necessary to create the pathology is unknown. In an effort to solve these problems researchers have been using lower magnitude peak overpressure shockwaves and looking for increasingly subtle behavioral changes and tissue damage.

In an attempt to replicate the cognitive impairment associated with mTBI researchers have devised a variety of behavioral tests including, the rotametric test, the forelimb grip-strength test, the acoustic startle response, the Morris water maze and other similar choice/movement tests (Moochhala et al., 2004, Bauman et al., 2009, Readnower et al., 2010, Saljo et al., 2010, Saljo et al., 2011). After conducting behavioral assays researchers sacrifice animals and look for damage to the neurons and glia in the brain. The majority of these behavioral studies of blast-induced brain injury have used rat models and peak overpressures below 40 psi and have found no evidence of mass apoptosis, necrosis or gross morphological changes to neurons in the brain (Park et al., 2011, Pun et al., 2011, Risling et al., 2011). Based on these studies as well as

MRIs of blast victims, it is believed that cell death does not play a significant role in the pathology of mTBI.

A number of different changes have been discovered in the brains of animals subjected to lower overpressure shockwaves. One study conducted on rats using an explosively generated blastwave recorded peak overpressures of 2.9 psi and detected evidence of axonal degeneration by Nissl staining along with some apoptosis (Moochhala et al., 2004). The administration of aminoguanidine, a known inhibitor of Inducible Nitric Oxide Synthatse (iNOS) either before or after blast exposure alleviated the cognitive impairment and reduced the number of degenerating and apoptotic neurons (Moochhala et al., 2004). Another study using rats exposed to peak overpressures from 1.45 to 4.35 psi generated in a Nitrogen driven shock-tube found cognitive impairment at both pressures in the Morris water maze test 2 days after exposure (Saljo et al., 2010). This impairment was alleviated or prevented by feeding the rats processed cereal which is known to have anti-inflammatory effects (Saljo et al., 2010).

1.7 Rationale for the cell culture technique

In an attempt to gain insight into the pathology of mTBI we proposed to reduce the complexity of brain tissue and employ a simple experimental system for exposing primary neuronal cell cultures to a controlled source of shockwaves. By using primary cell culture we wanted to examine the effects of shockwaves on

neurons both morphologically and biochemically. In this way we hoped to discover, what, if any, effects shockwaves may have on neurons directly.

CHAPTER 2

MATERIALS AND METHODS

2.1 Primary neuronal cultures

Primary hippocampal and cortical neuronal cultures were prepared by the Man Lab (Boston University) from embryonic day 18 rat embryos following a previously established method and plated at a density of $0.3x10^6$ cells per 60mm dish containing 5 cover slips (Man et al., 2000). Briefly, brain regions were dissected and digested with papain at 37C. Dissociated neurons were seeded on poly-L-lysine-coated coverslips and incubated at 37C in a humidified incubator with 5% CO_2. Cells were maintained in Neurobasal media (Invitrogen Cat # 2110304) supplemented with 2% B27, 1% horse serum, 1% penicillin/streptomycin and 0.4% L-glutamine for 2 weeks (14 days *in vitro* (DIV)) until use. After 1 week Fluorodeoxyuridine (FdU, 5μM) was added to the media to inhibit glial cell division. Media was changed every 72 hours for 2 weeks, at which time the cells were ready for shockwave-exposure.

2.2 Gene Gun pressure measurements

To determine applied pressure time histories delievered from the Helios Gene Gun (BioRad Cat # 165-2431), incident and reflected pressures were measured by Matthew Panzer, Garrett Woods and Dr. Cameron Bass of Duke University Biomedical Engineering, Durham, North Carolina. For reflected pressure, the Gene Gun was fixed rigidly to a stand with the Gene Gun spacer

positioned 2 cm above a flat plate constructed of delrin. A piezoresistive pressure sensor (Endevco Model 8530C) was mounted flush with the plate, coaxial with the center of the Gene Gun output, in the direction of the flow. Incident pressure was measured by mounting a piezoresistive pressure sensor 2 cm from the end of the Gene Gun spacer, perpendicular to the flow direction. The sleeve surrounded the Gene Gun spacer from the base of the gun to 3 cm from the end of the spacer and was open in the direction of the flow.

Gene Gun output was measured with helium input pressures of 50, 100, 150, 200, 300, 400, and 500 pounds per square inch (psi) for 9 tests for both reflected and incident pressure. To ensure repeatability, the Gene Gun was fired 3-4 times at each pressure before measurements were taken. Data were acquired using a multichannel signal conditioner (Vishay Model 2160) and LabVIEW (National Instruments). Incident pressure data was digitized at 500 kHz while stagnation pressure was digitized at 300 kHz. Data were post-filtered at 40 kHz using an 8-pole Butterworth filter. Acquired data were analyzed using MATLAB (Mathworks) to determine peak wave pressure and rise times from 20-80% of peak for incident pressures as well as reflected pressures and impulses.

2.3 Cell exposure to Gene Gun generated shockwaves

The Gene Gun was placed directly above the cells on a cover slip with the barrel guard placed 8-10 mm above the surface. The gun was discharged and

the media was immediately replaced back onto the cells such that the cells were uncovered for no more than 30 seconds.

2.4 Cell fixation

After shockwave-exposure the cells were cultured for an additional 24 or 48 hours. Prior to fixation cells were briefly washed in cold 1X Artificial Cerebral Spinal Fluid (ACSF ~750 μL) three times. Any removal or addition of liquid was done at the side of the well and not directly on any cover slip to avoid physically damaging cells. Cells were then fixed in a 4% PFA/sucrose solution (pH 7.4) for 10 minutes at room temperature.

2.5 Synaptic protein labeling by immunocytochemistry

After fixation cells were washed three times in cold 1X ACSF. Cells were then permeabilized with 500 μl of 0.3% TritonX100 in 1X Phosphate Buffered Saline (PBS) for 10 minutes at room temperature. Cells were then washed three times in cold 1X ACSF and blocked for 1hour at room temperature in 10% goat serum (in 1X PBS). Primary antibody was then added. For PSD95 a monoclonal antibody (Millipore Cat # AB9708) was used at a dilution of 1:2000, and incubation was carried out for 3 hours at 4C. For GluR1, a polyclonal antibody generated from the C-terminal fragment was used as previously described (Liao et al., 2001) at a 1:1000 dilution, and similar results were obtained with a commercially available version of the same antibody (Millipore Cat #AB1504). An anti-alpha tubulin monoclonal antibody (Sigma Cat # T9026) was used at a

1:3000 dilution and incubation was carried out for one hour at room temperature. Secondary antibodies (Invitrogen Cat # A11001 and A21422) were used at a 1:3000 dilution and incubations were carried out for one hour at room temperature. Cells were washed three times in cold 1X ACSF before the addition of secondary antibody as well as Hoescht stain (2μg/mL, Invitrogen Cat # 421491). Phalloidin actin staining (alexaFluor488 conjugated phalloidin, Invitrogen Cat # A12379) was also performed during the secondary antibody labeling. AlexaFluor488 conjugated phalloidin was diluted to 200units/mL, 5 units were added to the secondary stain, as per manufacturer's instructions. Cells were washed five times in cold 1X ACSF and then mounted for observation using Prolong Gold Antifade Reagent with 4',6-diamidino-2-phenylindole (DAPI) (Invitrogen Cat # P36930) and allowed to sit for at least 2 hours before imaging.

2.6 Fluorescent Imaging

2.6.1 Images were acquired using an inverted fluorescence Zeiss Axiovert 200M microscope with an AxioCam MRm camera and Axiovision software (Zeiss Imaging version 4.7.2.0 released 12-2008) and a 63x oil immersion objective (Zeiss Axiovert 200M). Cell exposure times were determined by the histogram saturation function making sure cells were within the dynamic range and not overexposed. Exposure times were kept constant for all samples within any given experiment.

2.6.2 Quantitation of synaptic staining was conducted using ImageJ (version 1.41K). First, neuronal processes were selected based solely on cytoskeletal (tubulin or actin) staining patterns from the green channel or the Differential Interference Contrast (DIC) image without examining the synaptic protein staining pattern whatsoever. All processes selected could be traced back to a cell body within the same field of view, and all segments analyzed were selected to be at least 30 microns long with as little background signal as possible. The process was then measured for length and a region of interest (ROI) was drawn around the segment using the Polygon tool with approximately 15 microns extra width on either side of the process. This ROI was then saved, and the synaptic markers (PSD95, GluR1 and Synapsin) were then analyzed. A threshold of 1500 (on a 4095 scale) was applied to the synaptic protein label channel, and the Analyze Particles function was used to count all particles in the ROI between 0.003-infinity square microns, as well as recording their mean grey value (MGV) and area. This information was imported into MS Excel and used to determine the number of particles per unit of length for that particular process. This was repeated at least 30 times with no more than 2 processes being chosen from any one field of view/image. The particles/micron measurements were then averaged and standardized to the 0 psi samples for plotting the resulting data.

2.7 Live cell labeling with Dextran-conjugated dyes

Briefly live 14DIV hippocampal neurons were subjected to shockwave-exposure as described above. After exposure fresh Neurobasal media was added containing a Dextran-conjugated Fluorescein. The 3 kilodalton (kDa), 40kDa, 70kDa and 500kDa Dextrans were conjugated to Fluorescein (Invitrogen Cat #; D3306, D1845, D1822, D7136). The 10kDa Dextran was conjugated to AlexaFluor546 (Invitrogen Cat # D22911). Dextrans were reconstituted in 1x PBS pH 7.5 at a concentration of 1mM. After shockwave-exposure, hippocampal neurons were incubated in media containing 10μM Dextran, similar to previous sonoporation studies (Khanna et al., 2006). Initial studies of Dextran cell loading after shockwave-exposure allowed 24 hours for dye penetration. Later it was determined that cell loading occurred within minutes of cell exposure and was reliably detectable 2-4 hours after exposure. Soma fluorescence was measured for at least 30 cells chosen based on DIC morphology and DAPI staining. The polygon tool in ImageJ was used to outline cell bodies in the DIC channel and that ROI was then applied to the Dextran fluorescence channel and pixel intensity was recorded. Recorded pixel intensities (Mean Grey Value, MGV) were exported to Microsoft Excel where values were averaged for each input pressure, standard deviations and standard error of the mean calculated. Values were converted to a percentage of the 0 psi input (set as 0% soma fluorescence). Cell recovery assays were conducted and analyzed in a similar manner described above with the addition that samples of shockwave-exposed cell cultures were

not immediately incubated with Dextran-conjugated dye. Cells were allowed to recover for 3-6 hours in Neurobasal media without Dextran before the Dextran-conjugated dye was introduced. After Dextran dye incubation, cells were washed, fixed and mounted as described above. Briefly, cells were washed in cold 1X ACSF 5 times to remove any Dextran not within the cells. Cells were then fixed in cold 4% paraformaldehyde (PFA) for 15 minutes and mounted using Prolong Gold Antifade reagent with DAPI (Invitrogen Cat # P36935). Cells were imaged on the inverted fluorescence microscope using the above described software and objective lens. Cells were selected based on DIC morphology; all cells had normal DAPI staining and processes determined to be connected to cell bodies. Dextran labeling was not viewed until after images were acquired. All images were acquired using identical exposure settings. Image analysis was conducted in a similar manner to that described above. Briefly, cell bodies were selected using the Polygon tool in ImageJ and MGV was measured for at least 30 cells in each experimental condition. Values were exported to Microsoft Excel where MGV of the soma for all cells under the same condition were averaged and standard deviation and standard error of the mean (SEM) were calculated. Data were displayed as averages with SEM error bars.

For the double labeling studies using synaptic proteins, cells underwent synaptic labeling as described above after 24 hours of Dextran loading followed by fixation. They were then mounted using Prolong Gold Antifade reagent containing DAPI (Invitrogen Cat # P36935). Cells were imaged using the inverted

fluorescence microscope and above described software and acquisition settings. Image collection was based on cell morphology as determined by DIC. All neurons selected had processes connected to visible cell bodies and normal DAPI staining. The histogram function was employed to insure no overexposure occurred and all input pressures were imaged using the same acquisition settings. Dextran labeling and synaptic protein labeling were not viewed until after images were acquired. Cell bodies were selected using the Polygon tool in ImageJ and MGV was measured for at least 30 cells from each experimental condition. At the same time two ROIs were selected using the Polygon tool along processes connected to the cell body by DIC imaging. The channel containing the synaptic protein being investigated then had the same ROIs applied to it. A threshold was set for the image and the number of puncta counted as described above. All images within an experiment had the same threshold applied. The length of the ROIs was then measured. All values were exported to Microsoft Excel, and the MGV of the soma for all cells under the same conditions were averaged and standard deviation and SEM were calculated. The average puncta/micron was calculated for each cell. Scatter plots of MGV vs Puncta/micron for all cells measured were created and a Pearson's linear regression analysis created a best fit line through the data points and displayed the correlation coefficient. Data were displayed as means with SEM error bars.

2.8 Preparation of extracts from whole cell and retinal cultures

After cells were incubated they were placed on ice, the media was removed and they were washed 3 times with cold 1X ACSF to remove any residual media. Cells were manually scraped from plates in 250μl of nonyl phenoxypolyethoxylethanol (NP40) lysis buffer with PhosSTOP phosphatase inhibitor cocktail (used according to manufacturer's instructions, Roche Cat # 04-906-837-001) and Complete Mini protease inhibitor cocktail (used according to manufacturer's instructions, Roche Cat # 04-693-124-001). The samples were then sonicated using a Branson Sonifier 150 with 3mm tip on power setting 2. Samples were sonicated 3 times for 10 seconds each, on ice with at least 30 seconds in between each sonication. Samples were then assayed for total protein using the bicinchoninic acid (BCA) assay and a Nanodrop 1000 spectrophotometer (used according to manufacturer's instructions, Thermo Fisher Cat #23225).

2.9 ATP quantification

Cells were subjected to shockwaves and then maintained for 6 hours to 5 days at 37C with regular media changes. Cell extracts were prepared as described above. An Invitrogen Adenosine Triphosphate (ATP) Determination Kit (Cat # A22066) was then used to quantitate total ATP levels of the extracts

derived from each culture. All samples and reagents were kept on ice prior to measurements. Aliquots were then taken in triplicate from each sample immediately following collection to which 200μl of the reaction solution (containing the D-luciferin and firefly luciferase) was added directly before being measured by a GloMax 20/20^{N} Luminometer (Turner BioSystems). ATP standards were used as positive controls. The data were recorded in Microsoft Excel and average light intensity, standard deviation and standard error of the mean were calculated for each sample.

2.9.1 Normalization to total protein levels Total protein levels were calculated using a Bicinchoninic Acid (BCA) total protein assay (Thermo Scientific Cat # 23227) and a Nanodrop 1000 spectrophotometer (Thermo Scientific Cat # ND1000). Bovine Serum Albumin (BSA) protein standards of known concentrations were diluted in the same cell lysis and collection buffer and used to create a standard curve, which in turn was used to calculate the total protein concentration of each experimental sample. Fresh protein standards were made for each experiment. All samples were normalized to the 0 psi control cultures from each experiment. Briefly, the ratio of the sample to the control was multiplied by the average ATP reading for the sample. Normalization of total ATP readings to total proteins is a standard practice when measuring total ATP (Chinopoulos et al., 2000, Ward et al., 2007, Weisova et al., 2009).

2.10 TUNEL assay of shockwave-exposed cultures

A terminal deoxynucleotidyl transferase dUTP nick end labeling (TUNEL) assay was used according to the manufacturer's instructions to assess cell survival after shockwave-exposure (Promega Cat # G7130). For comparison, a non-shockwave-exposed coverslip (0 psi) was fixed, permeabilized and incubated for 10 minutes at room temperature with 5-10units/mL of DNase I to artificially fragment the DNA (NEB Cat # M0303L). Cells were washed and labeled with the other experimental conditions. Cells were exposed to shockwaves as described above and incubated at 37C for 24 hours before being fixed in 4% PFA, as described above. Briefly, cells were permeabilized with 0.2% TritonX-100 in 1X PBS at room temperature for 5 minutes. Cells were then incubated in equilibration buffer for 10 minutes followed by 60 minutes of nicked end labeling by the Terminal Deoxynucleotidyl Transferase in a humidified 37C chamber. The reaction was halted by immersion in 2X saline-sodium citrate (SSC) for 15 minutes at room temperature. Cells were then washed 3 times in 1X PBS, blocked in 0.3% hydrogen peroxide for 5 minutes and washed 3 times in 1X PBS again. The cells were then incubated in a 1:500 of Streptavidin Horseradish peroxidase (HRP) for 30 minutes at room temperature. Cells were washed 3 times in 1X PBS and stained with freshly prepared diaminobenzidine (DAB) until a light brown background appeared. Cells were then washed in deionized water and mounted as described above. Shockwave-exposed cells were developed first and development was timed. All cells were developed for the same amount

of time to avoid overdevelopment and false positives due to prolonged development. Cells were imaged using an Olympus Provis AX70 fluorescent microscope and a 10X Olympus UPlanFl (0.30 Ph1) objective controlled by an Olympus U-MCB control panel. PictureFrame (version 2.3) software and a MicroFIRE camera (2.3A) were used to record images. DIC and DAPI images were recorded for all experimental conditions. Cells were counted using ImageJ software and the Cell Counter feature under Analysis. The brightness and contrast of the DNaseI-digested cells were manipulated to show the maximum signal. The same brightness and contrast settings were then applied to all images and positive cells were counted. To facilitate counting the total number of cells, DAPI staining was used to count cells for each image. Cell counts were then normalized to the 0 psi control. Data analysis was conducted in Microsoft Excel to determine average, standard deviation and standard error of the mean.

2.11 Western blotting

Western blotting was performed on harvested neuronal cells after exposure to shockwaves. Samples were thawed on ice and boiled for 10 minutes with 4x Laemmeli loading buffer plus 8% β-mercaptoethanol before being loaded onto SDS PAGE gels. Equal amounts of total protein (25-50 μg) were loaded into each well as determined by BCA total protein assay. 5μl of Precision Plus Protein Kaleidoscope ladder, range 10-250 kDa (BioRad Cat #161-0375EDU) was loaded for size comparisons. Gels were run at room temperature in 500mL of

Tris-HEPES-SDS running buffer (Thermo Fisher Cat # 28398) at 50 volts for 30 minutes followed by 60 minutes at 80 volts. Protein transfer occurred at 50 volts at room temperature for 2 hours in 1000mL of Tris-Glycine transfer buffer, pH 8 (Thermo Fisher Cat # 28380) with 15% methanol. Protein was transferred into Immobilon-FL low fluorescence PVDF membrane, pore size 0.45μm (Millipore Cat # IPFL00010). Transfer was assessed by visual confirmation of the entire ladder in the PVDF membrane. The membrane was washed in TBST, pH 7.4, and blocked in 2% nonfat pasteurized dry milk (Shaw's brand 4 lbs box) and 1% BSA for 1 hour at room temperature. After blocking, PVDF membranes were incubated with gentle agitation overnight at 4C or for 3 hours at room temperature, in primary antibody diluted in blocking solution, against the following synaptic proteins, PSD95 (Chemicon AB9708, 1:1000), SynapsinI (AbCam Ab8, 1:1000), GluR2 (NeuroMab Facility UC Davis/NIH clone L21/32, 1:1000), GluR2 phosphoS880 (AbCam Ab52180, 1:1000), Tau (AbCam Ab8763, 1:1000), Tau phosphoS396 (AbCam Ab32057, 1:500). Other synaptic proteins investigated include; αSynuclein (Millipore Cat #AB5038P, 1:1000), CAMII Kinase phosphoT305 (Millipore Cat # AB3865, 1:1000), CASK (NeuroMab Facility UC Davis/NIH clone 56A/50, 1:1000), GAP43 (Millipore Cat #AB5220, 1:500), GluR1 (Millipore Cat #AB1504, 1:1000), GluR1 phosphoS845 (AbCam Cat #Ab3901, 1:500), Grip1 (Millipore Cat # AB5547, 1:1000), Kinesin (Thermo Fisher Cat # MA1-19352, 1:500), Neurexin1b (NeuroMab Facility UC Davis/NIH clone N170A/1, 1:1000), Neuroligin1 (NeuroMab Facility UC Davis/NIH clone N97A/31,

1:1000), Neuronal Pentraxin2 (Millipore Cat #AB15520, 1:1000), Neuronal Specific Enolase (AbCam Ab16873, 1:1000), PSD93 (AbCam Cat # Ab2930, 1:1000), PSD95 phosphoS295 (Millipore Cat # 04-1065, 1:1000), S100β (AbCam Cat #Ab52642, 1:1000), SAP97 (AbCam Cat # Ab3437, 1:1000), Synapsinl phosphoS549 (Millipore Cat # AB9846, 1:1000), Synaptojanin (AbCam Cat # Ab19904, 1:1000) and Synaptophysin (AbCam Cat # Ab8049, 1:500).

As a loading control all blots were additionally probed for either αtubulin (AbCam Ab7291, 1:2000) or housekeeping gene eEFA1a (AbCam Ab37969). After primary antibody incubation, PVDF membranes were washed 3 times for 10 minutes each in TBST, pH 7.4. PVDF membranes were then incubated in the appropriated secondary antibody diluted in blocking buffer, either Cy5 conjugated Goat anti-mouse (Jackson Labs 115-175-003, 1:2000) or Cy5 conjugated Donkey anti-rabbit (Jackson Labs 711-175-152, 1:2000) for 1 hour at room temperature with shaking. They were then washed 3 times in TBST pH7.4 and air dried before imaging. Only samples initially harvested from the same rat and cultured together for preceding 2 weeks before shockwave-exposure were compared, ensuring that before shockwave-exposure treatment was identical.

Fluorescence in the PVDF membranes was imaged using a GE Healthcare Typhoon Trio flatbed scanner courtesy of Boston University Charles River Campus Biology Core. After image acquisition, protein levels were quantified using ImageJ software, Blot Analysis tool (NCBI). Relative band

intensities for all synaptic proteins assayed were calculated as follows: an initial measurement of pixel intensity was made for the control bands (either αTubulin or eEF1A1) of the 0 psi sample and the 250 psi sample, followed by pixel intensity values of the synaptic protein of interest. Any variation in the control bands was used to normalize pixel intensity values of the synaptic protein bands. Relative pixel intensity was then calculated as a fraction of the 0 psi control. All time points were repeated in triplicate and averages with standard deviation calculated using Microsoft Excel.

2.12 Rat retinal cultures

Rat retinas were harvested from adult *R. norvegicus* (Charles River Labs, Wilmington, MA) kept on a 12 hour light/dark cycles with free access to food and water. All animals were treated using protocols approved by the Boston University Charles River Campus Institutional Animal Care and Use Committee (IACUC). Animals were anesthetized using CO_2 before cervical separation. Briefly, the eyes were enucleated and the anterior chambers immediately removed on ice and placed in cold rodent balanced salt solution (BSS; 137mM NaCl, 5mM KCl, 2mM $CaCl_2$, 15mM D-glucose, 1mM $MgSO_4$, 1mM Na_2HPO_4, 10mM HEPES, pH 7.4). Retinas were then removed from enucleated eyecups and cultured in BSS. Dissected retinas were exposed to shockwaves similar to cultured neurons. Briefly, dissected retinas were placed in an empty well of a 6 well plate; the Gene Gun was positioned over the tissue, approximately 2 cm

centered about the well and the trigger pulled with either 0 psi of input pressure (control) or 250 psi of input pressure. After shockwave exposure the tissue was suspended in culture media and placed in a 37C, 5% CO_2, humidified incubator for 24 hours. Retinas were harvested similarly to cultured neurons. Briefly, the last 2 inches of a 3mL disposable transfer pipet (Samco Scientific Corp Cat # 225) was cut off and used to gently remove the retina and as little media as possible. The retina and media were placed in a 1.5mL Eppendorf tube and excess media was removed by aspiration. 250μl of NP40 lysis buffer with PhosSTOP phosphatase inhibitor cocktail (used according to manufacturer's instructions, Roche Cat # 04-906-837-001) and Complete Mini protease inhibitor cocktail (used according to manufacturer's instructions, Roche Cat # 04-693-124-001) was added. The samples were then sonicated using a Branson Sonifier 150 with 3mm tip on power setting 2. Sonications were performed on ice 3 times for 10 seconds each with at least 30 seconds in between each sonication. After sonication samples were immediately quantitated for total protein using the Promega BCA total protein assay as described above for cultured cells. Retinal samples were diluted 1:10 before being assayed to ensure samples were within the linear range of the assay. Samples were then aliquoted and stored at -20C. Western blots were performed on the rat retina samples for synaptic proteins found to change in primary neuronal cultures. 25-50 μg of total protein was added for each lane/experimental condition. Western blots and image analysis were identical as described above.

2.13 Statistical analysis

Two-tailed Students T-tests were conducted for all statistical analysis using Microsoft Excel and confirmed using the online t-test from www.Graphpad.com/quickcalcs/ttest. T-test results are reported as the degrees of freedom (df), the T-critical value and the p-value of the comparison. The statistical package JMP 9.0.0 from SAS Technologies was used to conduct the Pearson's Linear bivariate correlation analysis.

CHAPTER 3

GENE GUN AS A MODEL FOR PRODUCING SHOCKWAVES

3.1 Introduction

One of the many difficulties in researching the effects of shockwaves is creating them safely and reproducible in a controlled environment. A shockwave is a form of a spreading disturbance, the result of a near instantaneous change in the density of a substance. In this case, a shockwave is an abrupt change in air pressure. A pressure change, either above (overpressure) or below (underpressure) that occurs in less than 0.3 msec can be classified as a shockwave (de Candole, 1967). While the use of explosives to generate a shockwave is quite authentic and is employed by some researchers, it requires a specialized facility and increased lab safety protocols. As an alternative, the use of high pressure gas which is allowed to expand rapidly to generate a shockwave, has been well established to simulate shockwaves for analytical purposes. One device that utilizes such a system is a shock-tube, often used by researchers needing to expose everything from whole animals to cell cultures to shockwaves. Shock-tubes are long, hollow cylinders open at one end and connected to a pressurized gas source at the other, often Helium and occasionally Nitrogen. The subject to be exposed is secured at the opening of the tube at a predetermined distance from the pressurized gas source. When the gas is released a shockwave travels down the length of the tube, over the subject

to dissipate out the open end. Shock-tubes provide both a convenient and reproducible source of shockwaves in the laboratory setting.

Other devices have been designed to utilize shockwaves in a specific, directed manner. An extracorporeal shockwave (ESW) generating lithotripter creates high intensity shockwaves which can be focused by a trained user. The purpose of this device is to destroy specific matter within a body in a minimally invasive manner. It is commonly used to destroy kidney and gall stones in preference to surgical removal. These devices have also been used to destroy selective tissue, such as cancer cells by permeablizing the plasma membrane (Gambihler et al., 1994). Lithotripters have recently been employed as a long term analgesic for the relief of joint and tendon pain, though the mechanism of the action is not well understood (Hausdorf et al., 2008b). There is some evidence to suggest that ESWs act through selectively destroying unmyelinated nerve fibers in the peripheral nervous system in the area that they are applied (Hausdorf et al., 2008b).

3.2 Gene Gun is a biolistic transfection tool utilizing high pressure Helium

Biolistic Gene Guns utilize high Helium pressures to generate supersonic shockwaves that can be used to deliver DNA-coated microspheres to cell and tissue culture as well as whole animals (O'Brien and Lummis, 2006). The gold microspheres can be coated, through an electrostatic interaction with RNA, DNA or proteins (Wellmann et al., 1999, Wirth and Wahle, 2003, Uchida et al., 2006,

Uchida et al., 2009, Hao et al., 2010, Simon et al., 2010). The Helium is collected in a holding chamber located adjacent to the revolving cylinder holding the cartridges with the gold microspheres. When the safety is depressed and the trigger pulled, a solenoid switch releases the Helium extremely rapidly, generating a shockwave that moves over the microspheres picking them up as it expands out through the acceleration chamber and into the barrel (Figure 3.1). The microspheres hit randomly onto the target surface where some of the spheres penetrate the cells and release their bound cargo. Helium is used because it is one of the few gases with an atomic weight low enough to allow for the rapid expansion that produces a shockwave that is needed to propel the microspheres (Takeuchi et al., 1992). Helium has the added safety benefit of being inert under most conditions. Because of the similarity to a shock-tube, the biolistic Gene Gun also generates shockwaves that are similar to blastwaves. In the experiments that follow the cartridges in the revolver cylinder which usually holds microspheres were left empty such that the neurons were shot only with shockwaves.

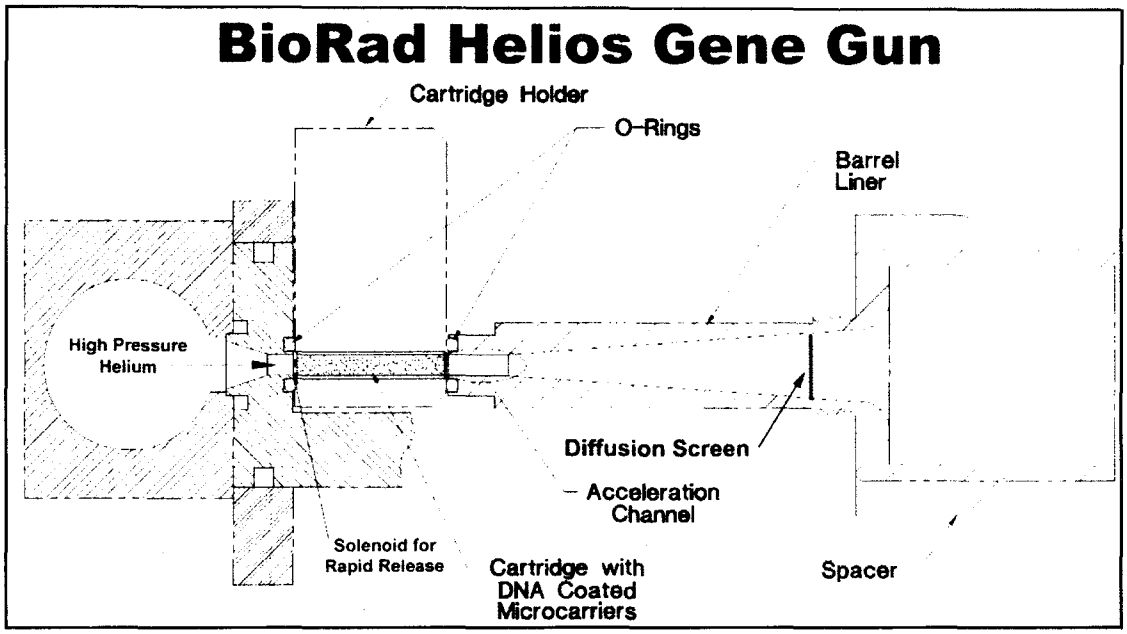

Figure 3.1: Schematic of the BioRad Helios Gene Gun in profile. The Helium is collected in an internal pressure chamber and released upon the trigger pull by rapid movement of the solenoid gate. It moves through the aligned barrel of the cartridge holder and cartridge, stripping any of the gold particles adhered to the inside of the cartridge. After exiting the cartridge the shockwave, Helium and gold particles enter a short acceleration chamber before expanding into the barrel and then to the cells. A diffuser screen can be placed in the barrel liner directly before the spacer to help dissipate the shockwave. For our experiments no diffuser screen was used, and there were no gold particles in the cartridge. BioRad Helios Gene Gun Cat. #165-2431.

The BioRad Helios Gene Gun has been used to successfully transfect cells in live animals, tissue slices as well as cultured cells (Wellmann et al., 1999, Gan et al., 2000, Wirth and Wahle, 2003, Goetze et al., 2004, Liu, 2007, Uchida et al., 2009, Hao et al., 2010, Simon et al., 2010). Transfection of brain slices is optimal with Helium input pressures between 90-120 psi with minimal tissue damage (Wellmann et al., 1999, Lechner et al., 2002). Some types of cultured cells, such as fibroblasts and lymphoid cancer cells can tolerate higher input pressures up to 300 psi, in the range of transfecting live animals (Lu et al., 2002, Martiniuk et al., 2002).

Like any protocol, Helios Gene Gun procedures require optimization for obtaining the best results. The shockwave is one of the main factors in cell death after exposure. In order to limit shockwave intensity one can vary the input pressure as well as the shooting distance (BioRad Helios Gene Gun manual). Another recommended method for limiting the shockwave is to use a diffusion screen, which can be placed in the barrel to disrupt the shockwave with limited interference of the gold particles (BioRad Helios Gene Gun Manual, (Wellmann et al., 1999). For each procedure these parameters need to be adjusted and optimized such that the desired effects of shockwaves under investigation are maximally detected while unwanted effects, such as cell death are minimized. For these experiments a diffusion screen was not used, input pressures varied between 0 and 400 psi and the end of the barrel was held fixed at 2 cm above the cells.

3.3 Mild vs. moderate shockwaves

It is believed that the overpressure phase of an in-air shockwave is the damaging portion since it is always much greater in magnitude than the accompanying underpressure phase. An idealized wave-form called a Friedlander Wave is often used as the typical profile of a shockwave. It is characterized by a near instantaneous rise in pressure (overpressure) followed by a longer lasting, but smaller magnitude decrease (underpressure). The rise time is the time required for the pressure wave to reach its peak overpressure

from the ambient pressure. For the entire range of Gene Gun pressure measurements, peak overpressures were collected. While the rise time of all shockwaves is generally defined as being less than 0.3 microseconds, the maximum overpressure reached as the wave passes the target can vary greatly. There is a great deal of research currently being undertaken to determine the pressure threshold for mild traumatic brain injury.

The damaging effects of high overpressure shockwaves from large magnitude explosions, such as those caused by IEDs, have been well documented in the brains of combat veterans suffering TBI (Taber et al., 2006, Sponheim et al., 2011). Animal models exposed to shockwaves with large peak overpressures have been able to replicate similar tissue damage as well as cognitive impairment found in soldiers suffering TBI (Cernak et al., 2001, Kato et al., 2007, Bauman et al., 2009, Saljo et al., 2010). However the lack of apparent tissue damage in veterans with shockwave-induced mTBI has prompted researchers to decrease peak overpressures in animal models and look for increasingly more subtle changes.

Animal models using low overpressure shockwaves have also suggested that cognitive impairment can occur with little to no discernable tissue damage (Cernak et al., 2001, Bauman et al., 2009). It is important to note that there is little to no cell death observed in veterans suffering mTBI, and it is a hallmark of the condition that there is very little damage which can be found with today's

imaging techniques which has led to the coining of the phrase 'invisible wounds' to describe mTBI (Cernak et al., 2001, Sponheim et al., 2011). A comprehensive study exposing live pigs to explosives of similar size and power to 'moderate' IEDs recorded peak overpressures outside of the subject's heads as well as multiple intracranial measurements. Peak overpressures outside and adjacent to the subject's head reached 50 psi while levels within the brain were less than half of that, 10- 20 psi (Bauman et al., 2009). This level of pressure was sufficient to cause cognitive dysfunction in the pigs as measured by Vicon motion analysis technology, which is similar to motion capture technology used to animate live action computer generated images (example, Gollum from Lord of the Rings). Pre- and post-exposure recordings showed a significant change in limb coordination and movement speeds (Bauman et al., 2009). Furthermore silver staining of coronal sections of the animals after sacrifice showed evidence of neuronal degeneration and increased astrocyte activation. This model is thought to represent a mild TBI due to the cognitive impairment coupled with lack of significant cell death and lack of visible brain damage in the form of lesions, hemorrhages or contusions. The swine used were roughly half the weight of the average American male (swine 90-110lbs, average male 190lbs) though a pig's skull is much thicker and stronger than the skull of a human. This difference in skull thickness could significantly alter the total force transmitted to the brain from the shockwave and thus the pressures recorded in the swine brain may not be applicable to the force required to cause mTBI in a human.

3.4 Gene Gun produces a shockwave within its operating input pressure ranges

According to the manufacturer, the BioRad Helios Gene Gun can function with up to 600 psi of input pressure. To calibrate the Gene Gun and determine the pressure and rise time delivered to cells in our experimental setup we varied input pressures from 50-400 psi in increments of 50 psi. Given the manufacturer's warning that the Gene Gun propels particles in excess of 1,000 feet/second, very near the speed of sound, we wanted to determine whether the Gene Gun produced a shockwave at a broad range of input pressures and to calculate the pressure delivered to cells at various input pressures in our system (BioRad Gene Gun manual). For example, it is specified in the manual that at 400 psi of input Helium pressure the Gene Gun produces approximately 108 decibels during discharge which is near the threshold for causing permanent hearing loss after a single exposure, consistent with a shockwave, but at lower input pressures we were not sure shockwaves would be produced (BioRad Gene Gun manual). Measurements of the rise time of the overpressure phase of the Gene Gun show it creates a reproducible shockwave at input pressures tested and as would be expected, rise times decreased as input pressure increased (Figure 3.2). These results provide confidence in our experimental system as a viable test system for characterizing the effects of sub-lethal shockwaves on neuronal cells.

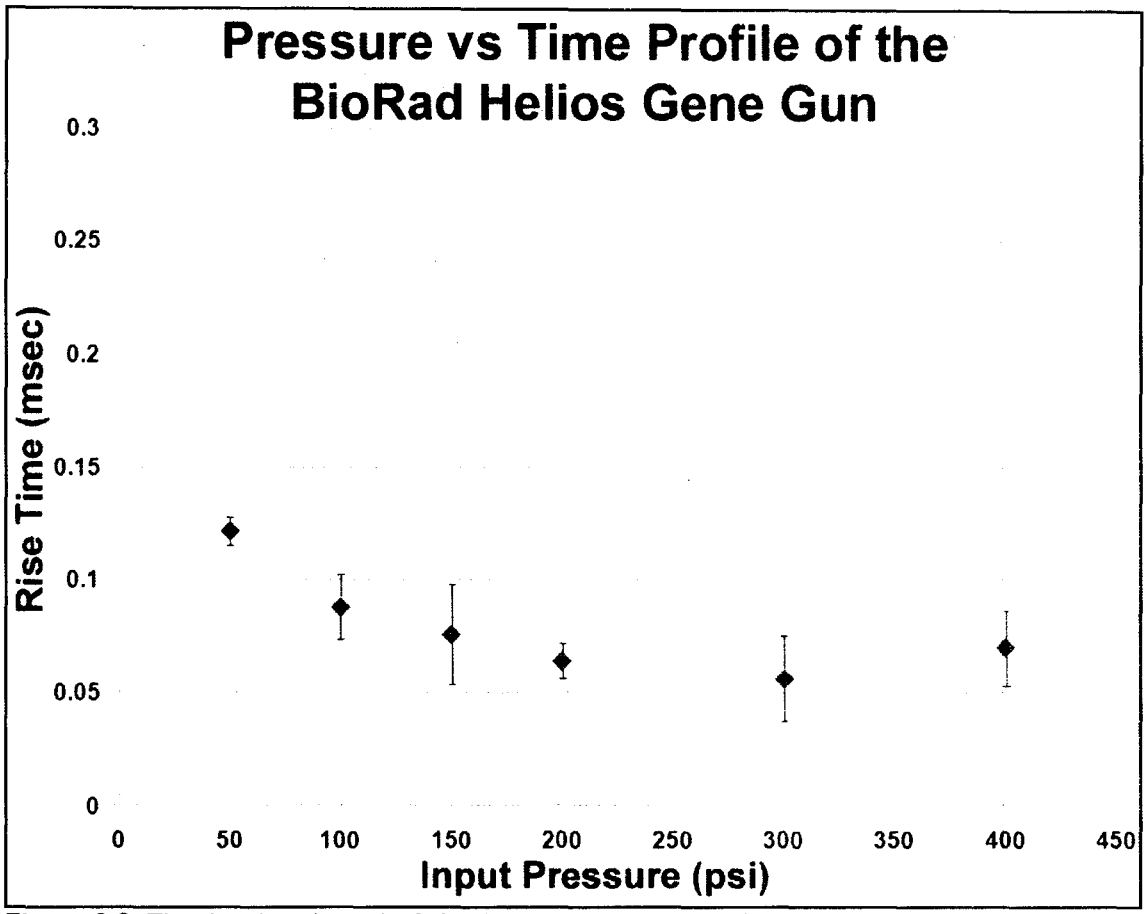

Figure 3.2: The rise time (msec) of shockwaves generated by increasing Helium input pressures with the BioRad Helios Gene Gun. Tested input pressures were found to produce pressure waves with rise times less than 0.3 msec indicating that at all input pressures tested a shockwave was indeed generated. Error bars are standard deviation. Measurements were made by Matthew Panzer, Garrett Woods and Dr. Cameron Bass of Duke University Biomedical Engineering, Durham, North Carolina.

3.5 At input pressures used in this experimental setup, the Gene Gun produces a shockwave with overpressures similar in magnitude to those detected intracranially in blastwave-exposed animals.

We have established that the Gene Gun produces shockwaves at the input pressures we tested. Next the magnitude of these shockwaves was

determined. In order for our experimental system to accurately model mTBI *in vitro* we needed to determine if the overpressures we could produce with the Gene Gun were similar in magnitude to those used to create mTBI models in animals. As expected, the magnitude of the overpressure phase increased as input pressure was increased, with the maximum pressure experience by the cells generated at the highest input pressure tested. With 400 psi of input pressure the Helios Gene Gun had a maximum peak overpressure of ~1.3 psi when positioned 2 cm from the end of the gun barrel as it was for all experiments (Figure 3.3). An animal mTBI model which used a Helium-driven shock-tube to expose adult rats to shockwaves of 10 psi measured adjacent to the head of the animals recorded peak overpressures in the brain between 1 and 2.3 psi. 10 psi overpressures were shown to cause cognitive impairment but not cell death in the rats (Moochhala et al., 2004, Saljo et al., 2010). These findings confirm our experimental system as a viable assay for replicating mTBI with cultured neurons using input pressures above 200 psi.

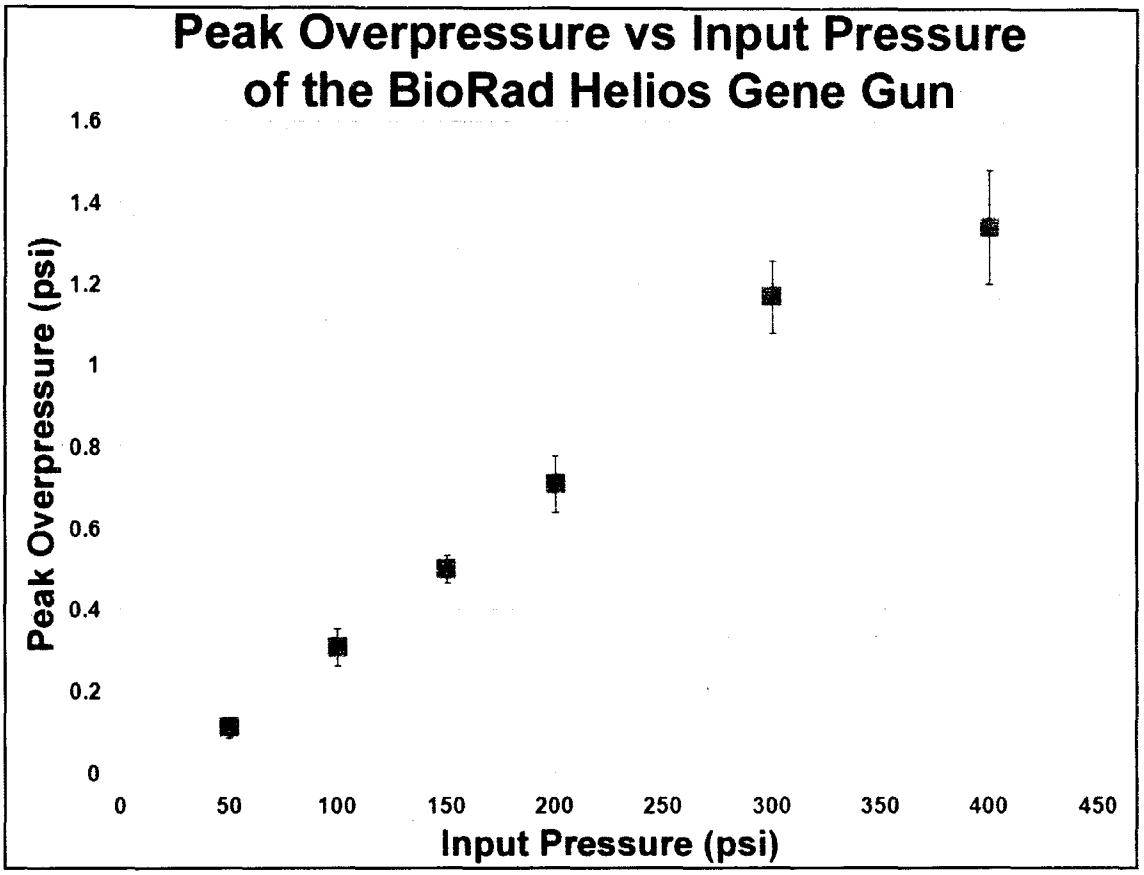

Figure 3.3: The peak overpressure of the shockwaves generated by the BioRad Helios Gene Gun increased with increased Helium input pressure. Peak overpressure was measured by a piezoresistive pressure sensor positioned 2 cm from the end of the barrel spacer. Error bars are the standard deviation. Measurements were made by Matthew Panzer, Garrett Woods and Dr. Cameron Bass of Duke University Biomedical Engineering, Durham, North Carolina.

3.6 At common operating input pressures the Gene Gun produced shockwave does not greatly alter cell morphology

Throughout these experiments, the majority of cells showed no major morphological changes after exposure to shockwaves generated by up to 300 psi of input pressure compared to mock shot cells (Figure 3.4). This finding is in accord with many mTBI studies suggesting that cell death does not seem to be a

major factor in mTBI. At input pressures over 300 psi in our *in vitro* system there was increasing visible cell damage as well necrotic cell death with increased input pressure. Damaged cells had processes which were sheared off and, in rare cases, cell somas became detached, tearing off the coverslip, appearing as processes leading to an empty area.

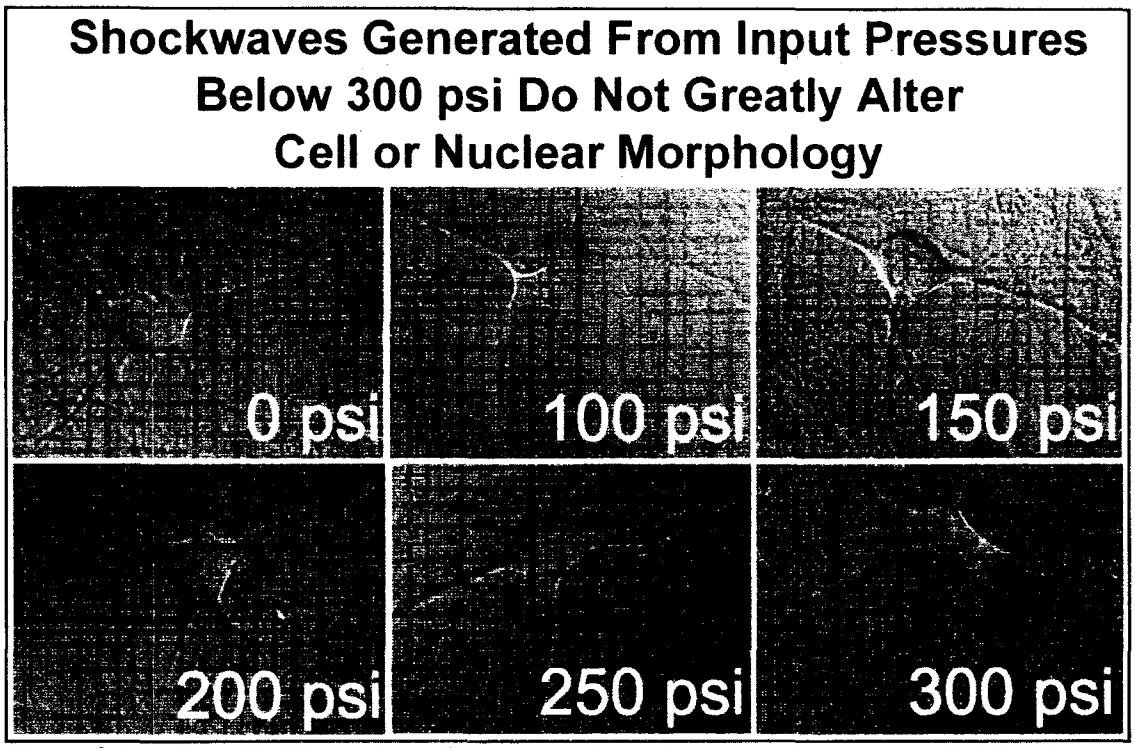

Figure 3.4: DIC and DAPI overlays of representative cells exposed to a range of Helium input pressures, images acquired 24 hours after exposure. Cell morphology is comparable between neurons exposed to a range of input pressures up to 300 psi.

All neurons fixed and imaged after shockwave exposure were stained with DAPI, a nuclear stain that binds tightly to double stranded DNA. Based on the density and pattern of the staining it is possible to determine the general health of the cell. Sick or dying cells will fragment their DNA which will be apparent as bright, punctuate staining. The majority of cells appeared healthy by both DAPI

staining and DIC morphology when exposed to shockwaves generated with input pressures up to 300 psi (Figure 3.4).

3.7 At common operating input pressures the Gene Gun produced shockwave does not cause apoptosis as shown by TUNEL assay

In order to be certain that shockwave exposure was not killing neurons a *T*erminal deoxynucleotidyl transferase d*U*TP *N*ick *E*nd *L*abeling (TUNEL) assay was employed. A TUNEL assay utilizes the nicks found in the double stranded DNA of unhealthy and dying cells to label apoptotic cells. Cells exposed to shockwaves generated with up to 250 psi of input pressure did not show any increased amount of TUNEL positive cells above background (Figure 3.5). Cell death started to become apparent at 300 psi of input pressure and was clearly evident at 400 psi of input pressure. As a result of the increased cell death observed at 400 psi but not at 250 psi, 250-300 psi was chosen as the maximum input pressure to be used. This finding is in accord with many other studies showing that cell death does not seem to be a major factor in mTBI.

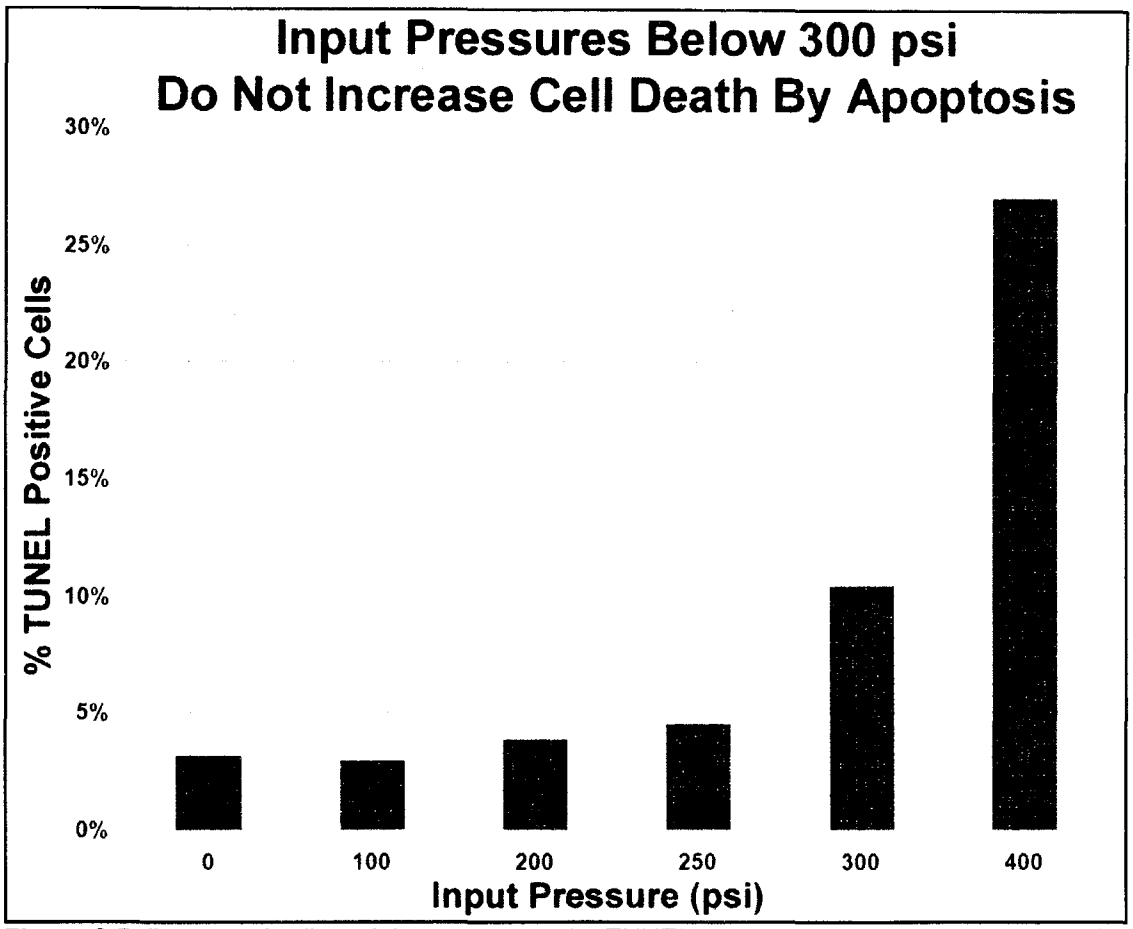

Figure 3.5: Percent of cells staining positive in the TUNEL assay over an increasing range of input pressures for the BioRad Helios Gene Gun. Increased cell death above background first became apparent at 300 psi of input pressure. Experiment was repeated 3 times with similar results.

3.8 Chapter 3 summary

Here, we have shown that the BioRad Helios Gene Gun can be used to conveniently produce a shockwave of consistent overpressures and rise times over a range of values that are close to the levels measured in animals subjected to sub-lethal blastwaves (Figure 3.2). The peak overpressures of the shockwaves generated within the operating parameters of the Gene Gun are approximately

10% of the overpressures observed in 'moderate-sized' blasts and are within the range of pressures shown to cause cognitive dysfunction, but no discernable tissue damage, in animal models, consistent with mTBI (Figure 3.3) (Bauman et al., 2009, Saljo et al., 2010). In order to best simulate mTBI *in vitro* we confirmed using a TUNEL assay as well as morphological assessment by DIC and DAPI staining that, at the pressure inputs measured, there was very little cell death by apoptosis or necrosis (Figure 3.4 and 3.5). For all subsequent experiments a maximum input pressure of 250-300 psi was chosen because there was little change in cell morphology by DIC imaging or DAPI staining observed (Figure 3.4).

CHAPTER 4

SHOCKWAVE EXPOSURE RESULTS IN TRANSIENT MEMBRANE PERMEABILITY

4.1 Introduction

I demonstrated in Chapter 3 that our *in vitro* system can accurately deliver shockwaves similar in magnitude to shockwaves that replicate the cognitive impairment of mTBI in a rat model of shockwave-induced mTBI and that these shockwaves do not greatly alter cell morphology or increase apoptosis above background levels, consistent with mTBI. Currently the mechanism of any possible damage caused by shockwaves is unknown, though evidence suggests that shockwaves do affect the brain. In order to learn how shockwaves may be causing damage to neurons, I investigated the membrane integrity of cultured neurons, because it is the first interface between the cells and the shockwave. Previous research has shown that high intensity shockwaves are capable of inducing membrane permeability in cells *in vivo* and I wanted to find out if our low intensity shockwaves could also permeabilize cells *in vitro* (Saljo et al., 2003, Khanna et al., 2006).

An extracorporeal shockwave-generating lithotripter is a device originally designed for the non-invasive destruction of kidney or gall stones by focusing externally generated shockwaves through the patient's body onto the stones. The high intensity shockwaves travel through the soft tissue of the body but reflect off

the dense stones, imparting a great deal of energy in the process. Repeated exposure eventually cracks the stone and reduces it to many smaller pieces which can then be passed out of the body. Recently lithotripters have been used to selectively destroy cancer cells *in vivo* by membrane permeabilization (Murata et al., 2006, Hausdorf et al., 2008a). Lithotripters generate high intensity shockwaves through one of three methods, electrohydraulic, piezoelectric or electromagnetic. The first lithotripter, the Dornier HM3 built in 1980s by Dornier MedTech Systems GmbH, was an electrohydaulic lithotripter that used a spark plug in a water tank to create a shockwave by vaporizing the small amount of water surrounding the spark plug. The bubble of vaporized water quickly collapsed back into liquid form and a shockwave was produced. Newer lithotripters use piezoelectric or electromagnetic mechanisms to create their shockwaves. Piezoelectric lithotripters rely on electrical current to rapidly alter the structure of crystals or ceramics that are in water. The rapid movement creates a shockwave that propagates through the water and into the patient. An electromagnetic lithotripter uses an electromagnetic coil, similar to a stereo speaker that induces high frequency vibrations in an adjacent metallic membrane, which are then transferred into a propagating medium such as water. We wanted to see if lower intensity shockwaves were capable of causing membrane permeabilization in our cultured neurons.

Sonoporation is a novel application of a lithotripter to transiently permeabilize the plasma membrane of a cell to facilitate the transfer of genetic

material into the cell (Fischer et al., 2006, Han et al., 2007, Zhou et al., 2008, Kudo et al., 2009, Kumon et al., 2009, Miller and Dou, 2009, Zhou et al., 2009, Lin et al., 2010). The magnitude of the overpressure of the shockwave generated for sonoporation is decreased dramatically compared to the kidney stone destruction. The growing use of sonoporation for transfection of a range of cell types, including a variety of neurons, is indicative of the relative ease of use and wide-ranging applicability of the technique (Fischer et al., 2006). Initial studies characterizing the size of the molecules which could be loaded into cells by sonoporation used various sized Dextran-conjugated dyes.

4.2 Overview of Dextran-conjugated dyes and prior uses

Dextran is a biologically inert hydrophilic polysaccharide. The glucose molecules are connected by α-1-6 linkages which are resistant to cleavage by most cellular glycosidases. Dextran can be purchased in a range of molecular weights based on the number of glucose molecules in the polysaccharide chain from 3kDa up to 2000kDa. When conjugated to a fluorescent dye the labeled Dextran molecule becomes a stable, non-reactive marker ideal for a number of different uses including neuronal cell tracing, cell lineage tracing and membrane permeability studies, among others. Dextran dyes have been used to study the mechanics of other cell permeabilization techniques including electroporation and sonoporation making them an ideal candidate to assess the membrane integrity

of our shockwave-exposed neuronal cultures (Zaharoff et al., 2008, Wei et al., 2010).

4.3 Mild shockwaves delivered with a Gene Gun permeabilize cultured neuronal cells with increased input pressure causing increased permeability

In order to determine what, if any, effect mild shockwaves have on the permeability of brain cells, I subjected cultured neurons to shockwaves from the Gene Gun, generated with increasing input pressure and immediately incubated the cells in Neurobasal media containing 20μM of 3 kilodalton (kDa) Dextran-conjugated fluorescein. Cells were incubated in dye for 2 hours, after which they were fixed and imaged. Membrane permeability was measure and plotted as increased fluorescein fluorescence in the cell soma greater than the soma fluorescence of the non-exposed (0 psi) cells. As seen in sonoporation studies, there was a positive relationship between input pressure and cell permeability with increasing input pressure leading to greater cell permeability (Figure 4.1). No difference in soma fluorescence was found between non-exposed cells and cells exposed to shockwaves generated from 100 psi of input pressure, suggesting that input pressures less than 150 psi do not cause membrane permeability. There was a 25.3 +/- 1.4% increase in soma fluorescence for 150 psi, a 37.0 +/-1.0% increase for 200 psi and a 75.6 +/-1.4% increase for 250 psi of input pressure (Figure 4.1). In a similar but less comprehensive study,

dissected guinea pig spinal cord white matter was exposed to increasing magnitude shockwaves generated from explosive blasts and incubated for 1 hour with horseradish peroxidase (HRP). Increased loading of HRP was observed with larger overpressures. Tissue exposed to a blast overpressure of 3.3psi had a 7.83 +/-1.39% increase in soma labeling over non-exposed cells, 5.95psi had a 24.67 +/-5.5% increase in soma labeling over non-exposed cells and 9.4psi had a 64.96 +/-10.16% increase in soma labeling over non-exposed cells (Connell et al., 2011).

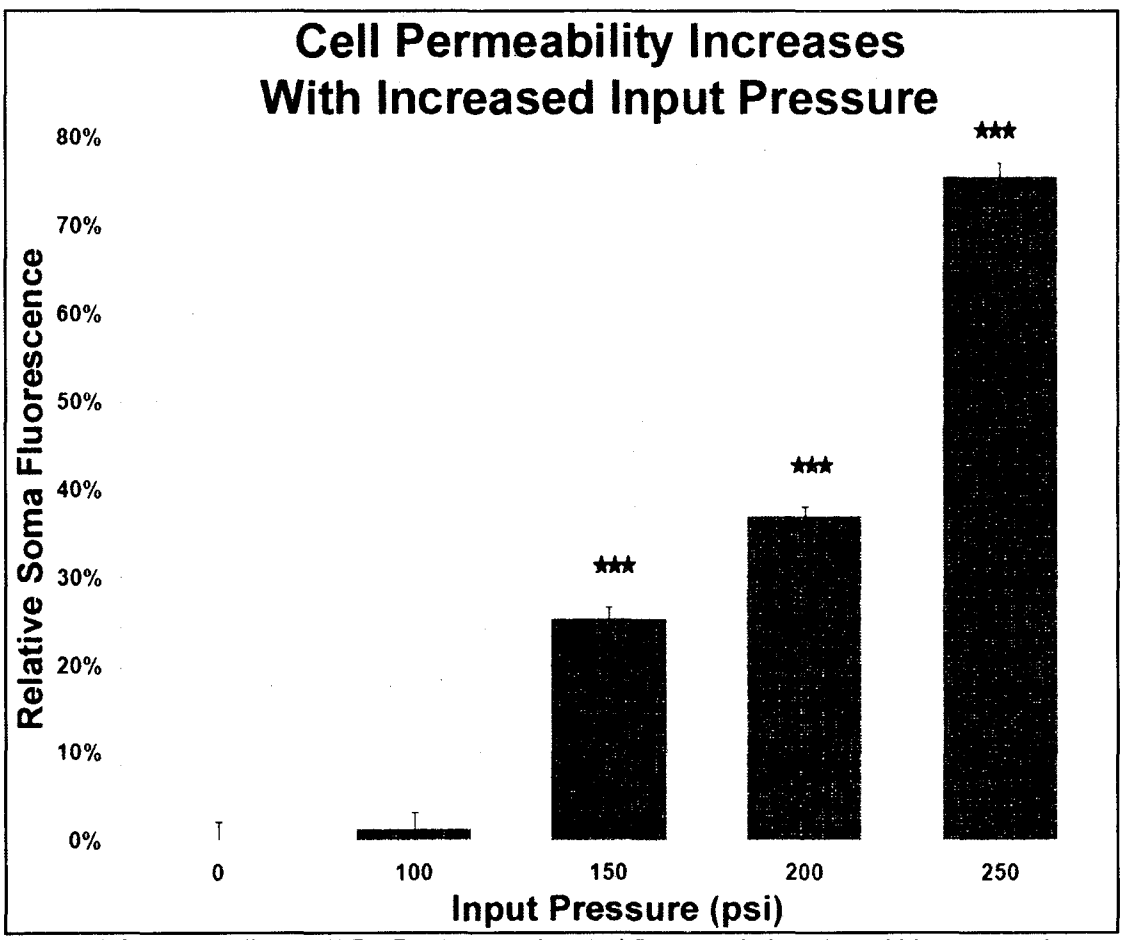

Figure 4.1: The loading of 3kDa Dextran-conjugated fluorescein in cultured hippocampal neurons increases with increased input pressure to the Gene Gun. Cells were exposed to increasing amounts of pressure and then incubated for 2 hours in the Dextran-conjugated dye before being

washed and fixed. The fluorescence of the soma was adjusted relative to the non-exposed (0 psi) control cells. *** = $p<0.0001$ for comparison between exposed and non-exposed cells for that time point.

Average soma fluorescence of each input pressure was normalized to the 0 psi control cells for this experiment and all subsequent Dextran experiments. Normalization of soma fluorescence to a control cell (0 psi) has been used previously for the quantitation of Dextran loading in electroporation studies (Wei et al., 2010, Connell et al., 2011). Shockwave-exposed cells always showed statistically significantly greater loading than non-exposed cells for all time points investigated.

4.4 The extent of cell permeability is directly related to Dextran size and shockwave intensity

Size cut-offs for cell permeability have been observed in sonoporation studies and depend on the number and magnitude of force applied to the cells. To determine the effective size of the shockwave-induced permeability in our system, I conducted pressure titration experiments with a range of commercially available Dextran conjugates. Using 3kDa, 10kDa, 40kDa, 70kDa and 500kDa Dextran conjugates the size restriction of the shockwave-induced membrane permeability was assessed.

At the lowest input pressure of 100 psi, the shockwave generated was not sufficient to permeabilize the cell membrane to any size Dextran we tested. Average soma fluorescence in cells exposed to shockwaves generated by 100

psi of input pressure was not increased above the non-exposed (0 psi) control cells for all Dextrans tested (Figure 4.2). The first indication of shockwave-induced membrane permeability was found with 150 psi of input pressure and the smallest Dextran. 3kDa Dextran soma fluorescence was 25.3 +/-1.4% above background, while the 10kDa, 70kDa and 500kDa soma fluorescence were not statistically significantly above background. Since only the smallest Dextran conjugate was able to penetrate the cell with 150 psi of input pressure, this could indicate that larger overpressures create larger holes in cell membranes.

In our system shockwaves generated from 200 psi of input pressure expose the cells to overpressures very near to what has been recorded in the brains of animal mTBI models. At this input pressure, there was significant loading of a range of Dextran conjugates, including the 3kDa, 10kDa and 70kDa conjugated Dextrans (Figure 4.2). 3kDa Dextran soma fluorescence was 37 +/-1.1% above background and significantly larger than the soma fluorescence at 150 psi of input pressure. The 10kDa Dextran soma fluorescence of 34.9 +/-3.7% above background was similar to the 3kDa Dextran. The 70kDa Dextran soma fluorescence was approximately half of the 3 and 10kDa Dextrans, at 15.4 +/-3.0% above background (Figure 4.2).

With 250 psi of input pressure the Gene Gun delivers shockwaves identical in magnitude to those recorded in the brains of mTBI animal models. As expected, membrane permeability after exposure to a shockwave generated by

250 psi of input pressure was much increased above the membrane permeability induced by lower input pressures. The 3kDa Dextran soma fluorescence of 250 psi exposed cells almost doubled compared to 200 psi, 75.6 +/-1.4% vs 37 +/-1.1% above background. The 10kDa Dextran continued to mirror the 3kDa Dextran with a similar jump, 34.9 +/-3.7% vs 71.2 +/-3.6% above background. The 40kDa Dextran and 70kDa Dextran were similar in soma fluorescence, 33.5 +/-2.5% and 32.1 +/-1.9% above background respectively. Previous research has demonstrated the ability of shockwaves generated from explosive blasts to permeabilize dissected guinea pig spinal cord white matter to HRP, an enzyme approximately 44kDa (Connell et al., 2011). The 500kDa Dextran was found to not be loaded into cells even after exposure to 250 psi of input pressure (Figure 4.2). There were no statistically significant differences between any of the average soma fluorescence for any input pressures measured for the 500kDa Dextran. This is similar to what has been found for single exposure sonoporation studies with 500kDa Dextran (Khanna et al., 2006, Zaharoff et al., 2008).

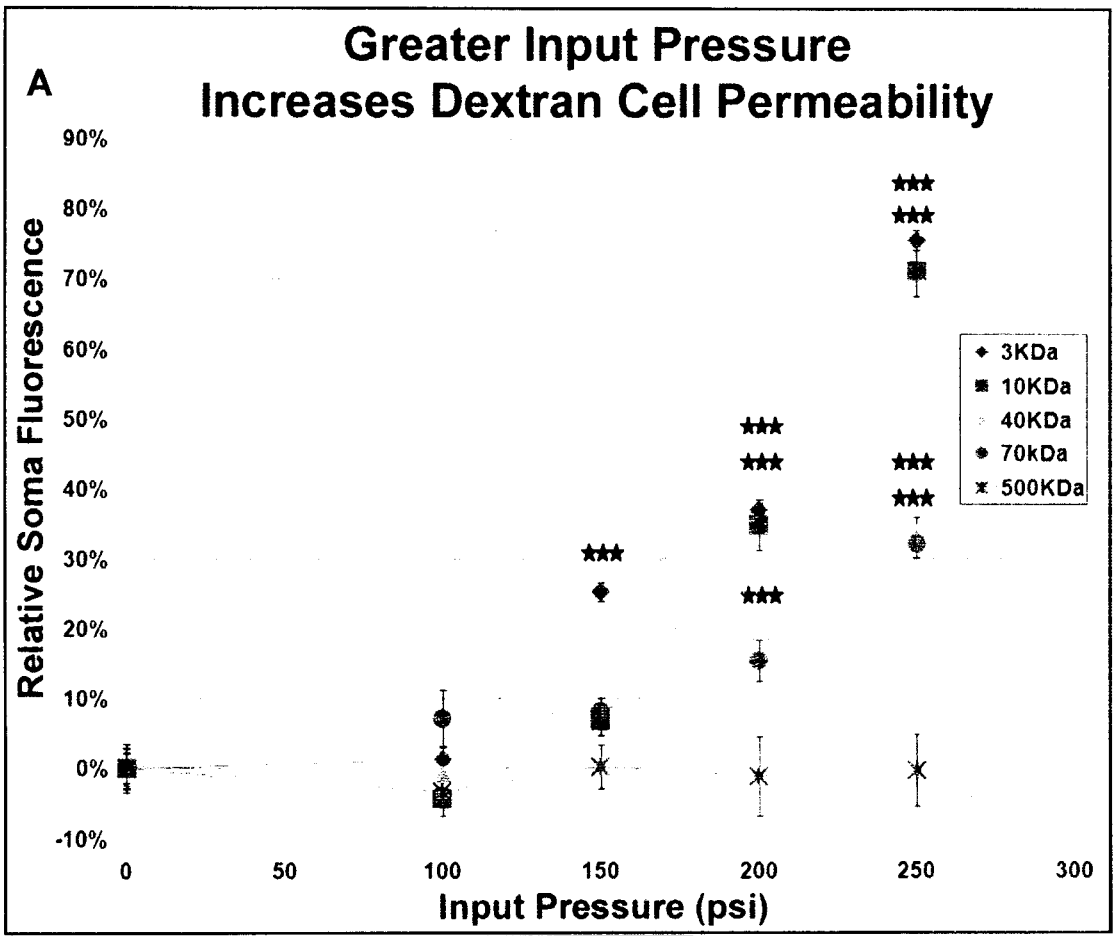

Figure 4.2: Cell loading of a range of different sized Dextran conjugates in cultured hippocampal neurons over a range of input pressures. A) Cultured primary hippocampal neurons were exposed to shockwaves generated from increasing input pressure and incubated with 3kDa, 10kDa, 40kDa, 70kDa or 500kDa Dextran-conjugated fluorescein before being washed, fixed and imaged. Cells were chosen based on DIC morphology and DAPI imaging. B) Fluorescence of the cell soma was measured and calculated relative to the non-exposed (0 psi) control for at least 40 cells for each pressure input and Dextran size. *** = $p<0.0001$ for comparison between exposed and non-exposed cells for any sized Dextran conjugate.

It can be seen in Figure 4.2 that at lower pressures the smaller Dextran conjugates more easily penetrated the shockwave-exposed cells than the larger Dextran conjugates. The relative size (in nanometers) of the Dextran conjugates and thus the size of the permeability of the cellular membrane can be approximated by the Stokes Radius (SR). The SR is the radius of a solid sphere of any given molecular weight that diffuses at the same rate as a molecule of the same molecular weight. The SR is almost always an underestimation of the size of a molecule since very few molecules exist as uniform spheres. The Stokes Radii for the Dextran-conjugated dyes used are shown in Table 4.1, with the lightest, 3kDa conjugates, approximately ten fold smaller than the heaviest, 500kDa conjugates (1.35nm vs 14.7nm). The largest conjugate shown to penetrate the cell was 70kDa and has a SR approximately one third (5.8nm) of the largest conjugate (500kDa, 14.7nm) which was found to not penetrate the cells.

Stokes Radius of All Size Dextrans Tested					
MW (kDa)	3	10	40	70	500
Stokes Radius (nm)	1.35	2.36	4.45	5.8	14.7

Table 4.1: The Stokes Radius in nanometers (nm) of the various sized Dextran conjugates used by their molecular weight in kilodaltons (kDa). 70kDa was the largest Dextran conjugate loaded into cells after shockwave-exposure. 500 kDa Dextran conjugates did not penetrate cells after shockwave-exposure of any pressure.

4.5 Shockwave-induced membrane permeability is lost within 2-6 hours after exposure

I next wanted to calculate how long after shockwave exposure would cells still be permeable to Dextran-conjugated dyes. Since the permeabilization effects of sonoporation are transient, we hypothesized a similar phenomenon was occurring in our experimental system. To determine the time required for cells to restore membrane integrity after shockwave exposure, cells were exposed to maximum overpressure shockwaves generated from 250 psi of input pressure and either incubated immediately in media containing dye or allowed to recover in media without dye before dye was then added. The maximum input pressure of 250 psi was chosen because it induced the greatest membrane permeability and best represents the overpressure recorded in the brains of animal mTBI models. After the recovery period, cells were incubated in dye for the same amount of time as cells immediately incubated with dye. All sizes of Dextran which were found to be loaded into shockwave-exposed cells were subsequently excluded in shockwave-exposed cells allowed to recover before incubation in the dye (Figure 4.4).

The 3 and 10kDa Dextran conjugates showed similar cell average soma fluorescence of 70% above background after exposure to shockwaves generated from 250 psi of input pressure and an initial recovery period of 6 hours was chosen for these two smallest Dextrans. Following shockwave exposure, cells

were given 6 hours before being incubated with Dextran-conjugated dye. Shockwave-exposed cells incubated with either the 3 or 10kDa Dextran after the 6 hour recovery period had average soma fluorescence that was not different from background (Figure 4.3). This finding indicates that membrane integrity is restored for the 3 and 10kDa Dextrans, which showed cell permeability with the lowest input pressures as well as overall highest soma fluorescence (Figure 4.2). The recovery period was decreased to 3 hours with the 40kDa Dextran in an attempt to narrow the recovery window. With only 3 hours recovery post-shockwave exposure cell soma fluorescence was not different from background for the 40kDa Dextran-conjugated dye (Figure 4.3). In the above pressure titration experiment, the 40 and 70kDa Dextrans demonstrated similar average soma fluorescence above background at 250 psi of input pressure. Since a 3 hour recovery was sufficient to exclude the 40kDa Dextran we shortened the recovery period to 2 hours for the 70kDa Dextran. A 2 hour recovery period was found to be sufficient to exclude the 70kDa Dextran from shockwave-exposed cells (Figure 4.3).

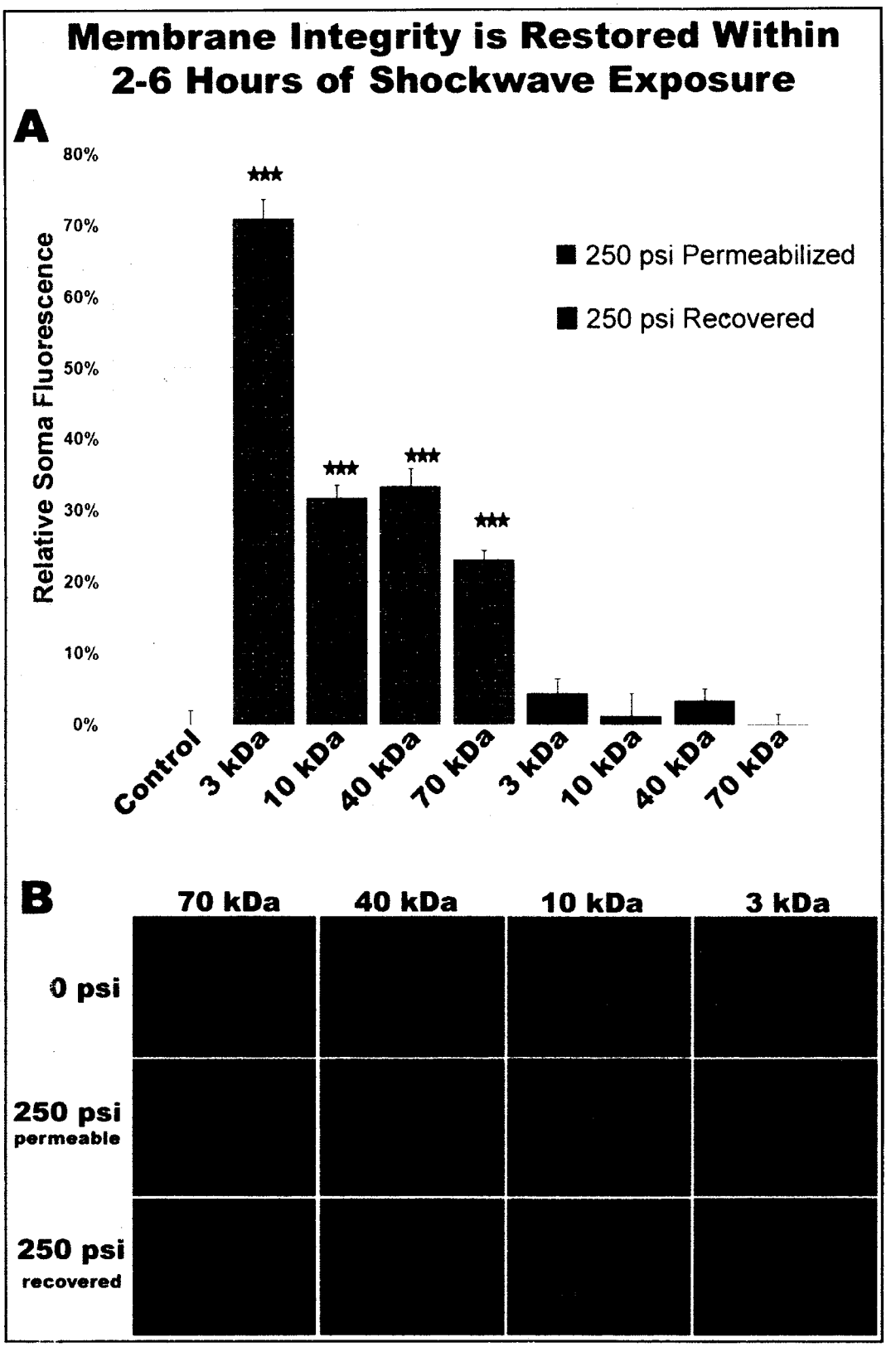
Membrane Integrity is Restored Within 2-6 Hours of Shockwave Exposure
A
Relative Soma Fluorescence
80%
70%
60%
50%
40%
30%
20%
10%
0%
***
***
***
***
250 psi Permeabilized
250 psi Recovered
Control
3 kDa
10 kDa
40 kDa
70 kDa
3 kDa
10 kDa
40 kDa
70 kDa
B
70 kDa
40 kDa
10 kDa
3 kDa
0 psi
250 psi
permeable
250 psi
recovered

Figure 4.3: Cell permeability to Dextran-conjugated dyes is lost with a pre-dye incubation recovery period of 2-6 hours, demonstrating repair of the cellular membrane. Cells were exposed to shockwaves generated by 250 psi of input pressure and either incubated directly in dye or allowed to recover for 2 to 6 hours before being incubated in dye. A) Cells allowed to recover before dye exposure were able to exclude the dye and did not show any statistically significant differences in soma fluorescence compared to non-exposed (0 psi) controls cells. B) Representative cells for each size Dextran at 0 psi and 250 psi permeabilized and 250 psi recovered. *** = $p<0.0001$ for comparison between exposed and non-exposed cells for any sized Dextran conjugate

The permeability caused by the shockwave is transient and the cells are able to re-establish the integrity of their plasma membrane within 2-6 hours after shockwave exposure. In accord with our findings, previous studies on the transient membrane permeability induced by sonoporation have shown that uptake of molecules occurs within seconds of exposure to the shockwave and that membrane integrity is restored within minutes after the exposure (Zhou et al., 2008, Kudo et al., 2009, Zhou et al., 2009).

4.6 Chapter 4 summary

I have shown that Gene Gun generated shockwaves of similar magnitude to those recorded in the brains of animal mTBI models increase permeability of cultured neuronal cells to 3-70kDa Dextran-conjugated dyes, with increased input pressure causing greater membrane permeability. I have also shown a permeability threshold of up to 70kDa, but not 500kDa Dextran, and this shockwave-induced permeability is lost within 2-6 hours after exposure. This finding of transient membrane permeability agrees with previous research in membrane permeabilization by sonoporation. The size cut off of 500kDa is similar to the limit of single exposure permeabilization in sonoporation (Khanna et

al., 2006, Zaharoff et al., 2008). It is possible that membrane permeabilization is occurring in the brains of animal mTBI models.

CHAPTER 5

SHOCKWAVE EXPOSURE DECREASES CELLULAR ENERGY LEVELS AS MEASURED BY ATP LUCIFERASE ASSAY

5.1 Introduction

It is estimated that the average human has 100 billion neurons in her/his brain with over 500 trillion connections (Drachman, 2005). These connections are called synapses. Neurons communicate via a traveling localized membrane depolarization event called an action potential which ends at a synapse. At the synapse the depolarization event triggers the release of vesicles containing neurotransmitters which diffuse across the gap to the adjacent neuron. In order to fire an action potential the neuron must maintain a very high electrochemical concentration gradient across its plasma membrane. This requires high amounts of energy which is stored and consumed in the form of Adenosine TriPhosphate (ATP). Most of the ion pumps require ATP to generate concentration gradients. These ion pumps maintain extracellular levels of Ca^{2+}, Cl^- and Na^+ greater than the intracellular levels, while the intracellular levels of K^+ are higher than the extracellular levels. The neuron maintains sequestered stores of intracellular Ca^{2+} within the endoplasmic reticulum (Hammond, 2001). The Na/K-ATPase pump moves Na^+ out of the cell and K^+ into the cell through the hydrolysis of ATP. The Ca-ATPase moves Ca^{2+} out of the cell or into a cellular organelle through the hydrolysis of ATP (Hammond, 2001). When the neuron fires an

action potential, voltage-gated ion channels open in response to the depolarization of the membrane, allowing Na^+, Cl^- and Ca^{2+} to enter the cell, further depolarizing the membrane and moving the reaction further down the axon. It has been estimated that roughly 2/3 of neuronal ATP is used to maintain the electrochemical gradient of the neuron (Blomqvist et al., 1991a, Blomqvist et al., 1991b, Gafaniz and Sanches, 2010). In order to meet the high energy demands of their function, neurons create and maintain many mitochondria throughout their complex, branching structure and specifically concentrate mitochondria at active and growing synapses (Cameron et al., 1991, Sheehan et al., 1997, Li et al., 2004, Popov et al., 2005).

Given the large amount of energy neurons devote to creating ion concentration gradients across their plasma membrane it seemed logical that after the shockwave-induced membrane permeability discovered in Chapter 4, the energy state of the neurons should be severely compromised. To investigate any possible shockwave-induced energy changes in our experimental system I assayed shockwave-exposed cultures for levels of ATP. In order to assay the amount of ATP in culture, the Invitrogen ATP Luciferase Assay was employed. Whole primary rat hippocampal cultures were exposed to increasing amounts of pressure and then allowed to recover for increasing periods of time. The cells were then lysed and total culture extracts collected for analysis. In order to account for any variation caused by a difference in the number of cells in each culture, total protein content was assayed and used to normalize the total ATP

values, as previously published work. Total protein levels were seen to vary between cultures but the differences were not reflected in the total ATP readings, and many times there was no significant difference in total protein content between any conditions.

There is evidence to suggest that shockwave exposure in both humans and animal models somehow alters the available energy in neurons. Functional MRI (fMRI) of blast-induced mTBI victims as has shown areas of decreased neuronal activity in the brain in a number of studies (Kim et al., 2004, Jantzen, 2010). Neuronal activity is measured by the turnover of oxygen from hemoglobin and has been linked to ATP levels (Lei et al., 2003, Gafaniz and Sanches, 2010).

5.2 Intracellular ATP levels in shockwave-exposed cell cultures were lower than in non-exposed control cultures

I showed in Chapter 4 that shockwave exposure increased membrane permeability in a pressure dependent manner, with greater pressure causing greater permeability. I found that total ATP levels decreased in a different manner, in that there was a pressure cut-off, above which increasing pressure caused the same decreases in total cellular culture ATP levels. Total ATP levels were expressed relative to the non-exposed control cells (Figure 5.1). There was no change in the amount of total ATP in cells exposed to shockwaves generated from 100 psi of input pressure compared to non-exposed cells. Above 100 psi of input pressure there was a significant decrease in total ATP. Unlike membrane

permeability, represented as increases in soma fluorescence (Chapter 4), increasing input pressure did not lead to further decreases in total ATP. Exposure to 200 or 300 psi of input pressure created a more than a 40% decrease in total culture ATP levels compared to the non-exposed control cells (Figure 5.1). This suggests that some level of membrane permeability can be compensated for by the cells before it begins to effect ATP levels.

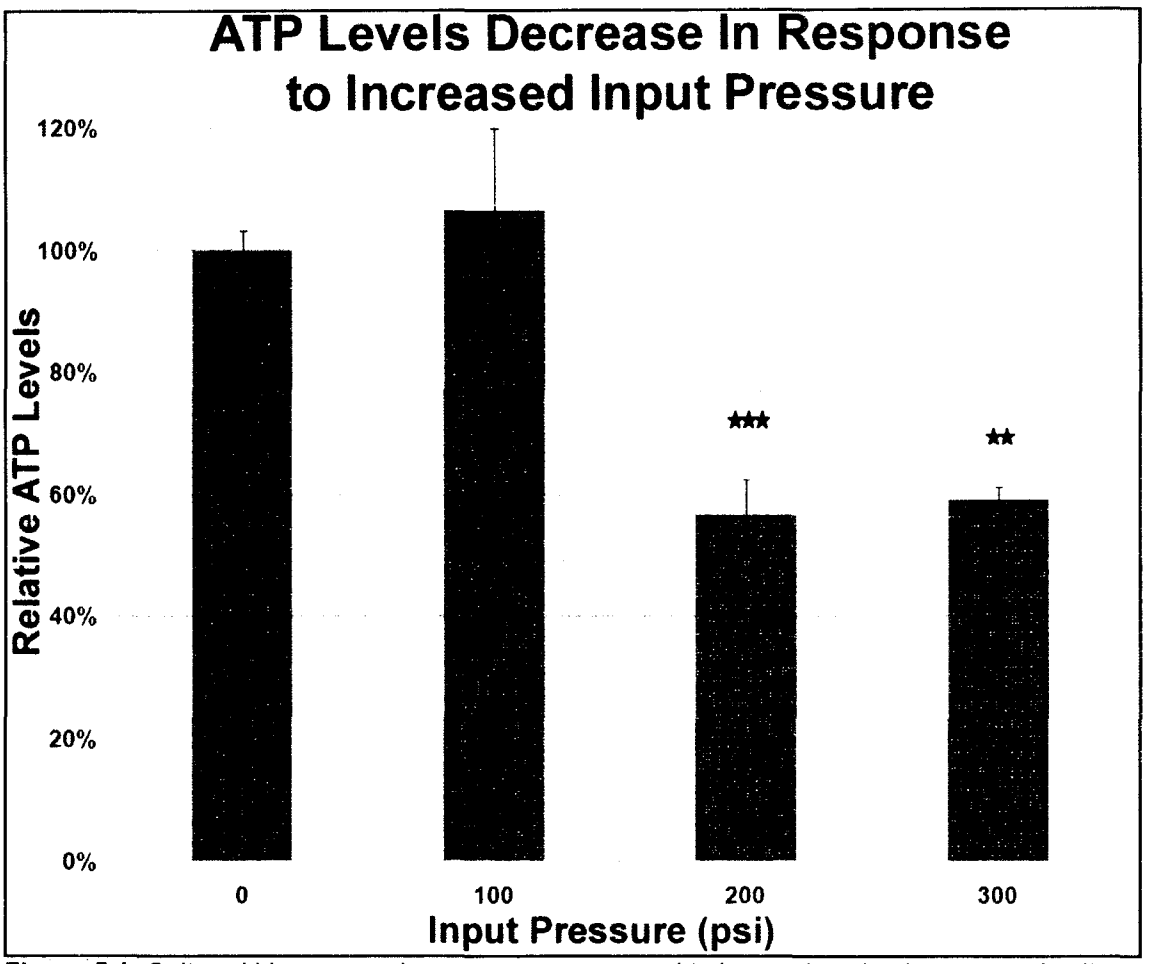

Figure 5.1: Cultured hippocampal neurons were exposed to increasing shockwaves and cultured for 24 hours before being harvested for the ATP luciferase assay. Total culture ATP levels were calculated relative to the 0 psi control cells. A decrease in total culture ATP levels was observed with increasing input pressure to a minimum of ~50% that of control culture ATP levels. *** = $p<0.0001$, ** = $p<0.001$ for comparison between exposed and non-exposed cells for any input pressure.

Previous work examining the excitotoxicity of prolonged glutamate stimulation on cultured neurons has found large decreases in whole culture ATP levels, which if not corrected led to apoptosis and necrosis (Chinopoulos et al., 2000, Maragos and Korde, 2004, Ward et al., 2007, Weisova et al., 2009, Cheng et al., 2010). It has also been demonstrated that cultured neurons can recover

from transient decreases in cellular ATP levels as large as 50% (Stout et al., 1998, Ward et al., 2007, Weisova et al., 2009).

5.3Total culture ATP levels were found to recover to non-exposed control levels within 2 days post shockwave-exposure

Since the shockwave-induced membrane permeability measured in Chapter 4 was found to recover with 2-6 hours of exposure I wanted to determine if the ATP level of the cells would recover as well. In order to determine the nature of the ATP decrease, a time course experiment was conducted. Total ATP levels were measured 1, 6 and 24 hours after shockwave exposure. A significant decrease in ATP levels of approximately 30% was observed in the first hour after exposure to a shockwave generated by 250 psi of input pressure. By 24 hours post-exposure, ATP levels continued to be significantly below the levels of non-exposed neurons (Figure 5.2).

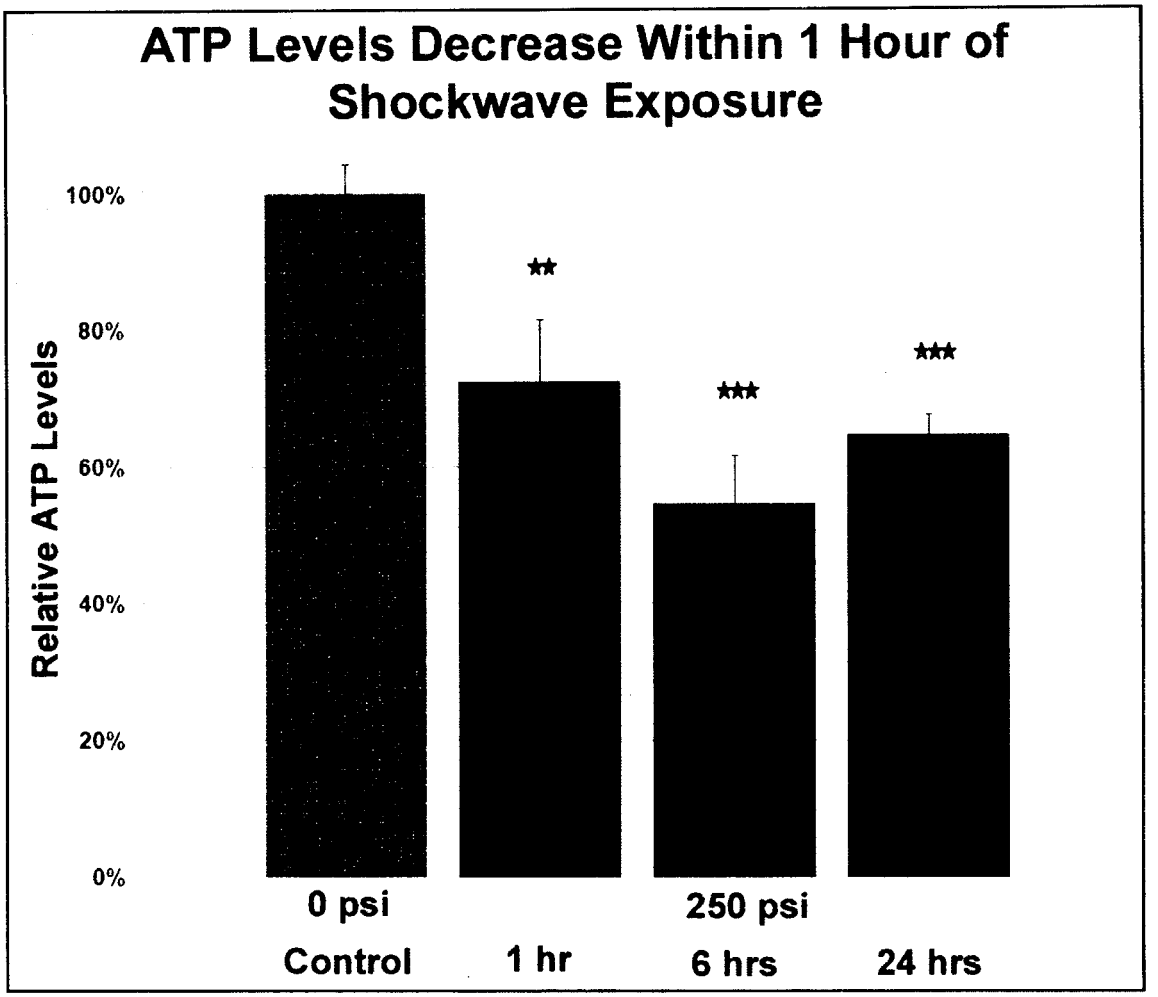

Figure 5.2: Shockwave-exposed hippocampal neuronal cultures showed a detectable decrease in total ATP levels within 1hr of exposure. At 6 hours post- exposure the decrease in total ATP was similar to the levels observed at 24 hours post-exposure. *** = $p<0.0001$, ** = $p<0.001$ for comparison between exposed and non-exposed cells for any time point.

ATP levels were found to recover to non-exposed levels within 48 hours after exposure (Figure 5.3). The recovery was maintained for an additional 3 days, at which point the experiment was halted (96 and 120 hours not shown). The cells fully recover to normal, non-exposed ATP levels and are able to maintain these levels within 48 hours of shockwave exposure.

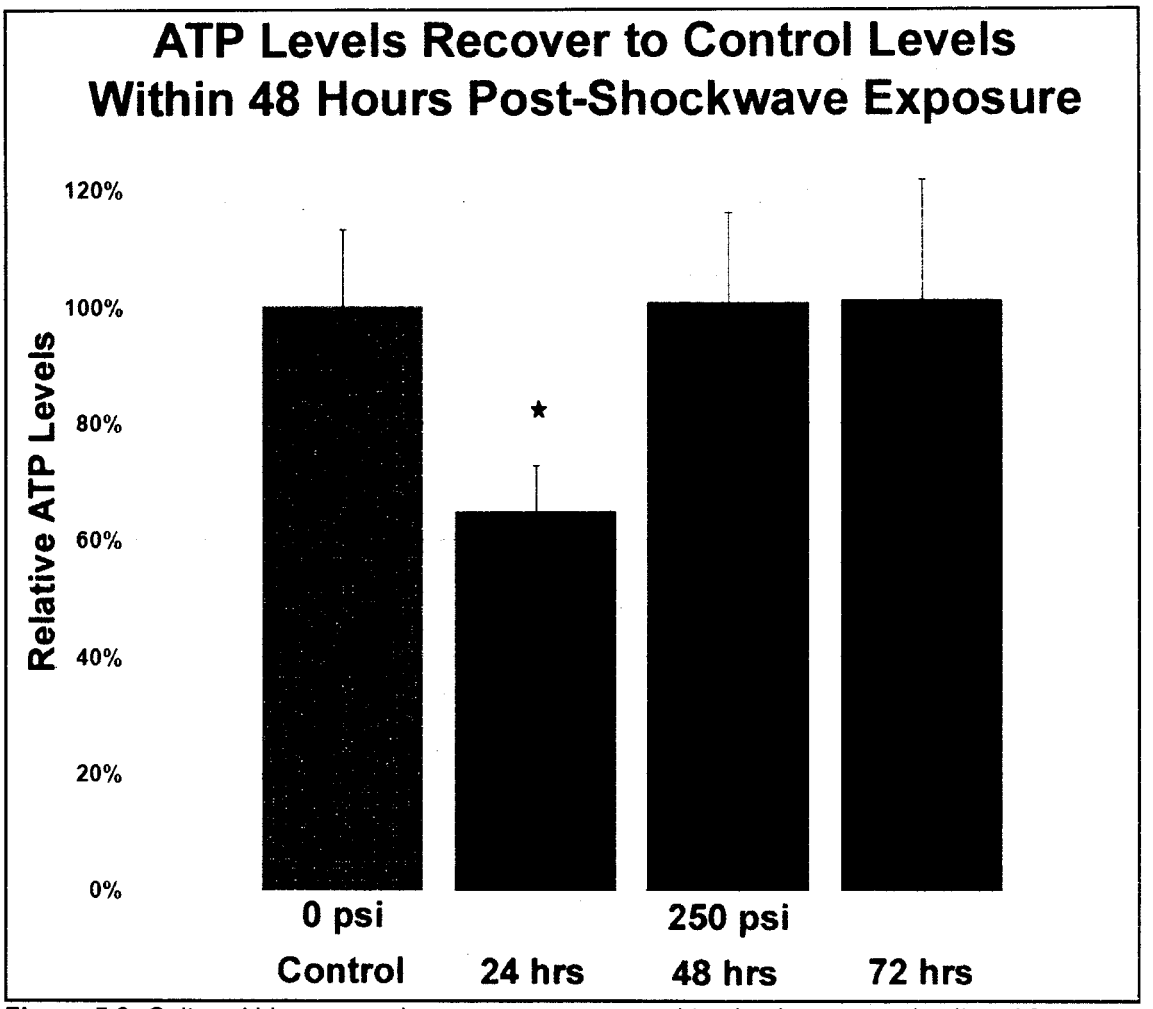

Figure 5.3: Cultured hippocampal neurons were exposed to shockwaves and cultured for increasing amounts to time to assay for possible recovery to non-exposed (0 psi) levels. Total culture ATP levels were calculated relative to the non-exposed cells for each time point assayed. A decrease in total culture ATP was observed at 24 hours and found to return to non-exposed levels by 48 hours after exposure. Cultures returned to and maintained non-exposed culture levels of ATP after 48 hours for at leats 5 days (data not shown).* = $p<0.01$ for comparison between exposed and non-exposed cells for any time point.

5.4 Implications of decreased cellular ATP in neurons

Prolonged energy depletion has been shown to cause apoptosis and necrosis in cultured neurons and is believed to be an important component in many neurodegenerative diseases. Excitotoxicity is a neuropathy associated with

a prolonged overactivation of excitatory receptors, particularly glutamate receptors of the N-methyl-D-aspartic acid (NMDA) type. This prolonged activation results in a disturbance in the cellular ion gradients which causes a decrease in cellular ATP levels that can lead to necrosis or apoptosis (Ward et al., 2007, Weisova et al., 2009, Concannon et al., 2010). When primary cultured neurons are briefly (<10 minutes) incubated with glutamate (~100μM) a decrease in cellular ATP levels can be seen within an hour after stimulation (Ward et al., 2007, Weisova et al., 2009, Concannon et al., 2010). This decrease is severe (>50%) compared to non-stimulated cells, but cells have been shown to recover back to pre-stimulation levels within 6 hours (Ward et al., 2007, Weisova et al., 2009, Concannon et al., 2010). Continuous exposure to the same glutamate signal causes prolonged depletion of cellular ATP levels and increased cell death (both necrotic and apoptotic) in the culture (Ward et al., 2007, Concannon et al., 2010). Often a delayed onset of apoptosis is observed after prolonged glutamate stimulation, with some cells surviving more than 24 hours after the removal of the stimulant before undergoing apoptosis. A key component to glutamate induced excitotoxicity is the increase in cellular Ca^{2+} levels which are believed to trigger a number of different cellular pathways leading to the delayed apoptosis. While there is still debate over the length of time required to induce apoptosis or cause necrosis it has been shown that cultured neurons can survive a transient ATP depletion.

Mitochondrial dysfunction and by extension energy (mis)regulation has been implicated in a number of different neurodegenerative diseases including Huntington's disease (HD) and Alzheimer's disease (AD). Mitochondria have been found to localize along neuronal processes and have been found at presynaptic terminals as well as dendritic spines (Cameron et al., 1991, Sheehan et al., 1997, Popov et al., 2005). Mitochondrial distribution in dendrites is regulated by neuronal activity and disruption of mitochondrial localization results in a decrease in the number of synapses (Li et al., 2004).

The exact mechanism of Huntington's disease is currently unclear and there are many different animal models used to study the condition. One method used to generate a mouse model very similar to the human condition is the administration of 3-nitropropionic acid or malonate both of which inhibit complex II of the electron transport chain in mitochondria (Beal et al., 1993, Greene et al., 1993). The Huntingtin gene has been shown to encode a protein that is known to associate with the mitochondrial membrane, though the nature of the interaction is unclear (Panov et al., 2002).

An early indicator of AD is a decrease in glucose metabolism in specific regions of the brain (Ferreira et al., 2010b). One of the known autosomal dominant forms of inheritable AD is a mutation in the presenilin-1 gene that encodes a protease which is known to regulate the activity of Notch. Notch signaling has been shown to be involved in synaptic plasticity and has been

shown to interact with mitochondrial remodeling proteins (Costa et al., 2003, Perumalsamy et al., 2010).

The onset of many of the neurodegenerative diseases, including AD, is a prolonged process that normally does not begin to manifest until late adulthood. The gradual progression suggests that while ultimately the loss of neurons is the visible and terminal result of the disease it is not the cause, and that perhaps an increasing loss of function plays an earlier role in its progression. The protracted time course observed in neurodegenerative diseases is similar to the symptoms observed in mTBI suffers. Often the onset of blast-induced mTBI takes a week or more to fully manifest and the symptoms can remain for years after the injury.

5.5 Chapter 5 summary

We have shown that there is a direct correlation between shockwave exposure and membrane permeability in cultured neurons and that shockwave-exposed cultures have lower total ATP levels compared to non-exposed cultures. We quantitated a pressure dependent decrease in cellular ATP levels in shockwave-exposed cultures which were able to recover to non-exposed levels after 2 days. ATP recovery lagged significantly behind membrane repair by almost 2 days and could be due to a number of reasons, including altered gene expression. Large scale transcript analysis on the brains of blast-exposed animals has revealed significant changes in the expression of dozens of genes occurring within 1 day of exposure and continuing to evolve as late as 7 days

after exposure (Pun et al., 2011, Risling et al., 2011). The largest changes in expression for most genes occurred between day 1 and day 4 post-exposure, which is well after our experimental system would predict that shockwave-induced membrane permeability and ATP depletion would be repaired. Given the prolonged evolution of symptoms many suffers of mTBI display, it seems likely that there is a mechanism(s) involved in the pathology of shockwave-induced mTBI that are slower acting or late to develop. This idea is supported by fMRI studies of soldiers who suffered a blast-induced mTBI and show prolonged decreases in the metabolism of specific areas of the brain months after injury.

CHAPTER 6

GENE GUN GENERATED SHOCKWAVES CAUSE SYNAPTIC DEGENERATION IN CULTURED NEURONS

6.1 Introduction

We have shown that our experimental system can produce a non-lethal shockwave of ~1 psi, similar in magnitude to the pressures recorded in the brains of animal mTBI models and this shockwave causes transient membrane permeability and transient decreases in cellular ATP levels in cultured neurons. We next wanted to investigate the downstream effects of the transient membrane permeability and energy decrease. An energy decrease should have a profound effect on a neuron, since neurons depends on a number of ATP-dependent processes including, ATP-dependent ion pumps to maintain the electrochemical gradient and ATP-dependent motor proteins to move macromolecular complexes and vesicles out to synapses. For example, the Na/K-ATPase pump moves Na^+ out of the cell and K^+ into the cell through the hydrolysis of ATP and the Ca-ATPase moves Ca^{2+} out of the cell or into a cellular organelle (Hammond, 2001). When the neuron fires an action potential, voltage-gated ion channels open in response to the depolarization of the membrane, allowing Na^+, Cl^- and Ca^{2+} to enter the cell, further depolarizing the membrane and moving the reaction further down the axon. Without constant maintenance, the electrochemical gradient is lost and the neuron is incapable of firing an action potential (Hammond, 2001).

Neurons also have other ATP-dependent processes including active transport of RNA, proteins and vesicles from the cell soma out to the synapses. Previous research has demonstrated that disruption of the active transport machinery results in a decrease in the number of synapses in cultured neurons and previous research from our lab has demonstrated that disruption of active transport is an early sign of decreased ATP levels (Goetze et al., 2006, Heinrich and Deshler, 2009). We therefore wanted to measure the density of synapses in neurons exposed to shockwaves in our system to determine if the drop in ATP levels we observed cause synaptic degeneration in cultured neurons and possibly in mTBI.

6.2 Overview of the synaptic markers assayed by immunocytochemistry after shockwave exposure

Synapses are the junction of two cells and have distinct sides, generally defined as pre-synaptic and post-synaptic. The pre-synaptic side belongs to the axon and is the origin of the signal being sent between the cells, while the post-synaptic side is the dendrite receiving the signal. In order to survey as many synapses as possible we used 3 different synaptic proteins that are known to be reliable markers for synapses due to their relative abundance at most synapses, and the availability of good antibodies to stain them. We assayed for 2 post-synaptic proteins, the ubiquitous scaffolding protein, Post Synaptic Density protein 95 (PSD95) and the Glutamate Receptor subunit 1 (GluR1) subunit of the

α-amino-3-hydroxy-5-methyl-4-isoxazolepropionic acid (AMPA) receptor family. PSD95 is a member of the Membrane Associated Guanylate Kinase (MAGUK) family, is a 95 kDa protein with three PDZ domains, a SRC Homology 3 (SH3) domain, and a guanylate kinase-like domain (GK) and it is found at the majority of all post synaptic sites. Together with PSD93, PSD95 forms a heteromultimer, binds the cytoplasmic domains of receptor proteins and ion channels, and has been shown to decrease in abundance at synapses as a result of loss of active transport (Goetze et al., 2006). GluR1 is a subunit of the AMPA receptor family, which is involved in fast synaptic transmission and synaptic plasticity. GluR1 is found at approximately 80% of all post-synaptic sites. It is a 50 kDa transmembrane protein that functions in a tetrameric manner with other Glutamate receptor subunits. The third protein chosen was a pre-synaptic marker, Synapsin1. Synapsins are involved in neurotransmitter release by helping to regulate vesicle fusion. Synapsin1 levels have been shown to decrease as a result of loss of active transport out to the synapses of cultured neurons (Goetze et al., 2006).

6.3 PSD95-labeled synapses decrease in a pressure dependent manner in hippocampal neurons

Hippocampal neurons were exposed to shockwaves generated with increasing amounts of input pressure and cultured for 24 to 48 hours before being fixed and stained for PSD95. PSD95 staining was quantitated with a non-

biased method which involved selecting a region of interest of a cellular process on one channel and exposing for synaptic labeling after the region of interest was selected. A decrease of approximately 45-60% was observed for input pressures of 200, 250 and 300 psi (Figure 6.1, 6.2). However, no difference was detected for cells exposed to shockwaves generated from 100 psi of input pressure compared to non-exposed cells. This pressure that leads to decreases in synapses correlates with the pressure that caused a drop in ATP levels and increased cell permeabilization. This indicates that an all-or-none pressure threshold effect is responsible for all these changes and may be linked. Input pressures of at least 200 psi caused a significant decrease in PSD95 synaptic density of approximately 60%. The decreases induced by input pressures of 200, 250 or 300 psi were not statistically different from one another.

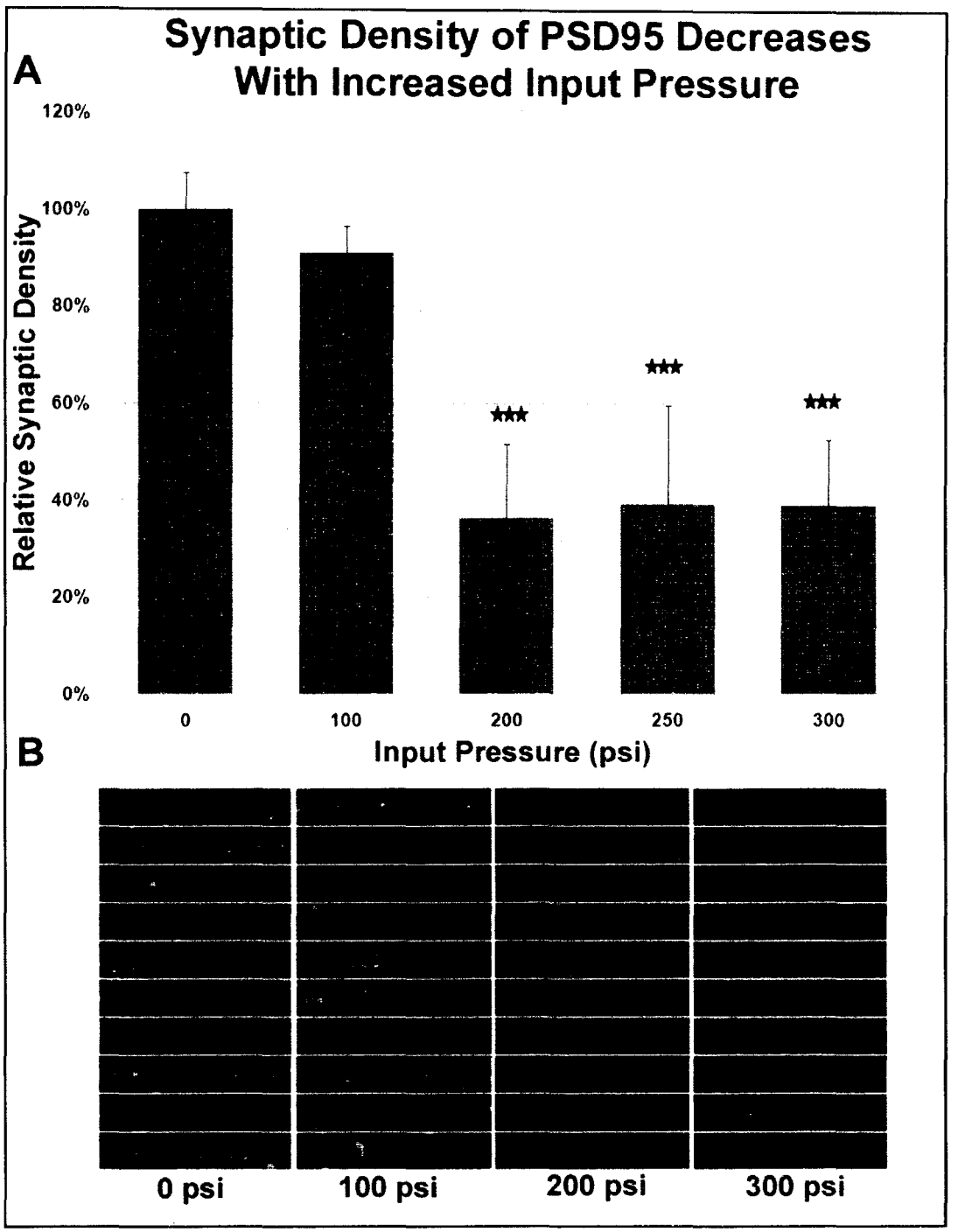

Figure 6.1: PSD95 staining in cultured hippocampal neurons decreases within 24 hours of exposure to Gene Gun generated shockwaves. A) Quantitation of at least 30 different 20 micron segments of neuronal processes. A significant decrease in the number of PSD95 puncta/micron was recorded in cells exposed to shockwaves generated with input pressures of 200 psi or greater. B) A selection of representative processes used in quantitation, each taken from a different cell. *** = $p<0.0001$, for comparison between exposed and non-exposed cells for any input pressure.

The 60% decrease observed in PSD95 synaptic density 24 hours after shockwave exposure is very similar to the 68% decrease in PSD95 synaptic density observed 3 days after siRNA knockdown of Staufen, a double-stranded RNA binding protein, required for active transport out to synapses (Goetze et al., 2006). Multiple replications of PSD95 synaptic density counting showed consistent decreases of ~50% 24 hours after exposure to shockwaves generated with 250 psi of input pressure.

In order to determine the duration of the PSD95 synaptic density decrease, neurons were cultured for 48 hours after shockwave exposure and PSD95 synaptic density was quantitated. Synaptic density of PSD95 remained well under the non-exposed control cells 48 hours after exposure (Figure 6.2).

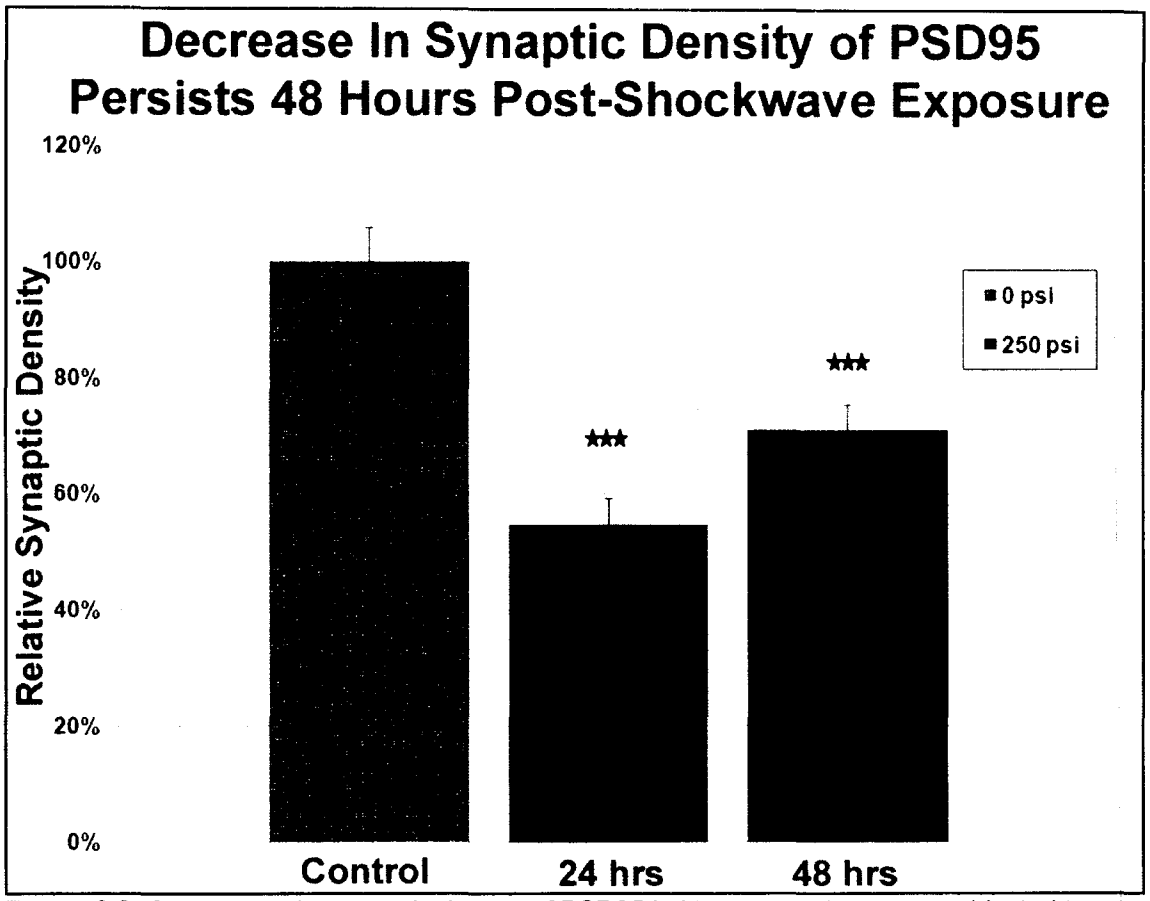

Figure 6.2: Changes in the synaptic density of PSD95 in hippocampal neurons subjected to shockwaves generated from 250 psi of input pressure show continued decreases 48 hours post-exposure. *** = $p<0.0001$, for comparison between exposed and non-exposed cells for any time point.

Unlike total ATP measurements, no recovery of PSD95 synaptic density was observed over the time points measured. By 48 hours post-exposure cells have repaired the shockwave-induced plasma membrane permeability and ATP decreases. It is possible that investigation of later time points post-exposure could show recover of PSD95 synaptic density to control levels.

6.4 GluR1 labeling decreases in cortical and hippocampal neuronal cultures exposed to Gene Gun generated shockwaves

We next investigated changes in synaptic density of the AMPA receptor subunit, GluR1, in cortical neurons. Cortical neurons were cultured identically to hippocampal neurons and exposed to shockwaves after 14 days *in vitro*. Cells were incubated for an additional 48 hours after shockwave exposure before being fixed and stained for GluR1. Images were quantitated with the same non-biased method used to quantitate PSD95. A similar pressure dependent effect was found for GluR1 in cortical neurons as was seen with PSD95 in hippocampal neurons, input pressures greater than 100 psi caused a consistent 40% decrease in the synaptic density of GluR1 (Figure 6.3). A decrease in the synaptic density of GluR1 was observed with an input pressure of 150 psi and increasing input pressure to 200 psi strengthened the decrease in GluR1 synaptic density.

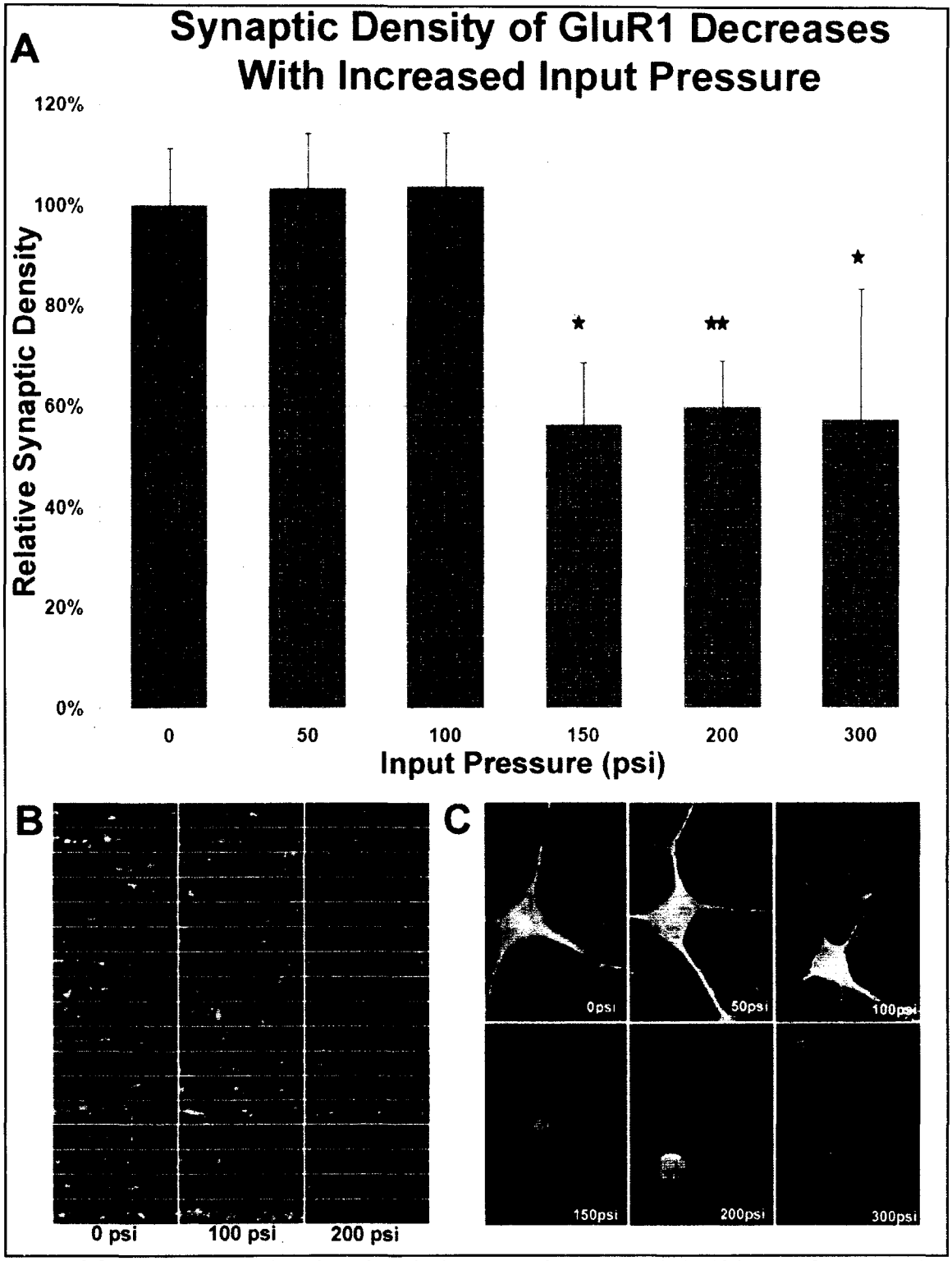

Figure 6.3: GluR1 staining in cultured cortical neurons decreases within 48 hours of exposure to Gene Gun generated shockwaves. A) Quantitation of at least 30 different 20 micron segments of neuronal processes. A significant decrease in the number of GluR1 puncta/micron was recorded

in cells exposed to shockwaves generated with input pressures of 150 psi or greater. B) A selection of representative processes used in quantitation, each taken from a different cell. C) Representative cells for 0 psi, 50 psi, 100 psi, 150 psi, 200 psi and 300 psi. ** = $p<0.001$, * = $p<0.01$ for comparison between exposed and non-exposed cells for any input pressure.

We also investigated changes in GluR1 synaptic density in hippocampal neurons at 24 and 48 hours post-exposure. A similar significant decrease of approximately 30% in GluR1 synaptic density was observed 24 and 48 hours after exposure (Figure 6.4).

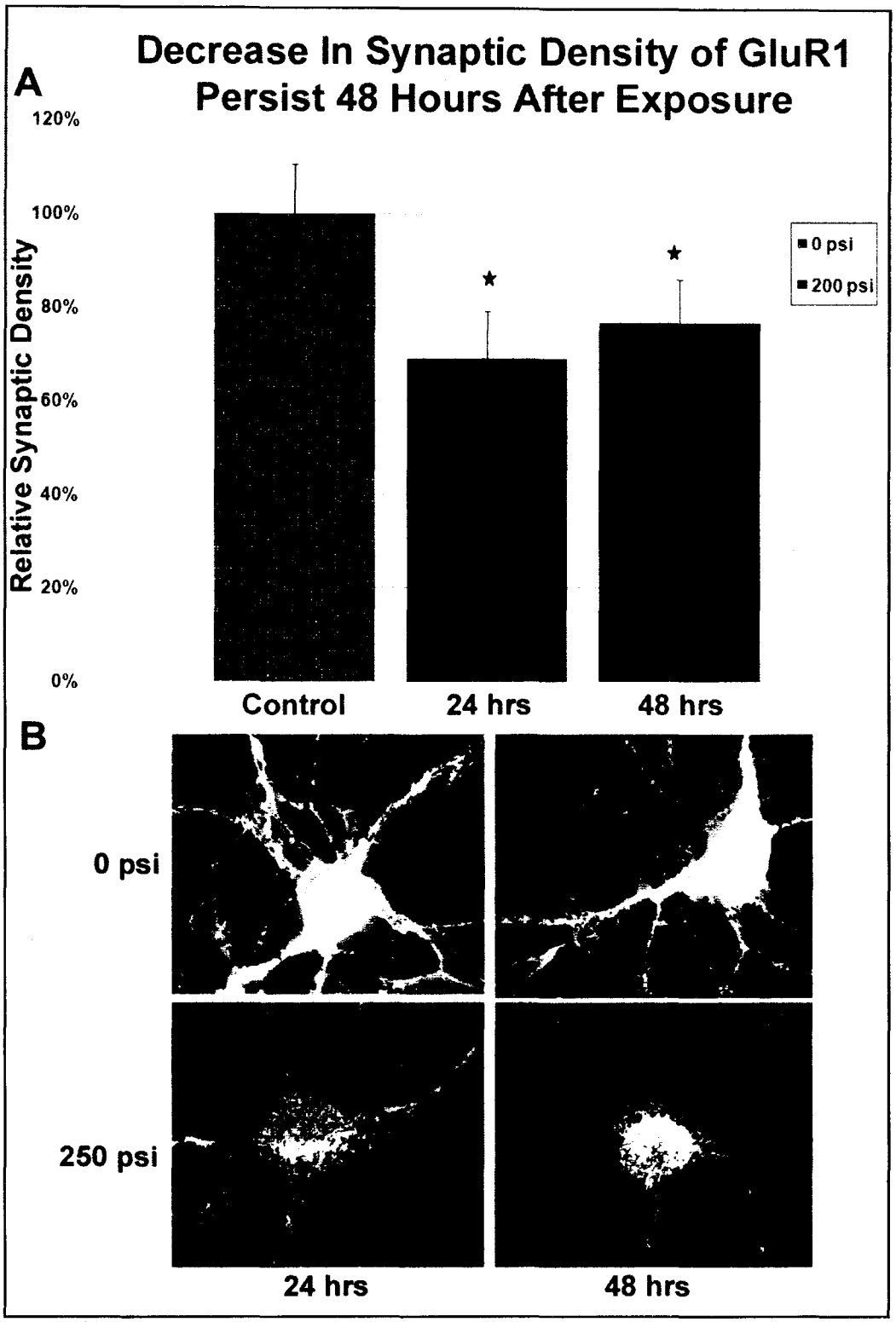

Figure 6.4: Changes in the synaptic density of GluR1 in hippocampal neurons subjected to shockwaves generated from 250 psi of input pressure show continued decreases 48 hours post-exposure. A) Quantitation of at least 30 different 20 micron segments of neuronal processes. B)

Representative cells from each time and pressure assayed in the quantitation. * = $p<0.01$ for comparison between exposed and non-exposed cells for any time point.

Similar decreases were observed in hippocampal neurons as were seen in cortical neurons, suggesting the effects of shockwave exposure are not specific to a single type of neuron and will therefore probably not be isolated to specific areas of the brain.

6.5 Synapsin1 labeling decreases in hippocampal cultures exposed to Gene Gun generated shockwaves

Next we investigated the response of the pre-synaptic marker, Synapsin1, to shockwaves. Thus far, we have shown large decreases in two post-synaptic proteins, which are found at the majority of post synaptic densities. Synapsin1 is abundant at the majority of pre-synaptic terminals and is a good representative of the axonal side of synapses. Hippocampal cultures were subjected to shockwaves generated with increasing input pressure and cultured for 24 hours after exposure. Cells were then fixed and stained for Synapsin1. Images were collected and quantitated with the same non-biased method used for PSD95 and GluR1. An approximate 40% decrease was observed in cells exposed to 250 psi-generated shockwaves, relative to controls (Figure 6.5). This decrease is similar to what was observed with PSD95 in hippocampal neurons as well as GluR1 in cortical and hippocampal neurons. Cells exposed to shockwaves generated from 100 psi of input pressure did not show any difference in Synapsin1 synaptic density compared to control cells.

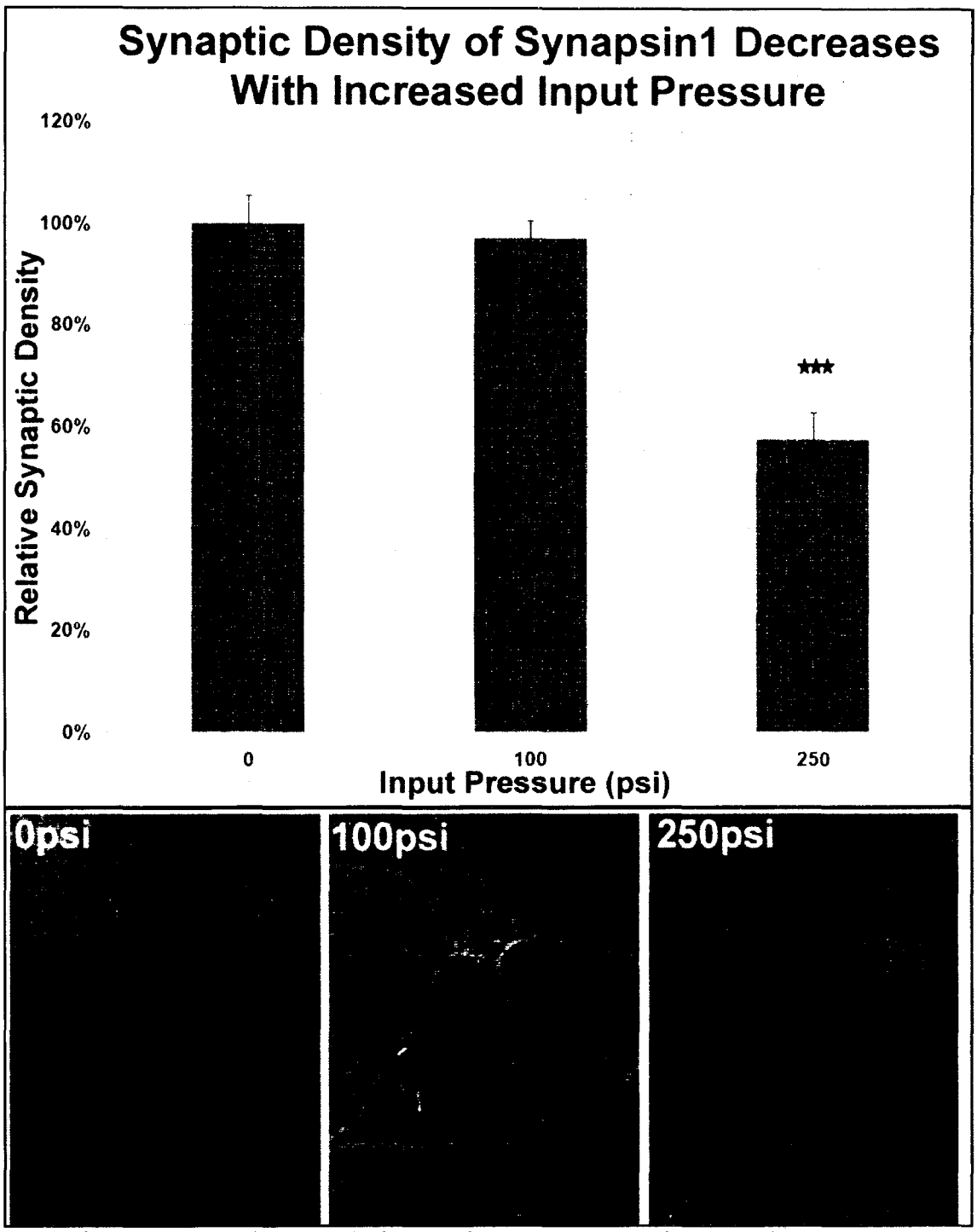

Figure 6.5: Changes in the synaptic density of synapsin1, shown in red, in hippocampal neurons subjected to shockwaves generated from 100 or 250 psi of input pressure show a pressure dependent decrease 24 hours post-exposure Quantitation of at least 30 different 20 micron segments of neuronal processes (Upper Panel). Representative cells from each pressure assayed in the quantitation (Lower Panel). *** = $p<0.0001$ for comparison between exposed and non-exposed cells.

The decrease we measured in Synapsin1 24 hours post-exposure is similar to the decrease measured in neuronal cells with disrupted trafficking (Goetze et al., 2006). Together, our results show decreased levels of pre- and post-synaptic markers with 250 psi shockwaves, which is consistent with a decrease in synaptic densities in shockwave exposed cells.

6.6 Synaptic labeling decreases correlate with increased Dextran permeability

Our experimental system has thus far demonstrated many shockwave-induced changes in cultured neurons. In an effort to definitively link the decrease in synaptic density with the increase in membrane permeability a co-labeling experiment was performed. In order to perform this experiment I needed to determine if cells could be incubated in Dextran-conjugated dye for 24 hours and still show a significant difference in average soma fluorescence between shockwave-exposed and non-exposed cells. A time course experiment was performed using the maximum input pressure and the 3kDa Dextran conjugate. Incubation time points of 10, 30, 60, 240 and 1440 minutes post-exposure were tested. I found that longer incubation times resulted in greater dye penetration for both exposed and non-exposed cultures, however relative differences in average soma fluorescence between exposed and non-exposed cells was maintained with increased incubation time and by 24 hours post-exposure had actually increased (Figure 6.6).

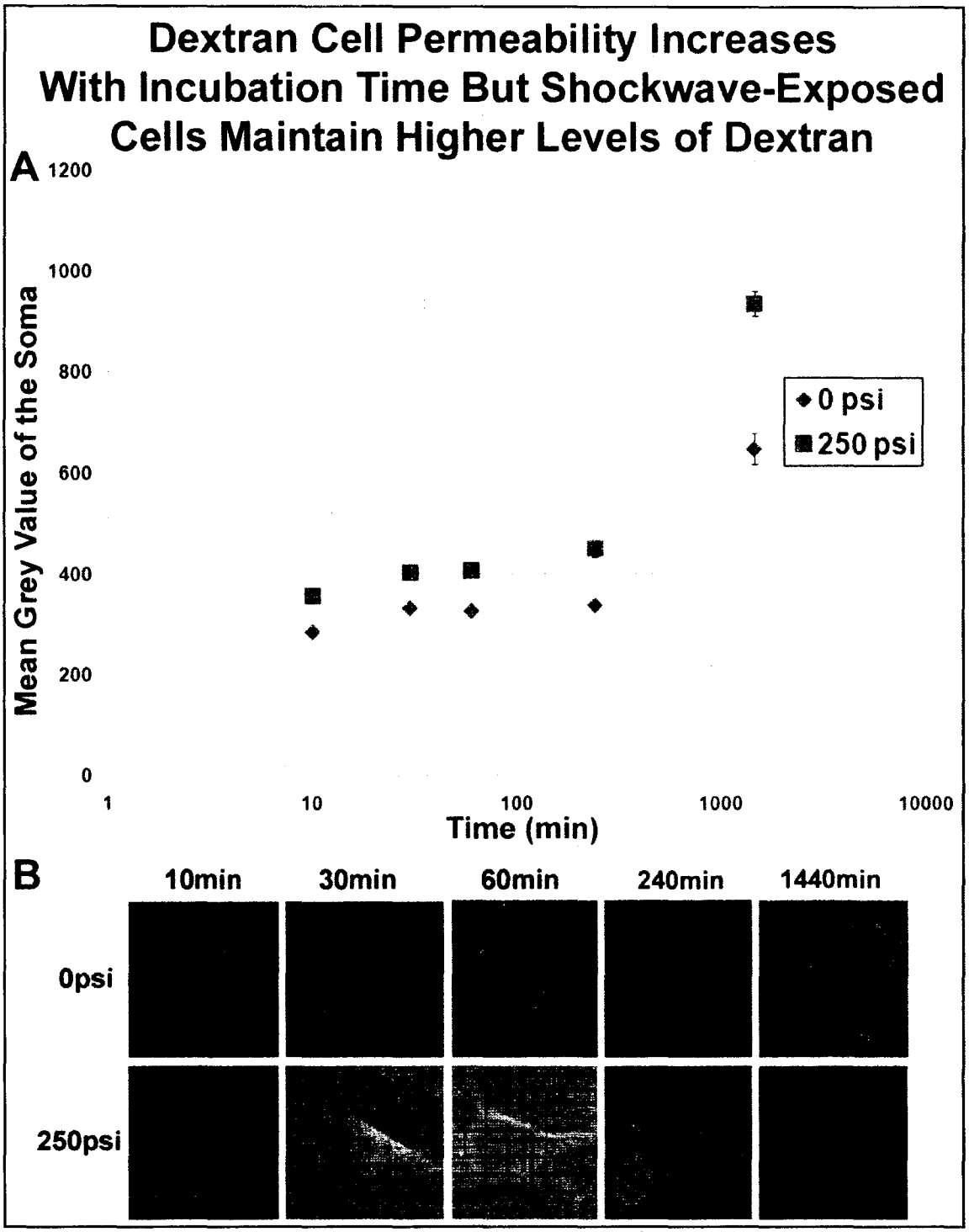

Figure 6.6: The soma loading of 3kDa Dextran-conjugated fluorescein increases with incubation time for both exposed and non-exposed cells, though the relative difference between exposed and non-exposed cells increases only slightly (1.2 to 1.4 fold) after 24 hours incubation. A) Neurons exposed to shockwaves generated from 250 psi of input pressure show increased loading at all time points compared to non-exposed (0 psi) control neurons. Time points

measured: 10min, 30min, 60min, 4 hours and 24 hours. B) Representative images of each time point are shown in panel B.

Having determined I could incubate cells for 24 hours with the 3kDa Dextran conjugate offered the possibility to do a correlation analysis, thus hippocampal neurons were exposed to 0 psi or 250 psi of input pressure and then incubated in media containing 3 kDa Dextran-conjugated fluorescein for 24 hours before being fixed and stained for pre- and post- synaptic markers. The pre-synaptic marker, Synapsin1, and the post-synaptic marker, PSD95, were used. Shockwave exposure, incubation and cell labeling were identical to the above labeling experiments for Synapsin1 and PSD95. Cells were incubated in 3kDa Dextran-conjugated fluorescein for 24 hours after shockwave exposure before being fixed and stained for the synaptic marker. Images were collected based on DIC morphology and DAPI staining. Images were quantitated using the same non-biased method employed above. At least 25 cells from each pressure were measured for both synaptic density as well as Dextran labeling in the soma.

Histograms of levels of each synaptic marker show distinct populations of cells based on shockwave exposure. A Pearson's linear Bivariate correlation analysis shows a negative correlation between increased Dextran labeling and decreased synaptic density labeling for both markers tested. The synaptic density of PSD95 was found to be negatively correlated to Dextran permeability from exposure to shockwaves produced from 250 psi of input pressure with a correlation coefficient of $r = -0.681$ (189) $p < 0.0001$ (Figure 6.7). A clear distinction can be seen between input pressures known to cause synaptic

degeneration and membrane permeability (250 psi vs 0 psi or 100 psi). We have strongly supported the hypothesis that there is an inverse correlation between shockwave-induced membrane permeability and decreases in synaptic densities.

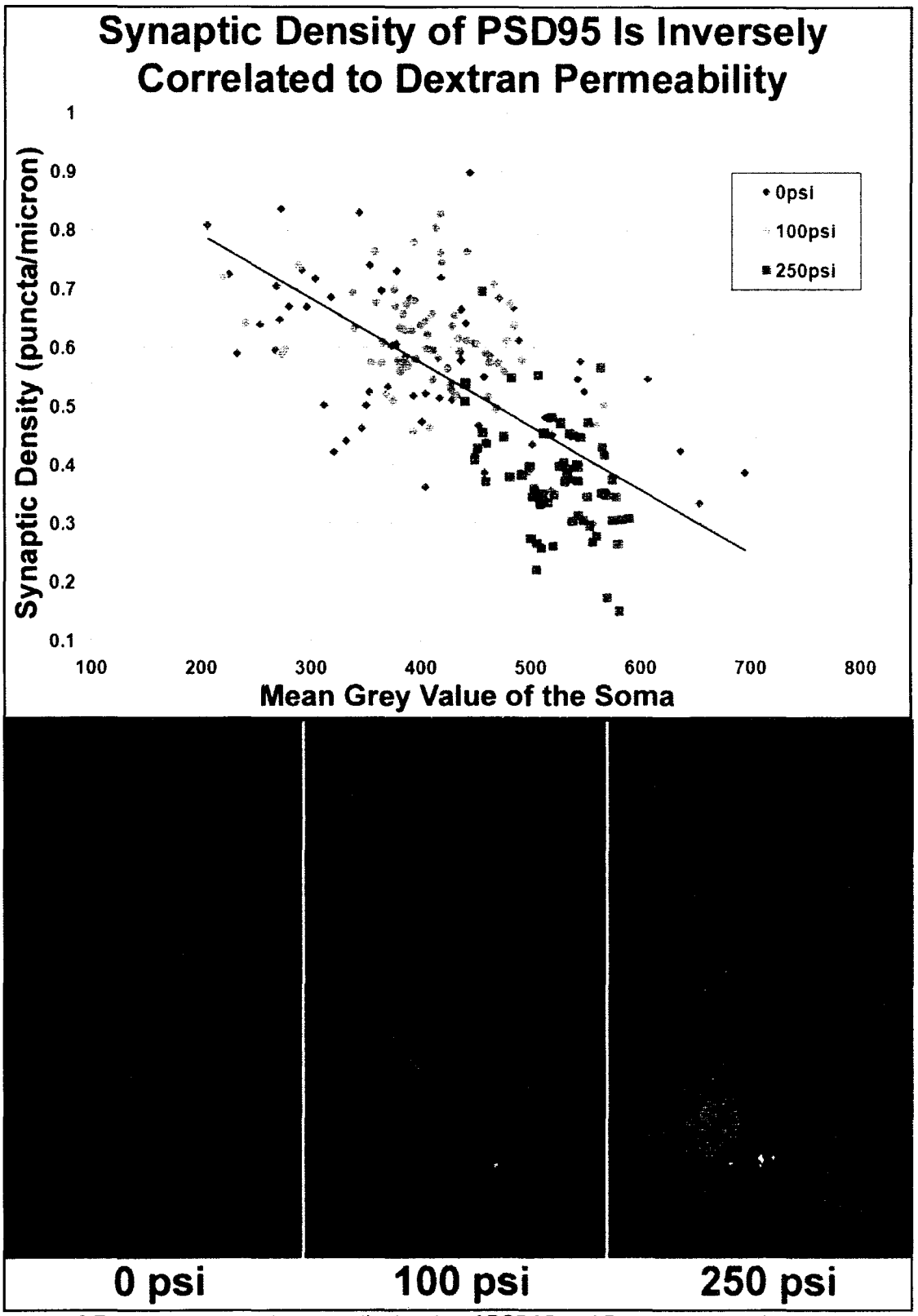

Figure 6.7: A histogram of the synaptic density of PSD95 and Dextran soma labeling for three

different input pressures. A Pearson's linear regression bivariate correlation shows a negative relationship between Dextran soma fluorescence and synaptic density of PSD95, r = -0.681 (189) p<0.0001. 0 psi are represented by blue diamonds, 100 psi by green circles and 250 psi by red squares. Representative cells from each pressure point are shown in the lower panel, PSD95 is red, Dextran is green and nuclear DAPI staining is blue.

In a similar finding to PSD95, Synapsin1 synaptic density was shown to also negatively correlate with Dextran soma labeling. Shockwaves generated by 250 psi of input pressure cause decreases in the synaptic density of Synapsin1 and increased membrane permeability with a correlation coefficient of r = -0.734 (119) p<0.0001 (Figure 6.8).

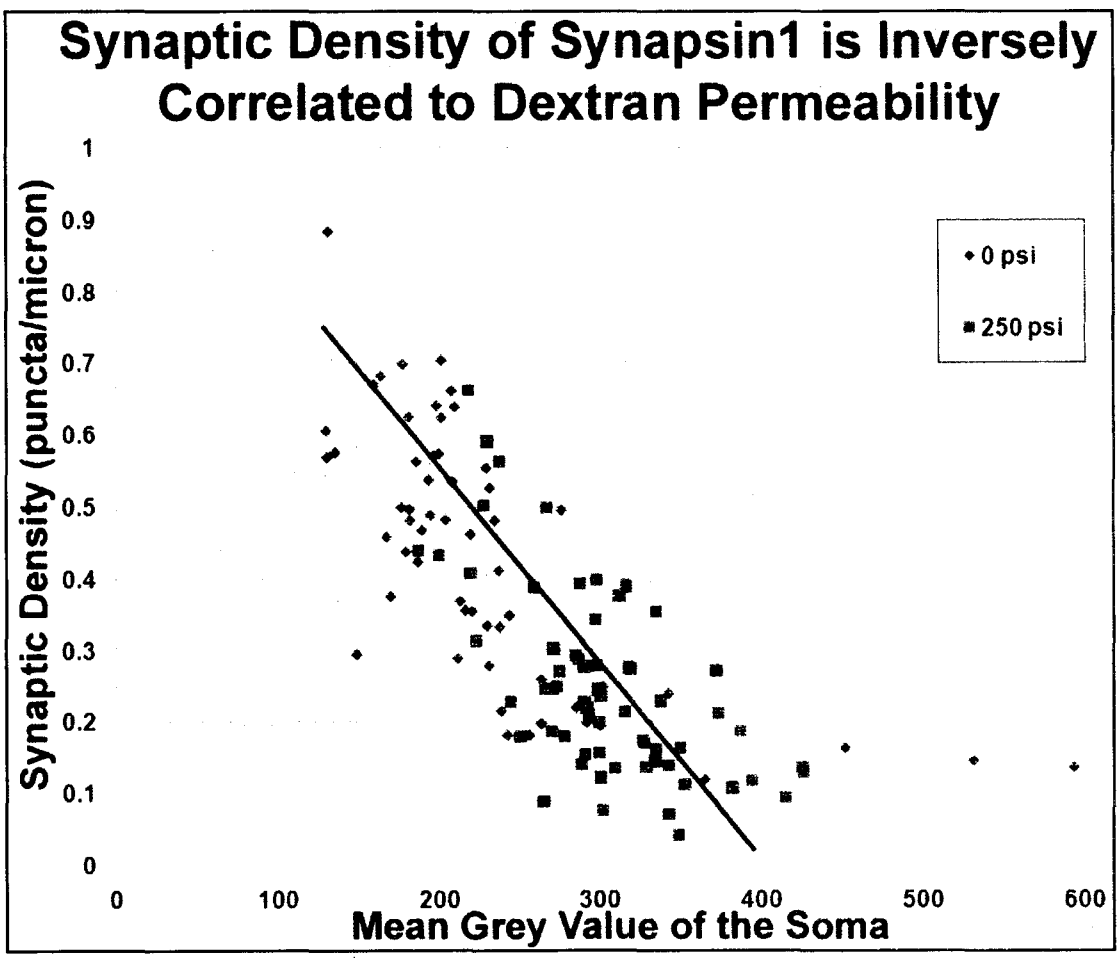

Figure 6.8: A histogram of the synaptic density of Synapsin1 and Dextran soma labeling for two different input pressures. A linear regression and bivariate correlation show a negative

relationship between Dextran soma fluorescence and synaptic density of Synapsin1, r = -0.734 (119) p<0.0001. 0 psi are represented by blue diamonds and 250 psi by red squares.

Together, these findings of very strong, significant negative correlation between Dextran soma labeling and decreases in two ubiquitous pre- and post-synaptic markers show that shockwaves cause synaptic degeneration through membrane permeabilization *in vitro* and suggest that a similar mechanism could be occurring in shockwave-induced mTBI.

6.7 Western blot data show similar decreases in some synaptic proteins

We have shown that shockwaves permeabilize cell membranes and decrease total ATP in cultured neurons and that this permeability is directly linked to synaptic degeneration. Loss of transport is known to cause synaptic degeneration and the decreases in synapse abundance observed with immunocytochemical analysis could be the result of decreased active transport out to synapses due to decreased ATP. Shockwave exposure has also been shown to cause increased proteolysis of certain cytoskeletal proteins leading to overall decreases in the total levels of these proteins. A blast-induced model of mTBI has shown increased proteolysis of the cytoskeletal protein αIIspectrin in rats after exposure to a blast overpressure of 1.7 psi starting at 12 hours post-exposure, with decreases still detectable at 7 and 14 days post-exposure (Park et al., 2011). Given this information, it is also possible that the decreases in numbers of synapses observed were the result of protein degradation and not disrupted transport.

In order to determine if the changes observed with immunocytochemistry were the result of decreased transport out to synapses, protein degradation or a combination of both of these mechanisms; western blots were performed for 20 different synaptic markers, including the PSD95, Synapsin1 and GluR1, found to decrease by immunocytochemistry. Hippocampal neurons were subjected to shockwaves generated from 250 psi of input pressure and cultured for 1 to 4 days after exposure. Cells were then collected on ice and assayed for total protein using the BCA total protein assay. Equal amounts of total protein were loaded in each western blot based on the BCA protein assay. In addition, as a loading control, either a housekeeping gene (eEF1A1) or cytoskeletal structure protein (αTubulin) was analyzed for each synaptic marker investigated. Our study focused a small set of proteins implicated in a variety of functions including synaptic structure (PSD93, PSD95, SAP97, Tau and αsynuclein), receptor localization (GRIP1, CaMII Kinase, CASK and Kinesin), neurotransmitter release (Synapsin1 and Synaptojanin), receptors (GluR1 and GluR2), synaptogenesis (GAP43, Synaptophysin, Neuroligin, Neuronal Pentraxin2 and Neurexin1β) (Table 6.1). A summary of all the proteins assayed as well as the changes observed are shown in Table 6.1.

We discovered only a small subset of the proteins assayed altered protein levels after shockwave exposure and that the time and amount of change in protein was unique for each. Out of the three synaptic proteins found to decrease by immunocytochemistry after shockwave exposure, only GluR1 failed to show

any change in protein levels by western blot (Figure 6.9). Levels of GluR1 protein remained similar to the non-exposed control at 24 hours, 3 and 4 days post-exposure. The loss of synaptic staining with GluR1 observed by immunocytochemistry could be the result of decreased active transport out to the synapses while the overall level of GluR1 protein remains the same in the cell. This result supports a mechanism where shockwave-induced disruption in the active transport out to synapses leads to synaptic degeneration.

In an opposite finding, Synapsin1 protein levels were found to decrease to ~65% of non-exposed control cells after 24 hours and did not show signs of recovery at 3 or 4 days post-exposure. Synapsin1 protein levels were found to decrease by 34.7 +/-11.3% within 24 hours of shockwave exposure, which is very similar to the 40 +/-9.1% decrease in synaptic staining observed by immunocytochemistry 24 hours after shockwave exposure (Figures 6.9 and 6.5). A similar decrease in Synapsin1 was observed by immunocytochemistry 3 days after siRNA knockdown of the RNA binding protein Staufen in cultured hippocampal neurons (Goetze et al., 2006). The decreases in Synapsin1 as measured by immunocytochemistry and western blot 24 hours after shockwave exposure were nearly identical and could indicate protein degradation as the cause of synaptic degeneration in this case. However, given the similarity of the decrease in synaptic staining of Synapsin1 measured after disruption of active transport by siRNA knockdown of Staufen to the decrease measure by western

blot, it seems likely that both protein degradation and disruption of active transport play a role in the shockwave-induced decrease of Synapsin1.

The final protein assayed by immunocytochemistry also assayed by western blot was PSD95. The changes in protein level for PSD95 were different from both those of GluR1 and Synapsin1. PSD95 protein levels were found to be similar to the non-exposed control 24 hours after shockwave exposure, suggesting the decreases observed by immunocytochemistry were the result of disrupted active transport. However, by 3 days post-exposure, levels of PSD95 showed a 17.6% +/-0.7% decrease compared to non-exposed cells, which is approximately half of the 30% +/- 11% decreased observed after 48 hours by immunocytochemistry (Figure 6.9). By 4 days post-exposure, levels of PSD95 protein were substantially lower, down by 60% +/-17.4% compared to non-exposed cells. These findings support the involvement of both loss of transport and protein degradation contributing to the decrease of PSD95 from synapses. Changes in PSD95 protein levels and localization have been associated with mental impairment in a rat model of age-related cognitive decline (VanGuilder et al., 2011). This association has been confirmed in human Alzheimer's patients with mild cognitive impairment. Western blot analysis of PSD95 protein levels was performed immediately post-mortem (<3 hours) on the brains of Alzheimer's patients with mild cognitive impairment and found a 30% decrease in total PSD95 protein levels compared to control samples (Sultana et al., 2010). Since the half-life of PSD95 is approximately 36 hours *in vitro*, the initial decrease

measured by immunocytochemistry could be the result of decreased transport of PSD95 out to the synapses due to decreased cellular ATP (El-Husseini Ael et al., 2002).

In addition to PSD95 and Synapsin1 another protein was found to decrease in response to shockwave exposure. Another subunit of the AMPA receptor, GluR2, was found to decrease to 64 +/-1.2% of the non-exposed control cells within 24 hours of shockwave exposure. However, unlike PSD95, the levels did not continue to decrease but rather eventually recovered to control levels by 4 days post-exposure (Figure 6.9). By 4 days post-exposure levels of GluR2 had risen to 94.2 +/-2.1% of non-exposed cells. GluR2 mRNA is known to be actively transported out along processes and undergoes local protein synthesis at synapses (Aranda-Abreu et al., 1999, Grooms et al., 2006). These findings further support the involvement of both disruption of active transport and protein degradation in the pathology of shockwave-induced synaptic degeneration.

Synaptic Proteins Assayed By Western Blot					
Synaptic Marker	**Results**		**Synaptic Marker**	**Results**	
αSynuclein	24 hours	no change	NSE	24 hours	83.6 +/- 12.6%
	3 day	no change		3 day	99 +/-0.7%
	4 days	no change		4 days	83.7 +/- 12.5%
CamKII Kinase phosphorylated Tyrosine 305	24 hours	101 +/- 0.7%	PSD93	24 hours	95.7 +/- 3.1%
	3 day	101.2 +/-0.8%		3 day	104.3 +/- 2.9%
	4 days	108.3 +/-5.6%		4 days	102.5 +/- 1.7%
CASK	24 hours	no change	PSD95	24 hours	109 +/-10%
	3 day	no change		*3 day*	*82.4 +/- 0.7%*
	4 days	90.7 +/-6.9%		*4 days*	*41 +/- 17.4%*
GAP43	24 hours	no change	PSD95 phosphorylated Serine 295	24 hours	107.6 +/- 5.2%
	3 day	no change		3 day	100.9 +/- 0.7%
	4 days	no change		4 days	86.1 +/- 10.6%
GluR1	24 hours	96.9 +/-2.2%	S100β	24 hours	93.7 +/- 4.6%
	3 day	106.4 +/-4.4%		3 day	102.1 +/- 1.5%
	4 days	99.1 +/-0.6%		4 days	90.2 +/- 7.3%
GluR1 phosphorylated Serine 845	24 hours	100.2 +/-0.1%	SAP97	24 hours	97.1 +/- 2.1%
	3 day	94.9 +/-3.7%		3 day	94.1 +/- 4.3%
	4 days	94.4 +/-4.1%		4 days	72.5 +/- 22.5%
GluR2	*24 hours*	*64.3 +/-1.2%*	Synapsin1	*24 hours*	*65.3 +/- 11.3%*
	3 day	*50.2 +/-33.7%*		*3 day*	*60.2 +/- 10.8%*
	4 days	*94.2 +/-2.1%*		*4 days*	*79.7 +/- 1.6%*
GluR2 phosphorylated Serine 880	*24 hours*	*19.8 +/-13.5%*	Synapsin1 phosphorylated Serine 549	24 hours	101 +/- 0.7%
	3 day	*22 +/-12.1%*		3 day	97.7 +/- 1.7%

	4 days	*14.6 +/-2.9%*		4 days	91 +/-6.7%
Grip1	24 hours	103.9 +/-2.7%	Synaptophysin	24 hours	97.8 +/-1.5%
	3 day	91.2 +/16.5%		3 day	90 +/-7.4%
	4 days	107.8 +/-5.3%		4 days	90 +/-7.4%
Kinesin	24 hours	117.5 +/-11.4%	Synaptojanin	24 hours	100.7 +/-0.5%
	3 day	99.5 +/-0.4%		3 day	101.9 +/-1.3%
	4 days	86.1 +/-10.6%		4 days	94.7 +/-3.9%
Neurexin1β	24 hours	97.2 +/-2%	Tau	*24 hours*	*203.5 +/-61%*
	3 day	95.1 +/-3.6%		*3 day*	*163.9 +/-8.3%*
	4 days	95.6 +/-3.2%		*4 days*	*223.6 +/-83.8%*
Neuroligin	24 hours	92.5 +/-5.5%	Tau phosphorylated Serine 396	*24 hours*	*143 +/-27.4%*
	3 day	105.7 +/-3.9%		*3 day*	*120.3 +/-7.2%*
	4 days	97.2 +/-2%		*4 days*	*125.4 +/-2.9%*
Neuronal Pentraxin1	24 hours	94.7 +/-3.9%			
	3 day	97.9 +/-1.5%			
	4 days	95.5 +/-3.3%			

Table 6.1: All Proteins assayed for changes in expression level or phosphorylation state over a 4 day period due to exposure to shockwaves generated from 250 psi of input pressure. Primary hippocampal neurons were exposed to shockwaves generated from 250 psi of input pressure and incubated for 24 hours, 3 or 4 days after the exposure. Cells were harvested and total protein of each sample was calculated. Western blots were performed for each protein at each time point and band intensity was quantitated. Shockwave-exposed cells were normalized to non-exposed control cells from the same time period. Significant changes in protein level or phosphorylation state were observed for 5 of the 25 proteins assayed. GluR2 and phosphorylated Serine 880 GluR2, PSD95, Tau and phosphorylated Serine 396 Tau all showed changes after shockwave-exposure. Western blots and quantitation performed by Vanessa Obourn, Deshler Lab.

Changes in protein levels in neurons has been associated with synaptic plasticity, with certain subpopulations of proteins increasing in response to excitatory signals and other decreasing due to lack of signals (Ehlers, 2003). Changes in the protein level of specific synaptic proteins, such as PSD95, can be indicative of overall synaptic strength and health.

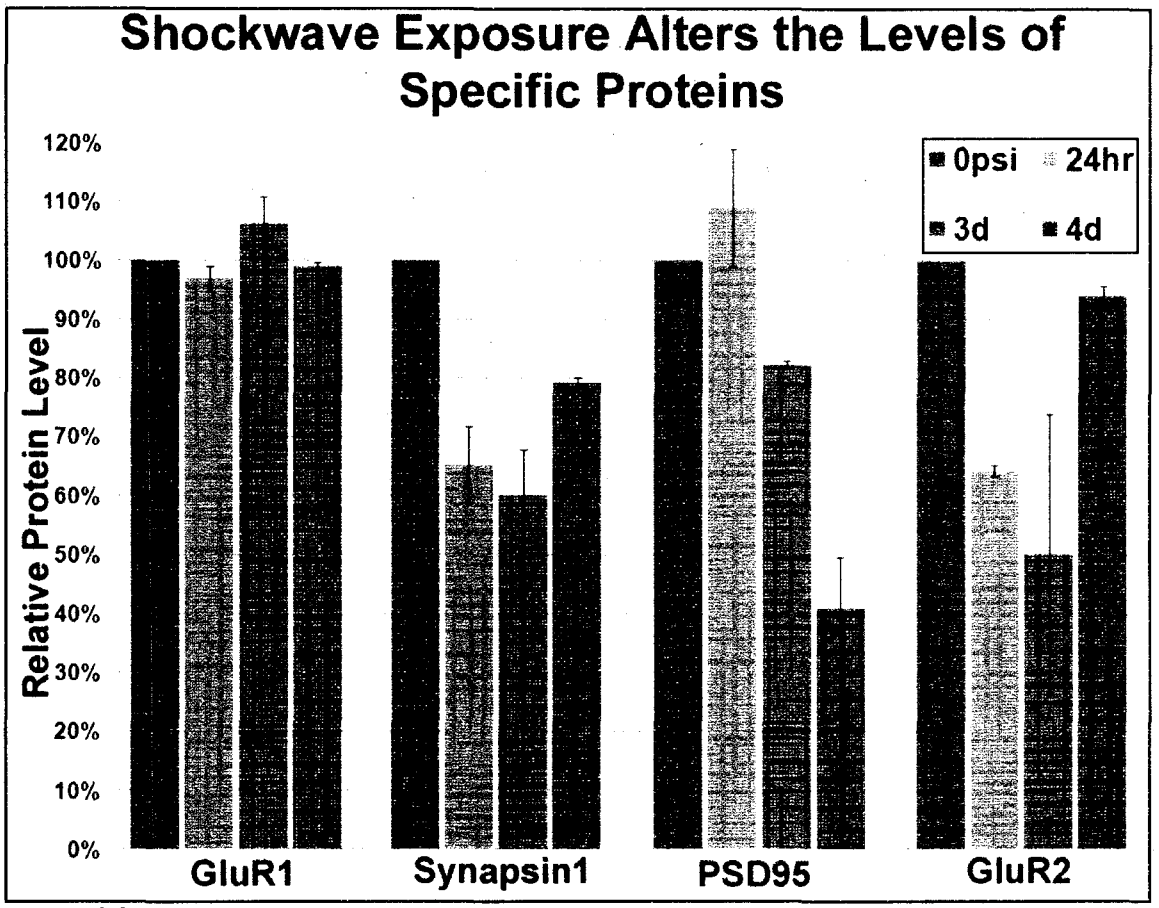

Figure 6.9: Western blot quantitation of all synaptic proteins found to change in response to exposure to shockwaves generated by 250 psi of input pressure. Primary hippocampal neurons were cultured for 14 days *in vitro* before shockwave-exposure and incubated for an additional 24 hours, 3 and 4 days after exposure. Cells were harvested and total protein calculated for all samples. Western blot analysis and quantitation were conducted by Vanessa Obourn.

6.8 Chapter 6 summary

We have shown that in our system Gene Gun generated shockwaves cause synaptic degeneration in cultured cortical and hippocampal neurons and that this degeneration is directly linked to increased membrane permeability. A pressure threshold for synaptic degeneration, similar to the pressure threshold for ATP decrease found in Chapter 5 was also observed. Unlike the ATP decreases in Chapter 5 and the synaptic degeneration shown in Chapter 6,

Dextran permeability increases with increased input pressure. This suggests that a certain amount of membrane permeability can be compensated for by the cell, allowing it to maintain ATP levels and synaptic protein densities. Increased membrane permeability by higher overpressure shockwaves cannot be compensated for and cause drastic decreases to total ATP and loss of synapses. The mechanism by which shockwaves cause synaptic degeneration seems to be a combination of both disruption of active transport as well as protein degradation.

CHAPTER 7

GENE GUN GENERATED SHOCKWAVES HAVE SIMILAR EFFECTS ON RETINAL TISSUE AS ON PRIMARY CELL CULTURE

7.1 Introduction

Thus far the efforts to discover the mechanism by which shockwaves cause mTBI have been unsuccessful. Our research into the effects of shockwaves on primary cultured neurons reveals a potential mechanism where shockwaves transiently permeabilize the cell membrane and cause synaptic degeneration. Membrane permeabilization presumably disrupts the electrochemical gradient which the cells would have to re-establish at a great energy cost. During this energy 'blackout', it is likely active transport to the synapses is decreased (Heinrich and Deshler, 2009) and decreases in active transport are known to result in synaptic degeneration (Goetze et al., 2006). In an effort to test this theory one step closer to the scale of a whole organism we tested the effects of shockwaves on intact rat retinas that had been removed from the animal via dissection.

The retina is a sheet of neurons and support cells at the back of the eye roughly 2 mm thick. The retina is responsible for the first steps in translating light into signals that can be processed by the brain. The retina develops from the embryonic forebrain and is considered part of the central nervous system. It contains a number of different types of neurons, many synapses and, due to its

easy accessibility, the retina is often studied as a surrogate for the brain (Kolb, 2003). As such, it is a perfect model tissue to test whether shockwave-induced synaptic degeneration occurs in neurons embedded in their neuronal tissue, as we have demonstrated occurs in culture.

Adult rat retinas were dissected from enucleated eyes and subjected to shockwaves generated from 250 psi of input pressure, as were cultured primary neurons. One retina from each rat served as a control (0 psi) and the other received shockwave exposure (250 psi). After shockwave exposure, retinas were cultured for 24 hours before collection. Total protein was measured for all samples and used to ensure equal amounts of protein were loaded during western blotting. As an additional loading control, samples were immunoblotted for either housekeeping gene eEF1A1 or cytoskeletal structure gene αTubulin. Western blots were performed for the 3 proteins found to change in cultured neurons after shockwave exposure, PSD95, Synapsin1 and GluR2.

7.2 Western blots of shockwave-exposed dissected rat retinas show similar changes in synaptic protein levels as seen in cultured neurons

Dissected rat retinas were exposed to shockwaves generated from 250 psi of input pressure and cultured for 24 hours before being harvested for western blot analysis. Samples were probed for PSD95, Synapsin1, and GluR2, all of which were found to change in response to shockwave-exposure in cultured primary hippocampal neurons (Figure 7.1).

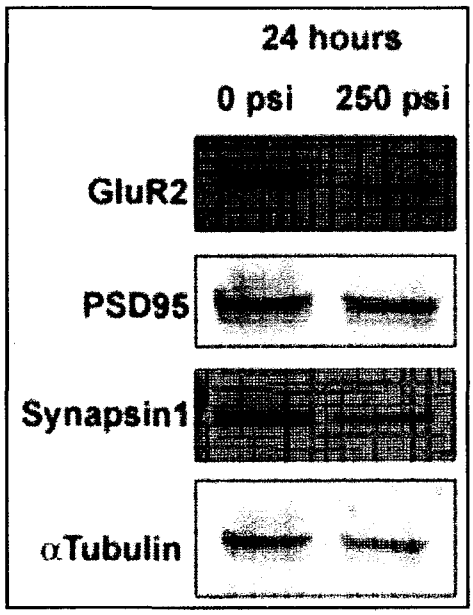

Figure 7.1: Western Blots of dissected rat retinas subjected to shockwaves generated from 250 psi of input pressure. Blots were probed for synaptic proteins shown to change from shockwave exposure in cultured hippocampal neurons. Similar changes were observed for all tested synaptic proteins. Intact rat retinas were removed from adult *R. norvegicus* rats and exposed to a shockwave generated by 250 psi input pressure *in vitro*. Synaptic proteins that exhibited changes in expression levels in cultured hippocampal neurons were blotted for expression 24 hours post-exposure in retina samples. Blots were quantified using Image J software and 250 psi band intensities are represented as a percentage of 0 psi band from the same blot corrected for tubulin loading control: GluR2: 82.4%±9.7%; PSD-95: 110±14.8%; Synapsin1: 54.4±17.0%. Western blot peformed by Vanessa Obourn, Deshler Lab.

Western blots on dissected rat retinas were quantitated to assess the degree of change in the specific synaptic proteins, PSD95, GluR2 and Synapsin1 (Figure 7.2).

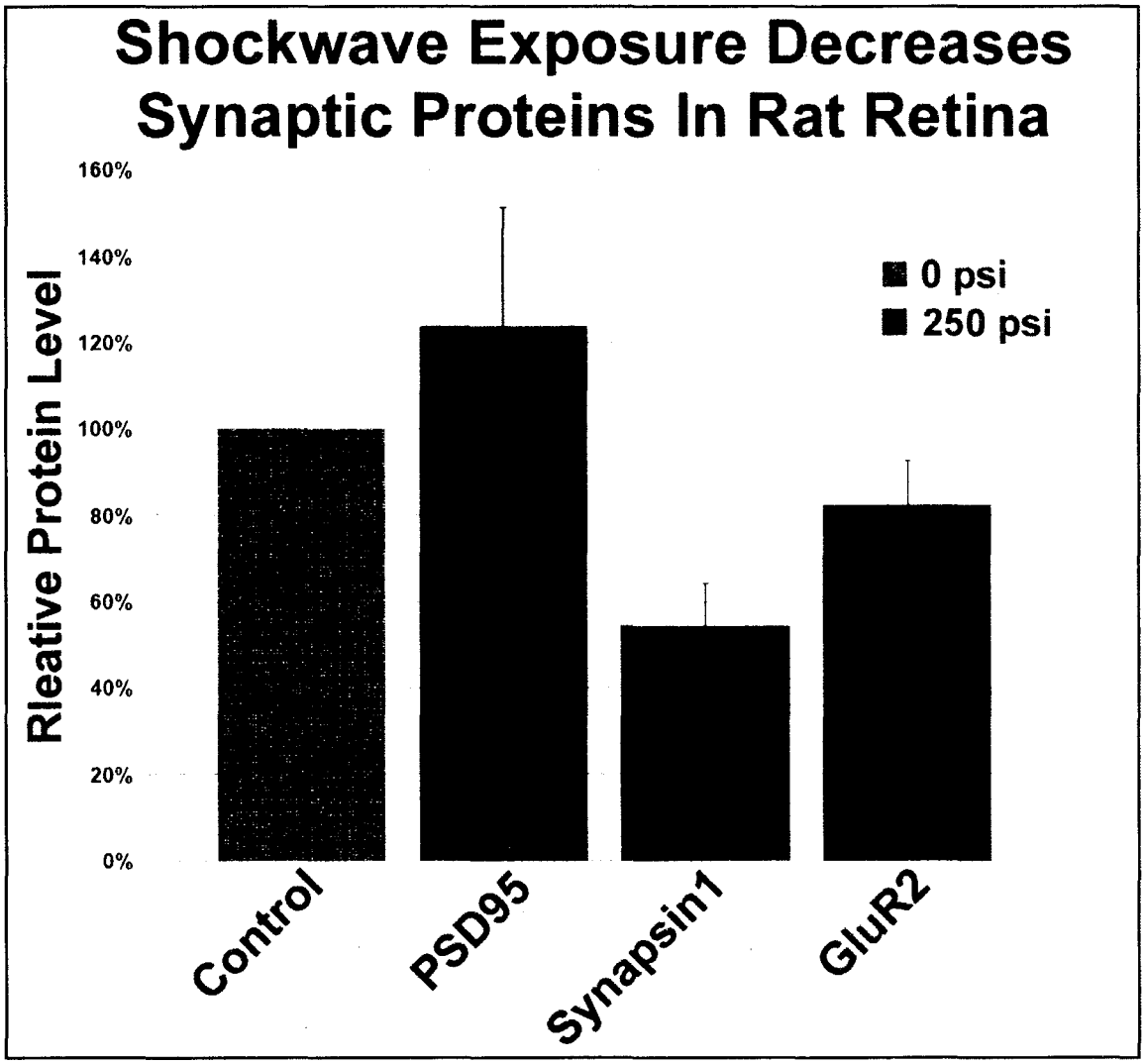

Figure 7.2: Dissected rat retinas exposed to shockwaves generated from 250 psi of input pressure show similar changes in synaptic protein expression as cultured primary neurons exposed to the same magnitude shockwave. GluR2 and Synapsin1 decreases were seen within 24 hours of shockwave exposure in dissected retinal tissue. PSD-95 showed no decrease in expression at 24 hours. Western blot quantitation performed by Vanessa Obourn, Deshler

Dissected rat retinas showed no change in expression in PSD95 within 24 hours after exposure, similar to what was observed in cultured primary neurons. Changes in PSD95 expression were not observed in cultured neurons until 3 days after exposure (Figure 6.9). It is reasonable to assume a similar change in

PSD95 would be observed in the retina in the same time frame as cultured neurons had it been investigated.

Similar to cultured primary hippocampal neurons there was a decrease in expression of the AMPA receptor subunit, GluR2. GluR2 showed a 37.1 +/- 1.2% decrease in shockwave-exposed cells 24 hours after exposure (Figure 7.2). A very similar decrease (35.7 +/- 1.2%) in GluR2 expression was observed in cultured primary hippocampal neurons subject to shockwave exposure and cultured for the same period of time (Figure 6.9).

Changes in Synapsin1 protein levels were more dramatic in shockwave-exposed dissected retinas than in cultured primary hippocampal neurons over the same time period. Retina Synapsin1 levels were down 45.6 +/-11.3% compared to non-exposed retinas (Figure 7.2). This decrease is larger than the decrease observed in cultured primary hippocampal neurons over the same period of time (34.7 +/-11.3%).

7.3 Chapter 7 summary

We have demonstrated in the previous chapters the damaging effects of shockwaves on cultured primary neurons and have now shown these effects in dissected tissue. The retina demonstrated similar changes in protein levels after shockwave exposure as primary cultured neurons, strengthening our hypothesis that shockwaves cause synaptic degeneration through membrane permeabilization. The retina is a particularly powerful model often employed to

represent the brain since it contains many similar types of neurons and synapses and is considered part of the central nervous system and easily cultured in its entirety (Kolb, 2003).

CHAPTER 8

DISCUSSION

8.1 Summary of Data

We have demonstrated that a BioRad Helios Gene Gun is capable of producing a shockwave within the input pressure range of 100 to 300 psi and that at input pressures less than 300 psi the shockwave generated is not lethal to cultured primary neurons (Figure 3.2, 3.4). We have shown that shockwave exposure causes decreases in cellular ATP levels of cultured neurons within 1 hour of exposure and that these decreases are restored within 48 hours of exposure (Figure 5.3, 5.4). We have also shown that shockwave exposure causes a transient membrane permeabilization in cultured neurons (Figures 4.3, 4.4). This permeabilization allows molecules with an effective radius of at least 5.8 nm, but less than 14.7nm, to cross the plasma membrane (Figure 4.2, Table 4.1). This permeabilization is repaired by within 2-6 hours of exposure. Furthermore, we demonstrated this membrane permeabilization is directly correlated to synaptic degeneration (Figure 6.7, 6.8). We showed that shockwave-induced synaptic degeneration was not limited to cultured hippocampal neurons, but also cultured cortical neurons (Figure 6.3). We confirmed the synaptic degeneration with western blot analysis and were able to show changes in the expression of multiple synaptic proteins (Figure 6.9). These biochemical changes were replicated in intact, dissected adult rat retinas

subjected to the same magnitude shockwaves (Figure 7.2). Together our data suggest a mechanism of shockwave pathology in which membrane permeabilization causes a disruption of the electrochemical gradient which results in significant energy depletion; this energy depletion alters active transport out to synapses and causes synaptic degeneration.

Shockwaves have been previously shown to cause membrane permeabilization in cultured cells, including primary hippocampal neurons (Saljo et al., 2003, Khanna et al., 2006). Shockwaves similar in magnitude to ours have also been shown to permeabilize neurons in cultured spinal cord tissue (Connell et al., 2011). Our study expands beyond the research of Connell et al, demonstrating both size restrictions for shockwave-induced membrane permeability as well the transient nature of the permeability. In addition, it also extends the findings by describing a plausible mechanism by which permeabilization leads to synaptic degeneration. Our findings are in agreement with previous research that a shockwave is capable of inducing a transient membrane permeabilization in cultured neurons (Kudo et al., 2009).

Many neurodegenerative diseases are thought to be the result of metabolic decreases in neurons rather than neuronal death. Energy deficiency in neurons results in reduced activity, and if not corrected, will eventually lead to cell death (Ward et al., 2007, Weisova et al., 2009, Ward et al., 2010). The cognitive deficits associated with Alzheimer's disease are thought to be the result

of impaired neuronal activity. A neuron requires two major components in order to be active; the ability to pass information via an action potential and a connection with another neuron to receive the information via a synapse. In order to fire an action potential a neuron must maintain a large electrochemical gradient at great metabolic expense (Hammond, 2001). Synapses require upkeep through continued use as well as internal maintenance in the form of local protein synthesis and active transport of RNP vesicles from the soma (Zukin et al., 2009, Morgado-Bernal, 2011). Any decrease in cellular ATP levels would have a major impact on both of these processes. Our research shows that shockwaves cause membrane permeability and drastic decreases in cellular ATP levels.

Synapse formation and function provide functional components of neurons that have much of the biochemistry of learning and memory, and synaptic degeneration has been linked to cognitive dysfunction (Hofer and Bonhoeffer, 2010, VanGuilder et al., 2011). Our research is the first to demonstrate that shockwave exposure causes synaptic degeneration and thus could be an underlying factor in the cognitive impairment associated with shockwave-induced mTBI. Furthermore we showed that this synaptic degeneration is directly correlated to membrane permeability. Disruption of the plasma membrane is known to cause drastic changes in the ion gradients maintained by the neuron and that the neuron expends great energy to reestablish these gradients. It has also been shown that loss of transport to synapses, an ATP dependent process,

results in synaptic degeneration similar to what we showed with shockwave exposure. Our research, in conjunction with previously published work, suggests a mechanism of shockwave pathology in neurons.

8.2 Implications for mTBI

It has been known since World War I that shockwaves cause damage to the brain and that this damage is sometimes only apparent as changes in memory, emotion and behavior without any obvious physical damage to an individual. To date the mechanism by which sub-lethal shockwaves damage the brain is unknown. Currently the damage caused by shockwaves is termed mild traumatic brain injury (mTBI). By definition, mTBI is not detectable by any widely used scanning technique, though certain advanced types of MRI have shown some promise in diagnosing the condition. Functional MRI (fMRI) has been used to detect mTBI as decreases in local neuronal metabolism as imaged by the turnover of oxygenated vs. deoxygenated hemoglobin (Kim et al., 2004, Jantzen, 2010). Unfortunately the equipment required for these techniques is large and costly and therefore not readily deployable to military field hospitals. Most of the data on mTBI are from civilian studies of blunt force induced mTBI. While there is still debate on whether or not blunt vs. blast-induced mTBI represent the same pathology, evidence is mounting that the two conditions are etiologically separate.

Based on the scanning data available, neuronal cell death is not considered to be a major factor in the pathology of either blunt or blast-induced mTBI. Animal models of mTBI which replicate the cognitive impairment of the injury, have not found evidence of significant cell death in the brains of animals exposed to shockwaves (Cernak et al., 2001, Moochhala et al., 2004, Bauman et al., 2009, Saljo et al., 2010). Our research confirms that mild shockwaves do not kill cultured primary hippocampal neurons nor greatly alter their morphology (Figure 3.4, 3.5). Furthermore, these shockwaves are similar in magnitude to shockwaves shown to cause cognitive impairment adult rats (Figure 3.3)(Moochhala et al., 2004).

Our research has shown that shockwaves induce transient membrane permeability in neurons (Figure 4.3). Previous research supports our findings that shockwaves can transiently permeabilize the plasma membrane of a cell *in vitro* (Murata et al., 2006, Lin et al., 2010). *In vivo* animal models of mTBI have suggested that shockwaves permeabilize cells measuring the blood serum levels of certain cytoplasmic proteins (Saljo et al., 2003). Human mTBI diagnosis has seen some limited success using blood serum levels of cytoplasmic proteins, neuronal specific enolase (NSE) and S100β, though the levels correlate most strongly with moderate and severe TBI (Bruns and Jagoda, 2009). This membrane permeability would account for the metabolic disruption seen by fMRI in patients with mTBI.

Our research has shown a drastic decrease in cellular ATP levels of cultured primary neurons immediately following shockwave exposure and that this decrease persists for 48 hours (Figure 5.1, 5.3, 5.4). This ATP decrease occurs in the same time frame as the membrane permeability and seems highly plausible that the membrane permeability is responsible for the ATP decrease. A neuron is dependent on ATP to move RNA and proteins from the cell soma out along dendrites and axons to synapses. Loss of transport out to synapses has been shown to cause synaptic degeneration similar to what we have shown here (Goetze et al., 2006). Furthermore, there is evidence to suggest that transport is disrupted in the brains of rats exposed to explosive blast overpressures of 22-34 psi as measured outside, adjacent to the head. Rats were exposed to shockwaves of 22 to 34 psi peak overpressure, generated by explosive charges. Animals were then sacrificed at 2, 6, and 18 hours as well as 2, 7 and 21 days post-exposure. Coronal brain slices were prepared and stained for the phosphorylated form of the heavy subunit of the neurofilament protein (NFH), which is the main structural component of axons (Saljo et al., 2000). NFH is synthesized in the cell soma and transported out to axons in its phosphorylated form (p-NFH, (Williamson and Cleveland, 1999)). Phosphorylated NFH is normally only detectable in the axons of healthy neurons and accumulation of the p-NFH in the cell soma is indicative of defects in axonal transport. Rats subjected to 22 to 34 psi blast overpressures showed accumulation of p-NFH in the cell soma layer of the temporal cortex 18 hours after exposure, which persisted up to

7 days post-exposure. Normal distribution of p-NFH was found in blast exposed animals 21 days after exposure, suggesting transport had been restored (Saljo et al., 2000).This restoration comes well after our *in vitro* model shows that cellular membranes have been repaired and the ATP balance restored. However, our research shows that synaptic degeneration occurs well after the ATP balance has been restored, with some synaptic proteins showing the biggest decreases 3 to 4 days after exposure (PSD95, Figure 6.9). Our research is the first to show that shockwaves specifically effect neuronal synapses and cause synaptic degeneration, probably through disruption of transport. Neuronal degeneration has been implicated in a number of diseases, including Alzheimer's disease. Many of the early symptoms of Alzheimer's disease and mTBI are identical, including insomnia, sleep disturbances, drowsiness, difficulty remembering, difficulty concentrating and changes in mood or personality (Helmick, 2006). Furthermore, decreased axonal transport has been implicated in Alzheimer's disease as well as decreases in neuronal energy levels (Julien and Mushynski, 1998, Ferreira et al., 2010a).

An area of TBI therapy that is gaining traction is the use of chemicals to increase intercellular ATP in the hopes of compensating for any irregularities or injuries. Currently this thinking is based on mitochondrial malfunction and has shown promise in preclinical animal models. Creatine is a dietary supplement used by all levels of athletes to help build muscle and maintain energy. In a blunt force induced model of TBI using both rats and mice it was found that animals

consuming a creatine supplement had a significant reduction in the extent of damage. Animals on the supplement showed increased mitochondrial membrane potentials, reduced levels of reactive oxygen species and there was no decrease in the levels of ATP(Sullivan et al., 2000).

8.3 Conclusions

Blast injury is the number one injury suffered by today's soldiers and as such it has become the 'signature injury' in modern warfare. Currently there are over 300,000 veterans who have suffered a mTBI and this number is expected to increase as the use of IEDs in OIF and OED increase. Currently there are no definitive diagnostic techniques for mTBI and the pathology of shockwave-induced mTBI is unknown. We have presented here the first evidence of shockwave-induced synaptic degeneration in both cultured primary neurons and dissected retinal tissue. Synaptic degeneration is the hallmark of many diseases that cause cognitive impairment, with a number of symptoms overlapping with those of mTBI. We have discovered several candidate proteins which could be used in future screening assays as well as further research into the mechanics of shockwave-induced synaptic degeneration.

LIST OF JOURNAL ABBREVIATIONS

Acta Physiol Scand	Acta Physiologica Scandinavica
Acta Radiol Suppl	Acta Radiologica Supplementum
Am J Epidemiol	American Journal of Epidemiology
Am J Physiol	The American Journal of Physiology
Am J Psychiatry	The American Journal of Psychiatry
Am J Public Health	American Journal of Public Health
Am J Sports Med	The American Journal of Sports Medicine
Am Surg	The American Surgeon
Ann Emerg Med	Annals of Emergency Medicine
Ann Neurol	Annals of Neurology
Appl Environ Microbiol	Applied and Environmental Microbiology
Arch Clin Neuropsychol	Archives of Clinical Neuropsychology
Arch Gen Psychiatry	Archives of General Psychiatry
Arch Phys Med Rehabil	Archives of Physical Medicine and Rehabilitation
ASN Neuro	American Society for Neurochemistry
Auton Neurosci	Autonomic Neuroscience
Biochim Biophys Acta	Biochimica et Biophysica Acta
Biophys J	Biophysical Journal

Biotechnol Lett	Biotechnology Letters
Br Med J	British Medical Journal
Brain Inj	Brain Injury
Brain Res	Brain Research
Brain Res Bull	Brain Research Bulletin
Can Med Assoc J	Canadian Medical Association Journal
Crit Care Med	Critical Care Medicine
Curr Biol	Current Biology
Curr Drug Targets	Current Drug Targets
DNA Cell Biol	DNA and Cell Biology
Exp Biol Med	Experimental Biology and Medicine
Front Neural Circuits	Frontiers in Neural Circuits
Front Neurol	Frontiers in Neurology
Gene Ther	Gene Therapy
Trans Biomed Eng	Transactions on Bio-medical Engineering
Int Rev Psychiatry	International Review of Psychiatry
Int Tinnitus J	The International Tinnitus Journal
J Athl Train	Journal of Athletic Training
J Biomed Sci	Journal of Biomedical Science
J Biotechnol	Journal of Biotechnology

J Cell Biol	The Journal of Cell Biology
J Comp Neurol	The Journal of Comparative Neurology
J Control Release	Journal of Controlled Release
J Head Trauma Rehabil	The Journal of Head Trauma Rehabilitation
J Int Neuropsychol Soc	Journal of the International Neuropsychological Society
J Membr Biol	The Journal of Membrane Biology
J Neurobiol	Journal of Neurobiology
J Neurochem	Journal of Neurochemistry
J Neuropsychiatry Clin Neurosci	The Journal of Neuropsychiatry and Clinical Neurosciences
J Neurosci	The Journal of Neuroscience
J Neurosci Methods	The Journal of Neuroscience Methods
J Neurosci Res	The Journal of Neuroscience Research
J Neurosurg	Journal of Neurosurgery
J Neurotrauma	Journal of Neurotrauma
J Rehabil Med	Journal of Rehabilitation Medicine
J Rehabil Res Dev	Journal of Rehabilitation Research and Development
J Spec Oper Med	Journal of Special Operations Medicine
J Trauma	The Journal of Trauma

J Trauma Stress	Journal of Traumatic Stress
Mil Med	Military Medicine
Mt Sinai J Med	The Mount Sinai Journal of Medicine
N Engl J Med	The New England Journal of Medicine
Nat Neurosci	Nature Neuroscience
Nat Protoc	Nature Protocols
Neurobiol Dis	Neurobiology of Disease
Pain Med	Pain Medicine
Plant Mol Biol	Plant Molecular Biology
Proc Natl Acad Sci USA	Proceedings of the National Academy of Sciences of the United States of America
Prog Nucleic Acid Res Mol Biol	Progress in Nucleic Acid Research and Molecular Biology
Ultrasound Med Biol	Ultrasound in Medicine and Biology
World J Surg	World Journal of Surgery

REFERENCES

(AMEDD) AMD (Evacuation Statistics for OEF and OIF. wwwarmymedicinearmymil/news/medevacstats/medevacstatshtm.2006).

Alexander C (The Shock of War. Smithsonian Magazine.2010).

American Psychiatric Association. (2000) Diagnostic criteria from DSM-IV-TR. Washington, D.C.: American Psychiatric Association.

Aranda-Abreu GE, Behar L, Chung S, Furneaux H, Ginzburg I (Embryonic lethal abnormal vision-like RNA-binding proteins regulate neurite outgrowth and tau expression in PC12 cells. J Neurosci 19:6907-6917.1999).

Bauman RA, Ling GS, Tong L, Januszkiewicz A, Agoston D, Delanerolle N, Kim J, Ritzel D, Bell R, Ecklund JM, Armonda R, Bandak F, Parks S (An introductory characterization of a combat-casualty-care relevant swine model of closed head injury resulting from exposure to explosive blast. J Neurotrauma.2009).

Beal MF, Brouillet E, Jenkins BG, Ferrante RJ, Kowall NW, Miller JM, Storey E, Srivastava R, Rosen BR, Hyman BT (Neurochemical and histologic characterization of striatal excitotoxic lesions produced by the mitochondrial toxin 3-nitropropionic acid. J Neurosci 13:4181-4192.1993).

Bellamy RF, Zajtchuk R, Buescher TM (1991) Conventional warfare : ballistic, blast, and burn injuries. Washington, D.C.
Bethesda, Md.
San Antonio, Tex.: Walter Reed Army Institute of Research
Uniformed Services University of the Health Sciences ;
United States Army Institute for Surgical Research.

Blomqvist G, Gjedde A, Gutniak M, Grill V, Widen L, Stone-Elander S, Hellstrand E (Facilitated transport of glucose from blood to brain in man and the effect of moderate hypoglycaemia on cerebral glucose utilization. Eur J Nucl Med 18:834-837.1991a).

Blomqvist G, Stone-Elander S, Halldin C, Roland PE, Swahn CG, Haaparanta M, Solin O, Lindqvist M, Widen L (Cerebral glucose utilization measured by positron emission tomography. [1-11C]-D-glucose compared with [2-18F]-2-fluoro-2-deoxy-D-glucose. Acta Radiol Suppl 376:171-172.1991b).

Bochicchio GV, Lumpkins K, O'Connor J, Simard M, Schaub S, Conway A, Bochicchio K, Scalea TM (Blast injury in a civilian trauma setting is associated with a delay in diagnosis of traumatic brain injury. Am Surg 74:267-270.2008).

Bruns JJ, Jr., Jagoda AS (Mild traumatic brain injury. Mt Sinai J Med 76:129-137.2009).

Cameron HA, Kaliszewski CK, Greer CA (Organization of mitochondria in olfactory bulb granule cell dendritic spines. Synapse 8:107-118.1991).

CDC (2003) Report to Congress on Mild Traumatic Brain Injury in the United States: Steps to Prevent a Serious Public Health Problem. . (Prevention,

C. f. D. C. a., ed) Atlanta: National Center for Injury Prevention and Control.
Cernak I, Savic J, Ignjatovic D, Jevtic M (Blast injury from explosive munitions. J Trauma 47:96-103; discussion 103-104.1999).
Cernak I, Wang Z, Jiang J, Bian X, Savic J (Ultrastructural and functional characteristics of blast injury-induced neurotrauma. J Trauma 50:695-706.2001).
Cheng A, Hou Y, Mattson MP (Mitochondria and neuroplasticity. ASN Neuro 2.2010).
Chinopoulos C, Tretter L, Rozsa A, Adam-Vizi V (Exacerbated responses to oxidative stress by an Na(+) load in isolated nerve terminals: the role of ATP depletion and rise of [Ca(2+)](i). J Neurosci 20:2094-2103.2000).
Clemedson CJ, Granstom SA (Studies on the genesis of "rib markings" in lung blast injury. Acta Physiol Scand 21:131-144.1950).
Coldren RL, Kelly MP, Parish RV, Dretsch M, Russell ML (Evaluation of the Military Acute Concussion Evaluation for use in combat operations more than 12 hours after injury. Mil Med 175:477-481.2010).
Concannon CG, Tuffy LP, Weisova P, Bonner HP, Davila D, Bonner C, Devocelle MC, Strasser A, Ward MW, Prehn JH (AMP kinase-mediated activation of the BH3-only protein Bim couples energy depletion to stress-induced apoptosis. J Cell Biol 189:83-94.2010).
Connell S, Gao J, Chen J, Shi R (Novel Model to Investigate Blast Injury in the Central Nervous System. J Neurotrauma.2011).
Costa RM, Honjo T, Silva AJ (Learning and memory deficits in Notch mutant mice. Curr Biol 13:1348-1354.2003).
de Candole CA (Blast injury. Can Med Assoc J 96:207-214.1967).
Drachman DA (Do we have brain to spare? Neurology 64:2004-2005.2005).
DVBIC (Military Acute Concussion Evalutaion. Defense and Veterans Brain Injury Center.2006).
Ehlers MD (Activity level controls postsynaptic composition and signaling via the ubiquitin-proteasome system. Nat Neurosci 6:231-242.2003).
El-Husseini Ael D, Schnell E, Dakoji S, Sweeney N, Zhou Q, Prange O, Gauthier-Campbell C, Aguilera-Moreno A, Nicoll RA, Bredt DS (Synaptic strength regulated by palmitate cycling on PSD-95. Cell 108:849-863.2002).
Elsayed NM (Toxicology of blast overpressure. Toxicology 121:1-15.1997).
Faux S, Sheedy J (A prospective controlled study in the prevalence of posttraumatic headache following mild traumatic brain injury. Pain Med 9:1001-1011.2008).
Ferreira IL, Resende R, Ferreiro E, Rego AC, Pereira CF (Multiple Defects in Energy Metabolism in Alzheimer's Disease. Curr Drug Targets.2010a).
Ferreira IL, Resende R, Ferreiro E, Rego AC, Pereira CF (Multiple defects in energy metabolism in Alzheimer's disease. Curr Drug Targets 11:1193-1206.2010b).

Fischer AJ, Stanke JJ, Omar G, Askwith CC, Burry RW (Ultrasound-mediated gene transfer into neuronal cells. J Biotechnol 122:393-411.2006).

Gafaniz R, Sanches J (ATP consumption and neural electrical activity: a physiological model for brain imaging. Conf Proc IEEE Eng Med Biol Soc 2010:5480-5483.2010).

Gambihler S, Delius M, Ellwart JW (Permeabilization of the plasma membrane of L1210 mouse leukemia cells using lithotripter shock waves. J Membr Biol 141:267-275.1994).

Gan WB, Grutzendler J, Wong WT, Wong RO, Lichtman JW (Multicolor "DiOlistic" labeling of the nervous system using lipophilic dye combinations. Neuron 27:219-225.2000).

Goetze B, Grunewald B, Baldassa S, Kiebler M (Chemically controlled formation of a DNA/calcium phosphate coprecipitate: application for transfection of mature hippocampal neurons. J Neurobiol 60:517-525.2004).

Goetze B, Tuebing F, Xie Y, Dorostkar MM, Thomas S, Pehl U, Boehm S, Macchi P, Kiebler MA (The brain-specific double-stranded RNA-binding protein Staufen2 is required for dendritic spine morphogenesis. J Cell Biol 172:221-231.2006).

Gondusky JS, Reiter MP (Protecting military convoys in Iraq: an examination of battle injuries sustained by a mechanized battalion during Operation Iraqi Freedom II. Mil Med 170:546-549.2005).

Greene JG, Porter RH, Eller RV, Greenamyre JT (Inhibition of succinate dehydrogenase by malonic acid produces an "excitotoxic" lesion in rat striatum. J Neurochem 61:1151-1154.1993).

Grooms SY, Noh KM, Regis R, Bassell GJ, Bryan MK, Carroll RC, Zukin RS (Activity bidirectionally regulates AMPA receptor mRNA abundance in dendrites of hippocampal neurons. J Neurosci 26:8339-8351.2006).

Guskiewicz KM, Bruce SL, Cantu RC, Ferrara MS, Kelly JP, McCrea M, Putukian M, Valovich McLeod TC (National Athletic Trainers' Association Position Statement: Management of Sport-Related Concussion. J Athl Train 39:280-297.2004).

Hammond C (2001) Cellular and molecular neurobiology. San Diego: Academic Press.

Han YW, Ikegami A, Chung P, Zhang L, Deng CX (Sonoporation is an efficient tool for intracellular fluorescent dextran delivery and one-step double-crossover mutant construction in Fusobacterium nucleatum. Appl Environ Microbiol 73:3677-3683.2007).

Hao J, Li SK, Kao WW, Liu CY (Gene delivery to cornea. Brain Res Bull 81:256-261.2010).

Hart T, Dijkers M, Fraser R, Cicerone K, Bogner JA, Whyte J, Malec J, Waldron B (Vocational services for traumatic brain injury: treatment definition and diversity within model systems of care. J Head Trauma Rehabil 21:467-482.2006).

Hausdorf J, Lemmens MA, Heck KD, Grolms N, Korr H, Kertschanska S, Steinbusch HW, Schmitz C, Maier M (Selective loss of unmyelinated nerve fibers after extracorporeal shockwave application to the musculoskeletal system. Neuroscience 155:138-144.2008a).

Hausdorf J, Lemmens MA, Kaplan S, Marangoz C, Milz S, Odaci E, Korr H, Schmitz C, Maier M (Extracorporeal shockwave application to the distal femur of rabbits diminishes the number of neurons immunoreactive for substance P in dorsal root ganglia L5. Brain Res 1207:96-101.2008b).

Heinrich B, Deshler JO (RNA localization to the Balbiani body in Xenopus oocytes is regulated by the energy state of the cell and is facilitated by kinesin II. Rna 15:524-536.2009).

Helmick K, Guskiewicz, K, Barth, J, Cantu, R, Kelly, JP, McDonald, E, Flaherty, S, Bazarian, J, Bleiberg, J, Carter, T, Cooper, J, Drake, A, French, L, Grant, G, Holland, M, Hunt, R, Hurtado, T, Jenkins, D, Johnson, T, Kennedy, J, Labutta, R, Lopez, M, McCrea, M, Montgomery, H, Riechers, R, Ritchie, E, Ruscio, B, Schneider, T, Schwab, K, Tanner, W, Zitnay, G, Warden, D (2006) Defense and Veterans Brain Injury Center Working Group on the Acute Management of Mild Traumatic Brain Injury in Military Operational Settings. (VA, D. a. V. B. I. C., ed) Washington DC.

Hettich T, Whitfield E, Kratz K, Frament C (Case report: use of the Immediate Post Concussion Assessment and Cognitive Testing (ImPACT) to assist with return to duty determination of special operations soldiers who sustained mild traumatic brain injury. J Spec Oper Med 10:48-55.2010).

Hofer SB, Bonhoeffer T (Dendritic spines: the stuff that memories are made of? Curr Biol 20:R157-159.2010).

Hoffer ME, Donaldson C, Gottshall KR, Balaban C, Balough BJ (Blunt and blast head trauma: different entities. Int Tinnitus J 15:115-118.2009).

Hoge CW, McGurk D, Thomas JL, Cox AL, Engel CC, Castro CA (Mild traumatic brain injury in U.S. Soldiers returning from Iraq. N Engl J Med 358:453-463.2008).

Hooker DR (Physiological effects of air concussion. Am J Physiol 67:219-274.1924).

Huang MX, Theilmann RJ, Robb A, Angeles A, Nichols S, Drake A, D'Andrea J, Levy M, Holland M, Song T, Ge S, Hwang E, Yoo K, Cui L, Baker DG, Trauner D, Coimbra R, Lee RR (Integrated imaging approach with MEG and DTI to detect mild traumatic brain injury in military and civilian patients. J Neurotrauma 26:1213-1226.2009).

Jantzen KJ (Functional magnetic resonance imaging of mild traumatic brain injury. J Head Trauma Rehabil 25:256-266.2010).

Jones E, Fear NT, Wessely S (Shell shock and mild traumatic brain injury: a historical review. Am J Psychiatry 164:1641-1645.2007).

Julien JP, Mushynski WE (Neurofilaments in health and disease. Prog Nucleic Acid Res Mol Biol 61:1-23.1998).

Kang HK, Hyams KC (Mental health care needs among recent war veterans. N Engl J Med 352:1289.2005).

Kato K, Fujimura M, Nakagawa A, Saito A, Ohki T, Takayama K, Tominaga T (Pressure-dependent effect of shock waves on rat brain: induction of neuronal apoptosis mediated by a caspase-dependent pathway. J Neurosurg 106:667-676.2007).

Kessler RC, Berglund P, Demler O, Jin R, Merikangas KR, Walters EE (Lifetime prevalence and age-of-onset distributions of DSM-IV disorders in the National Comorbidity Survey Replication. Arch Gen Psychiatry 62:593-602.2005).

Khanna S, Hudson B, Pepper CJ, Amso NN, Coakley WT (Fluorescein isothiocynate-dextran uptake by chinese hamster ovary cells in a 1.5 MHz ultrasonic standing wave in the presence of contrast agent. Ultrasound Med Biol 32:289-295.2006).

Kim DS, Ronen I, Olman C, Kim SG, Ugurbil K, Toth LJ (Spatial relationship between neuronal activity and BOLD functional MRI. Neuroimage 21:876-885.2004).

Kolb H (How the Retina Works. American Scientist 91:28-35.2003).

Kudo N, Okada K, Yamamoto K (Sonoporation by single-shot pulsed ultrasound with microbubbles adjacent to cells. Biophys J 96:4866-4876.2009).

Kumon RE, Aehle M, Sabens D, Parikh P, Han YW, Kourennyi D, Deng CX (Spatiotemporal effects of sonoporation measured by real-time calcium imaging. Ultrasound Med Biol 35:494-506.2009).

Lechner HA, Lein ES, Callaway EM (A genetic method for selective and quickly reversible silencing of Mammalian neurons. J Neurosci 22:5287-5290.2002).

Lei H, Ugurbil K, Chen W (Measurement of unidirectional Pi to ATP flux in human visual cortex at 7 T by using in vivo 31P magnetic resonance spectroscopy. Proc Natl Acad Sci U S A 100:14409-14414.2003).

Leibovici D, Gofrit ON, Stein M, Shapira SC, Noga Y, Heruti RJ, Shemer J (Blast injuries: bus versus open-air bombings--a comparative study of injuries in survivors of open-air versus confined-space explosions. J Trauma 41:1030-1035.1996).

Leibovici D, Gofrit, ON, Shapira, SC (Eardrum perforation in explosion survivors: Is it a marker of pulmonary blast injury? Ann Emerg Med 34:168-172.1991).

Levin HS, Wilde E, Troyanskaya M, Petersen NJ, Scheibel R, Newsome M, Radaideh M, Wu T, Yallampalli R, Chu Z, Li X (Diffusion tensor imaging of mild to moderate blast-related traumatic brain injury and its sequelae. J Neurotrauma 27:683-694.2010).

Lew HL, Otis JD, Tun C, Kerns RD, Clark ME, Cifu DX (Prevalence of chronic pain, posttraumatic stress disorder, and persistent postconcussive symptoms in OIF/OEF veterans: polytrauma clinical triad. J Rehabil Res Dev 46:697-702.2009).

Li Z, Okamoto K, Hayashi Y, Sheng M (The importance of dendritic mitochondria in the morphogenesis and plasticity of spines and synapses. Cell 119:873-887.2004).

Liao D, Scannevin RH, Huganir R (Activation of silent synapses by rapid activity-dependent synaptic recruitment of AMPA receptors. J Neurosci 21:6008-6017.2001).

Lin CR, Chen KH, Yang CH, Cheng JT, Sheen-Chen SM, Wu CH, Sy WD, Chen YS (Sonoporation-mediated gene transfer into adult rat dorsal root ganglion cells. J Biomed Sci 17:44.2010).

Lippa SM, Pastorek NJ, Benge JF, Thornton GM (Postconcussive symptoms after blast and nonblast-related mild traumatic brain injuries in Afghanistan and Iraq war veterans. J Int Neuropsychol Soc 16:856-866.2010).

Liu Y (Impact studies of high-speed micro-particles following biolistic delivery. IEEE Trans Biomed Eng 54:1507-1513.2007).

Lovell M, Collins, M, Maroon, J (Inaccuracy of symptom reporting following concussions in athletes. Medicine and Science in Sports and Exercise 34:S298.2002).

Lu CY, Chou AK, Wu CL, Yang CH, Chen JT, Wu PC, Lin SH, Muhammad R, Yang LC (Gene-gun particle with pro-opiomelanocortin cDNA produces analgesia against formalin-induced pain in rats. Gene Ther 9:1008-1014.2002).

Mahoney PF RJ, Brooks AJ (2004) Ballistic Trauma: A Practical Guide. New York: Springer.

Man HY, Lin JW, Ju WH, Ahmadian G, Liu L, Becker LE, Sheng M, Wang YT (Regulation of AMPA receptor-mediated synaptic transmission by clathrin-dependent receptor internalization. Neuron 25:649-662.2000).

Maragos WF, Korde AS (Mitochondrial uncoupling as a potential therapeutic target in acute central nervous system injury. J Neurochem 91:257-262.2004).

Martiniuk F, Chen A, Mack A, Donnabella V, Slonim A, Bulone L, Arvanitopoulos E, Raben N, Plotz P, Rom WN (Helios gene gun particle delivery for therapy of acid maltase deficiency. DNA Cell Biol 21:717-725.2002).

Mayorga MA (The pathology of primary blast overpressure injury. Toxicology 121:17-28.1997).

McCrea M, Kelly JP, Randolph C, Kluge J, Bartolic E, Finn G, Baxter B (Standardized assessment of concussion (SAC): on-site mental status evaluation of the athlete. J Head Trauma Rehabil 13:27-35.1998).

Mellor SG (The relationship of blast loading to death and injury from explosion. World J Surg 16:893-898.1992).

Miller DL, Dou C (Induction of apoptosis in sonoporation and ultrasonic gene transfer. Ultrasound Med Biol 35:144-154.2009).

Mitchell T, Smith, GM (Medical Services, Casualties, and Medical Statistics of the Great War. London, His Majesty's Stationary Office.1931).

Moochhala SM, Md S, Lu J, Teng CH, Greengrass C (Neuroprotective role of aminoguanidine in behavioral changes after blast injury. J Trauma 56:393-403.2004).

Morgado-Bernal I (Learning and memory consolidation: linking molecular and behavioral data. Neuroscience 176:12-19.2011).

Mott FW (The Microscopic Examination of the Brains of Two Men Dead of Commotio Cerebri (Shell Shock) without Visible External Injury. Br Med J 2:612-615.1917).

Murata R, Ohtori S, Ochiai N, Takahashi N, Saisu T, Moriya H, Takahashi K, Wada Y (Extracorporeal shockwaves induce the expression of ATF3 and GAP-43 in rat dorsal root ganglion neurons. Auton Neurosci 128:96-100.2006).

Murray CK, Reynolds JC, Schroeder JM, Harrison MB, Evans OM, Hospenthal DR (Spectrum of care provided at an echelon II Medical Unit during Operation Iraqi Freedom. Mil Med 170:516-520.2005).

Murthy JM, Chopra JS, Gulati DR (Subdural hematoma in an adult following a blast injury. Case report. J Neurosurg 50:260-261.1979).

O'Brien JA, Lummis SC (Biolistic transfection of neuronal cultures using a hand-held gene gun. Nat Protoc 1:977-981.2006).

Panov AV, Gutekunst CA, Leavitt BR, Hayden MR, Burke JR, Strittmatter WJ, Greenamyre JT (Early mitochondrial calcium defects in Huntington's disease are a direct effect of polyglutamines. Nat Neurosci 5:731-736.2002).

Park E, Gottlieb JJ, Cheung B, Shek PN, Baker AJ (A model of low-level primary blast brain trauma results in cytoskeletal proteolysis and chronic functional impairment in the absence of lung barotrauma. J Neurotrauma 28:343-357.2011).

Perumalsamy LR, Nagala M, Sarin A (Notch-activated signaling cascade interacts with mitochondrial remodeling proteins to regulate cell survival. Proc Natl Acad Sci U S A 107:6882-6887.2010).

Popov V, Medvedev NI, Davies HA, Stewart MG (Mitochondria form a filamentous reticular network in hippocampal dendrites but are present as discrete bodies in axons: a three-dimensional ultrastructural study. J Comp Neurol 492:50-65.2005).

Pun PB, Kan EM, Salim A, Li Z, Ng KC, Moochhala SM, Ling EA, Tan MH, Lu J (Low level primary blast injury in rodent brain. Front Neurol 2:19.2011).

Readnower RD, Chavko M, Adeeb S, Conroy MD, Pauly JR, McCarron RM, Sullivan PG (Increase in blood-brain barrier permeability, oxidative stress, and activated microglia in a rat model of blast-induced traumatic brain injury. J Neurosci Res 88:3530-3539.2010).

Risling M (Blast Induced Brain Injuries - A Grand Challenge in TBI Research. Front Neurol 1:1.2010).

Risling M, Plantman S, Angeria M, Rostami E, Bellander BM, Kirkegaard M, Arborelius U, Davidsson J (Mechanisms of blast induced brain injuries, experimental studies in rats. Neuroimage 54 Suppl 1:S89-97.2011).
Ritenour AE, Baskin TW (Primary blast injury: update on diagnosis and treatment. Crit Care Med 36:S311-317.2008).
Rosenfeld JV, Ford NL (Bomb blast, mild traumatic brain injury and psychiatric morbidity: a review. Injury 41:437-443.2010).
Saljo A, Bao F, Haglid KG, Hansson HA (Blast exposure causes redistribution of phosphorylated neurofilament subunits in neurons of the adult rat brain. J Neurotrauma 17:719-726.2000).
Saljo A, Bolouri H, Mayorga M, Svensson B, Hamberger A (Low-level blast raises intracranial pressure and impairs cognitive function in rats: prophylaxis with processed cereal feed. J Neurotrauma 27:383-389.2010).
Saljo A, Huang YL, Hansson HA (Impulse noise transiently increased the permeability of nerve and glial cell membranes, an effect accentuated by a recent brain injury. J Neurotrauma 20:787-794.2003).
Saljo A, Mayorga M, Bolouri H, Svensson B, Hamberger A (Mechanisms and pathophysiology of the low-level blast brain injury in animal models. Neuroimage 54 Suppl 1:S83-88.2011).
Sayer NA, Chiros CE, Sigford B, Scott S, Clothier B, Pickett T, Lew HL (Characteristics and rehabilitation outcomes among patients with blast and other injuries sustained during the Global War on Terror. Arch Phys Med Rehabil 89:163-170.2008).
Schatz P, Pardini JE, Lovell MR, Collins MW, Podell K (Sensitivity and specificity of the ImPACT Test Battery for concussion in athletes. Arch Clin Neuropsychol 21:91-99.2006).
Schneiderman AI, Braver ER, Kang HK (Understanding sequelae of injury mechanisms and mild traumatic brain injury incurred during the conflicts in Iraq and Afghanistan: persistent postconcussive symptoms and posttraumatic stress disorder. Am J Epidemiol 167:1446-1452.2008).
Schnurr PP, Kaloupek D, Sayer N, Weiss DS, Cohen J, Galea S, Weaver TL (Understanding the impact of the wars in Iraq and Afghanistan. J Trauma Stress 23:3-4.2010).
Schretlen DJ, Shapiro AM (A quantitative review of the effects of traumatic brain injury on cognitive functioning. Int Rev Psychiatry 15:341-349.2003).
Schwartz I, Tuchner M, Tsenter J, Shochina M, Shoshan Y, Katz-Leurer M, Meiner Z (Cognitive and functional outcomes of terror victims who suffered from traumatic brain injury. Brain Inj 22:255-263.2008).
Seal KH, Metzler TJ, Gima KS, Bertenthal D, Maguen S, Marmar CR (Trends and risk factors for mental health diagnoses among Iraq and Afghanistan veterans using Department of Veterans Affairs health care, 2002-2008. Am J Public Health 99:1651-1658.2009).
Sheehan JP, Swerdlow RH, Miller SW, Davis RE, Parks JK, Parker WD, Tuttle JB (Calcium homeostasis and reactive oxygen species production in cells

transformed by mitochondria from individuals with sporadic Alzheimer's disease. J Neurosci 17:4612-4622.1997).

Simon B, Sandhu M, Myhr KL (Live FISH: imaging mRNA in living neurons. J Neurosci Res 88:55-63.2010).

Sponheim SR, McGuire KA, Kang SS, Davenport ND, Aviyente S, Bernat EM, Lim KO (Evidence of disrupted functional connectivity in the brain after combat-related blast injury. Neuroimage 54 Suppl 1:S21-29.2011).

Stout AK, Raphael HM, Kanterewicz BI, Klann E, Reynolds IJ (Glutamate-induced neuron death requires mitochondrial calcium uptake. Nat Neurosci 1:366-373.1998).

Sullivan PG, Geiger JD, Mattson MP, Scheff SW (Dietary supplement creatine protects against traumatic brain injury. Ann Neurol 48:723-729.2000).

Sultana R, Banks WA, Butterfield DA (Decreased levels of PSD95 and two associated proteins and increased levels of BCl2 and caspase 3 in hippocampus from subjects with amnestic mild cognitive impairment: Insights into their potential roles for loss of synapses and memory, accumulation of Abeta, and neurodegeneration in a prodromal stage of Alzheimer's disease. J Neurosci Res 88:469-477.2010).

Taber KH, Warden DL, Hurley RA (Blast-related traumatic brain injury: what is known? J Neuropsychiatry Clin Neurosci 18:141-145.2006).

Takeuchi Y, Dotson M, Keen NT (Plant transformation: a simple particle bombardment device based on flowing helium. Plant Mol Biol 18:835-839.1992).

Tanielian T, Jaycox LH (2008) Invisible wounds of war: psychological and cognitive injuries, their consequences, and services to assist recovery. Santa Monica, California: RAND Corporation

Tanielian TL, Jaycox L, Rand Corporation. (2008) Invisible wounds of war : psychological and cognitive injuries, their consequences, and services to assist recovery. Santa Monica, CA: RAND.

Uchida M, Li XW, Mertens P, Alpar HO (Transfection by particle bombardment: delivery of plasmid DNA into mammalian cells using gene gun. Biochim Biophys Acta 1790:754-764.2009).

Uchida M, Natsume H, Kishino T, Seki T, Ogihara M, Juni K, Kimura M, Morimoto Y (Immunization by particle bombardment of antigen-loaded poly-(DL-lactide-co-glycolide) microspheres in mice. Vaccine 24:2120-2130.2006).

Van Kampen DA, Lovell MR, Pardini JE, Collins MW, Fu FH (The "value added" of neurocognitive testing after sports-related concussion. Am J Sports Med 34:1630-1635.2006).

VanGuilder HD, Farley JA, Yan H, Van Kirk CA, Mitschelen M, Sonntag WE, Freeman WM (Hippocampal dysregulation of synaptic plasticity-associated proteins with age-related cognitive decline. Neurobiol Dis 43:201-212.2011).

von Holst H, Cassidy JD (Mandate of the WHO Collaborating Centre Task Force on Mild Traumatic Brain Injury. J Rehabil Med 8-10.2004).

Ward MW, Concannon CG, Whyte J, Walsh CM, Corley B, Prehn JH (The amyloid precursor protein intracellular domain(AICD) disrupts actin dynamics and mitochondrial bioenergetics. J Neurochem 113:275-284.2010).

Ward MW, Huber HJ, Weisova P, Dussmann H, Nicholls DG, Prehn JH (Mitochondrial and plasma membrane potential of cultured cerebellar neurons during glutamate-induced necrosis, apoptosis, and tolerance. J Neurosci 27:8238-8249.2007).

Warden D (Military TBI during the Iraq and Afghanistan wars. J Head Trauma Rehabil 21:398-402.2006).

Wei ZL, Ogawa R, Takasaki I, Zhao QL, Zheng HC, Ahmed K, Hassan MA, Kondo T (Mild hyperthermia prior to electroporation increases transfection efficiency in HCT 116, HeLa S3 and SGC 7901 cells. Biotechnol Lett 32:367-371.2010).

Weisova P, Concannon CG, Devocelle M, Prehn JH, Ward MW (Regulation of glucose transporter 3 surface expression by the AMP-activated protein kinase mediates tolerance to glutamate excitation in neurons. J Neurosci 29:2997-3008.2009).

Wellmann H, Kaltschmidt B, Kaltschmidt C (Optimized protocol for biolistic transfection of brain slices and dissociated cultured neurons with a hand-held gene gun. J Neurosci Methods 92:55-64.1999).

White CS, Bowen IG, Richmond DR (Biological tolerance to air blast and related biomedical criteria. CEX-65.4. CEX Rep Civ Eff Exerc 1-239.1965).

White CS, Bowen IG, Richmond DR, Corsbie RL (Comparative nuclear effects of biomedical interest. Memo Rep Nav Med Res Inst (US) 8:1-83.1961).

Wightman JM, Gladish SL (Explosions and blast injuries. Ann Emerg Med 37:664-678.2001).

Williamson TL, Cleveland DW (Slowing of axonal transport is a very early event in the toxicity of ALS-linked SOD1 mutants to motor neurons. Nat Neurosci 2:50-56.1999).

Wirth MJ, Wahle P (Biolistic transfection of organotypic cultures of rat visual cortex using a handheld device. J Neurosci Methods 125:45-54.2003).

Xydakis MS, Bebarta VS, Harrison CD, Conner JC, Grant GA, Robbins AS (Tympanic-membrane perforation as a marker of concussive brain injury in Iraq. N Engl J Med 357:830-831.2007).

Zaharoff DA, Henshaw JW, Mossop B, Yuan F (Mechanistic analysis of electroporation-induced cellular uptake of macromolecules. Exp Biol Med (Maywood) 233:94-105.2008).

Zhou Y, Kumon RE, Cui J, Deng CX (The size of sonoporation pores on the cell membrane. Ultrasound Med Biol 35:1756-1760.2009).

Zhou Y, Shi J, Cui J, Deng CX (Effects of extracellular calcium on cell membrane resealing in sonoporation. J Control Release 126:34-43.2008).

Zukin RS, Richter JD, Bagni C (Signals, synapses, and synthesis: how new proteins control plasticity. Front Neural Circuits 3:14.2009).